SSC-369

REDUCTION OF S-N CURVES FOR SHIP STRUCTURAL DETAILS

SHIP STRUCTURE COMMITTEE

1993

SHIP STRUCTURE COMMITTEE

The SHIP STRUCTURE COMMITTEE is constituted to prosecute a research program to improve the hull structures of ships and other marine structures by an extension of knowledge pertaining to design, materials, and methods of construction.

RADM A. E. Henn, USCG (Chairman)
Chief, Office of Marine Safety, Security and Environmental Protection
U. S. Coast Guard

Mr. Thomas H. Peirce
Marine Research and Development Coordinator
Transportation Development Center
Transport Canada

Mr. H. T. Haller
Associate Administrator for Ship-building and Ship Operations
Maritime Administration

Dr. Donald Liu
Senior Vice President
American Bureau of Shipping

Mr. Alexander Malakhoff
Director, Structural Integrity Subgroup (SEA O5P)
Naval Sea Systems Command

Mr. Thomas W. Allen
Engineering Officer (N7)
Military Sealift Command

Mr. Warren Nethercote
Head, Hydronautics Section
Defence Research Establishment-Atlantic

EXECUTIVE DIRECTOR

CDR Stephen E. Sharpe, USCG
Ship Structure Committee
U. S. Coast Guard

CONTRACTING OFFICER TECHNICAL REPRESENTATIVE

Mr. William J. Siekierka
SEA 05P4
Naval Sea Systems Command

SHIP STRUCTURE SUBCOMMITTEE

The SHIP STRUCTURE SUBCOMMITTEE acts for the Ship Structure Committee on technical matters by providing technical coordination for determinating the goals and objectives of the program and by evaluating and interpreting the results in terms of structural design, construction, and operation.

AMERICAN BUREAU OF SHIPPING

Mr. Stephen G. Arntson (Chairman)
Mr. John F. Conlon
Mr. Phillip G. Rynn
Mr. William Hanzelek

NAVAL SEA SYSTEMS COMMAND

Mr. W. Thomas Packard
Mr. Charles L. Null
Mr. Edward Kadala
Mr. Allen H. Engle

TRANSPORT CANADA

Mr. John Grinstead
Mr. Ian Bayly
Mr. David L. Stocks
Mr. Peter Timonin

MILITARY SEALIFT COMMAND

Mr. Robert E. Van Jones
Mr. Rickard A. Anderson
Mr. Michael W. Touma
Mr. Jeffrey E. Beach

MARITIME ADMINISTRATION

Mr. Frederick Seibold
Mr. Norman O. Hammer
Mr. Chao H. Lin
Dr. Walter M. Maclean

U. S. COAST GUARD

CAPT T. E. Thompson
CAPT W. E. Colburn, Jr.
Mr. Rubin Scheinberg
Mr. H. Paul Cojeen

DEFENCE RESEARCH ESTABLISHMENT ATLANTIC

Dr. Neil Pegg

SHIP STRUCTURE SUBCOMMITTEE LIAISON MEMBERS

U. S. COAST GUARD ACADEMY

LCDR Bruce R. Mustain

U. S. MERCHANT MARINE ACADEMY

Dr. C. B. Kim

U. S. NAVAL ACADEMY

Dr. Ramswar Bhattacharyya

CANADA CENTRE FOR MINERALS AND ENERGY TECHNOLOGIES

Dr. William R. Tyson

SOCIETY OF NAVAL ARCHITECTS AND MARINE ENGINEERS

Dr. William Sandberg

NATIONAL ACADEMY OF SCIENCES - MARINE BOARD

Dr. Robert Sielski

NATIONAL ACADEMY OF SCIENCES - COMMITTEE ON MARINE STRUCTURES

Mr. Peter M. Palermo

WELDING RESEARCH COUNCIL

Dr. Martin Prager

AMERICAN IRON AND STEEL INSTITUTE

Mr. Alexander D. Wilson

OFFICE OF NAVAL RESEARCH

Dr. Yapa D. S. Rajapaske

Member Agencies:

United States Coast Guard
Naval Sea Systems Command
Maritime Administration
American Bureau of Shipping
Military Sealift Command
Transport Canada

Ship Structure Committee

An Interagency Advisory Committee

Address Correspondence to:

Executive Director
Ship Structure Committee
U. S. Coast Guard (G-MI/R)
2100 Second Street, S.W.
Washington, D.C. 20593-0001
PH: (202) 267-0003
FAX: (202) 267-4677

August 20, 1993

SSC-369
SR-1336

REDUCTION OF S-N CURVES FOR SHIP STRUCTURAL DETAILS

This report presents a set of fatigue S-N curves for design and analysis of ship structural details. The set of fatigue curves is based on a reanalysis of fatigue data presented in SSC-318. The methodology used to develop the fatigue S-N curves is presented. Examples are presented to illustrate the application of S-N curves for plating under 1 inch thick. A glossary of terms used is provided and recommendations are presented for future research.

A. E. Henn

A. E. HENN
Rear Admiral, U.S. Coast Guard
Chairman, Ship Structure Committee

Technical Report Documentation Page

1. Report No. SSC-369	2. Government Accession No. PB94-121926	3. Recipient's Catalog No.
4. Title and Subtitle Reduction of S-N Curves for Ship Structural Details		5. Report Date September 1992
		6. Performing Organization Code
7. Author(s) Karl A. Stambaugh, David H. Leeson, Dr. Frederick Lawrence, C-Y, Hou, Grzegorz Banas		8. Performing Organization Report No. SR-1336
9. Performing Organization Name and Address Columbia Research Corp. 2531 Jefferson Davis Highway Arlington, VA 22202		10. Work Unit No. (TRAIS)
		11. Contract or Grant No. DTCG23-90-C-20001
12. Sponsoring Agency Name and Address Ship Structure Committee U.S. Coast Guard (G-M) 2100 Second Street, SW Washington, DC 20593		13. Type of Report and Period Covered Final Report
		14. Sponsoring Agency Code G-M

15. Supplementary Notes

Sponsored by the Ship Structure Committee and its member agencies.

16. Abstract

This report presents a set of fatigue S-N curves for design and analysis of ship structural details. The set of fatigue curves is based on a reanalysis of fatigue data presented in SSC-318. The methodology used to develop the fatigue S-N curves is presented. Examples are presented to illustrate the application of S-N curves for plating under one inch thick. A glossary of terms used is provided. Recommendations are presented for future research.

17. Key Words	18. Distribution Statement
Fatigue Ship Structure Structural Details S-N Curves	Available from: National Technical Information Service U.S. Department of Commerce Springfield, VA 22151

19. Security Classif. (of this report)	20. Security Classif. (of this page)	21. No. of Pages	22. Price
Unclassified	Unclassified	178	

Form DOT F 1700.7 (8-72) Reproduction of completed page authorized

METRIC CONVERSION FACTORS

Approximate Conversions to Metric Measures

Symbol	When You Know	Multiply by	To Find	Symbol
		LENGTH		
in	inches	*2.5	centimeters	cm
ft	feet	30	centimeters	cm
yd	yards	0.9	meters	m
mi	miles	1.6	kilometers	km
		AREA		
in^2	square inches	6.5	square centimeters	cm^2
ft^2	square feet	0.09	square meters	m^2
yd^2	square yards	0.8	square meters	m^2
mi^2	square miles	2.6	square kilometers	km^2
	acres	0.4	hectares	ha
		MASS (weight)		
oz	ounces	28	grams	g
lb	pounds	0.45	kilograms	kg
	short tons (2000 lb)	0.9	tonnes	t
		VOLUME		
tsp	teaspoons	5	milliliters	ml
Tbsp	tablespoons	15	milliliters	ml
fl oz	fluid ounces	30	milliliters	ml
c	cups	0.24	liters	l
pt	pints	0.47	liters	l
qt	quarts	0.95	liters	l
gal	gallons	3.8	liters	l
ft^3	cubic feet	0.03	cubic meters	m^3
yd^3	cubic yards	0.76	cubic meters	m^3
		TEMPERATURE (exact)		
°F	Fahrenheit temperature	5/9 (after subtracting 32)	Celsius temperature	°C

*1 in ≡ 2.54 (exactly). For other exact conversions and more detailed tables, see NBS Misc. Publ. 286, Units of Weights and Measures, Price $2.25, SD Catalog No. C13.10:286.

Approximate Conversions from Metric Measures

Symbol	When You Know	Multiply by	To Find	Symbol
		LENGTH		
mm	millimeters	0.04	inches	in
cm	centimeters	0.4	inches	in
m	meters	3.3	feet	ft
m	meters	1.1	yards	yd
km	kilometers	0.6	miles	mi
		AREA		
cm^2	square centimeters	0.16	square inches	in^2
m^2	square meters	1.2	square yards	yd^2
km^2	square kilometers	0.4	square miles	mi^2
ha	hectares (10,000 m^2)	2.5	acres	
		MASS (weight)		
g	grams	0.035	ounces	oz
kg	kilograms	2.2	pounds	lb
t	tonnes (1000 kg)	1.1	short tons	
		VOLUME		
ml	milliliters	0.03	fluid ounces	fl oz
l	liters	2.1	pints	pt
l	liters	1.06	quarts	qt
l	liters	0.26	gallons	gal
m^3	cubic meters	35	cubic feet	ft^3
m^3	cubic meters	1.3	cubic yards	yd^3
		TEMPERATURE (exact)		
°C	Celsius temperature	9/5 (then add 32)	Fahrenheit temperature	°F

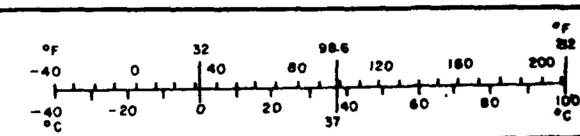

REDUCTION OF S-N CURVES FOR
SHIP STRUCTURAL DETAILS
SR-1336

September 30, 1992

Prepared by

Karl A. Stambaugh
David H. Leeson
Columbia Research Corporation
2531 Jefferson Davis Highway
Arlington, VA 22202

and

Dr. Frederick Lawrence
C-Y. Hou
Grzegorz Banás
University of Illinois
Urbana Champaign Campus
Urbana, Illinois

Project Number 192-01

for

Ship Structures Committee
Under Contract To
United States Coast Guard
Washington, DC

Contract No. DTCG23-90-C-20001

TABLE OF CONTENTS

LIST OF TABLES

LIST OF FIGURES

LIST OF FIGURES
(continued)

LIST OF FIGURES
(continued)

LIST OF FIGURES
(continued)

LIST OF FIGURES
(continued)

LIST OF SYMBOLS

a	=	Crack depth
b	=	Fatigue strength exponent
C	=	Constant relating to the mean S-N curve
COV	=	Coefficient of variation
HAZ	=	Heat affected zone
K_f	=	Fatigue notch factor
$K_{f\,max}^{A}$	=	Value of K_f for axial component of applied stress
$K_{f\,max}^{B}$	=	Value of K_f for bending component of applied stress
$K_{f\,max}^{eff}$	=	Value of K_f representing combined effects of axial and bending stresses
K_t	=	Elastic stress concentration factor
L	=	Load effect
m	=	Inverse slope of mean S-N regression line, also used as exponent controlling the thickness effect
M_k	=	Correction factor for effect of weld shape in N_p model
M_w	=	Wave induced bending movement
N	=	Number of cycles corresponding to a particular fatigue strength; total number of nominal stress range cycles also known as fatigue life
n_i	=	Number of stress cycles in stress block i
N_i	=	Number of cycles of failure at a constant stress range
N_I	=	Life devoted to crack initiation and early growth
N_p	=	Life devoted to fatigue crack propagation
N_T	=	Total fatigue life
R	=	Ratio of minimum to maximum applied stress
s	=	Standard deviation
S_{ref}	=	Design stress for the reference thickness
S_a^A	=	Axial component of applied stress
S_a^B	=	Bending component of applied stress
S_a^T	=	Applied mean stress
$s_{R=0}$	=	Standard deviation for stress ratio of 0
S_u	=	Ultimate strength
S_y	=	Yield strength

LIST OF SYMBOLS
(continued)

S_W	=	Wave induced bending stress
t	=	Plate thickness
V_C	=	Variation due to uncertainty in equivalent stress range; includes effects of fabrication, workmanship, and uncertainty in slope
V_F	=	Variation due to errors in fatigue model and use of Miner's Rule
V_N	=	Variation in fatigue test data about mean S-N line
V_R	=	Total COV of resistance in terms of cycles to failure
V_S	=	Variation due to uncertainty in equivalent stress range; includes effects of error in stress analysis
x	=	Ratio of applied bending to applied total stresses
α	=	Geometry factor
β	=	Number of stress blocks
ΔS_R	=	Design stress range
η	=	Limit damage ratio
σ'_f	=	Fatigue strength coefficient
σ_r	=	Local (notch root) residual stress
σ_B	=	Bending stress
τ	=	Shear Stress

1.0 INTRODUCTION

Cyclic loading causes fatigue cracking in a ship's welded structural details. If these details are not designed to resist fatigue cracking, the ship's profitability may be affected by repair costs and its economic life shortened. Fatigue cracks, for instance, may lead to fractures in ship's primary hull structure, an event resulting in catastrophic failure. It is therefore necessary that structural designers use techniques for minimizing fatigue damage and ensuring structural integrity for the ship's intended service life.

One technique for predicting and assessing fatigue cracking uses empirical data derived from laboratory tests of representative structural details. After details undergo fatigue tests, test data are analyzed in terms of stress applied to each detail and the number of cycles required to reach failure. The test results are commonly referred to as S-N data and are presented in S-N curves.

This report presents a set of S-N curves for typical welded structural details. The S-N curves are reduced from an extensive data base described by Munse et al. in SSC 318 (1-1) and Lawrence et al. in SSC project SR-1298 (1-2). To provide data that are independent of method and compatible with cumulative damage assessments, the S-N data are presented in graphs and tables as well as in S-N curves. Fatigue loading and factors affecting fatigue response are briefly discussed as preliminary guidance for the designer. For those interested in developing fatigue loading stress curves, supporting literature is cited. Examples that illustrate the relationship between the S-N data and structural details are provided. For all sets of S-N curves, however, the designer's knowledge of fatigue response and his engineering judgement are critical to identifying the proper S-N curve for each application. A correction for detail members thicker than one inch is recommended. The reanalysis and development of S-N curves is presented in Appendix A; development of thickness correction in Appendix B; and a glossary of terms in Appendix C.

2.0 FATIGUE IN SHIP STRUCTURAL DETAILS

Throughout its service life a ship experiences environmental loading which causes cyclic stress variations in structural members. Those variations can cause fatigue cracking in welded structural details if the details are inadequately designed. A fatigue assessment, supported when appropriate by fatigue analysis, should ensure that structural members do not lead to catastrophic failure. Fatigue-critical locations have been identified in a survey of standard structural details by Jordan et al. in SSC 272 (2-1) and SSC 294 (2-2). Stambaugh (2-3) presents fatigue- critical locations for special details that may lead to fracture. Fatigue analysis should be considered for these locations and wherever special or new details are introduced in the ship's primary structure.

2.1 FATIGUE STRESS IN SHIP DETAILS

2.1.1 Ship Hull Girder Loading and Resulting Stresses

Hull loads from waves and other sources must be transformed to stress distributions in the structural detail. Because it depends on the type of ship and operational environment, predicting and analyzing fatigue stresses is complex. The designer must estimate the magnitude of the stresses and determine their impact on fatigue response.

In a ship's steel structure, stress cycles are generally caused by the seaway and by changes in still water bending moments. These loads produce bending stress and shear stress in the ship's hull girder. These global stresses are illustrated in Figure 2-1 for a typical tanker where vertical, lateral, and torsional bending combine in the primary structural members. Local stresses caused by changes in hydrostatic pressure and local loading from cargo or ballast are also superimposed on the hull girder. If pertinent to a particular ship, other loading from

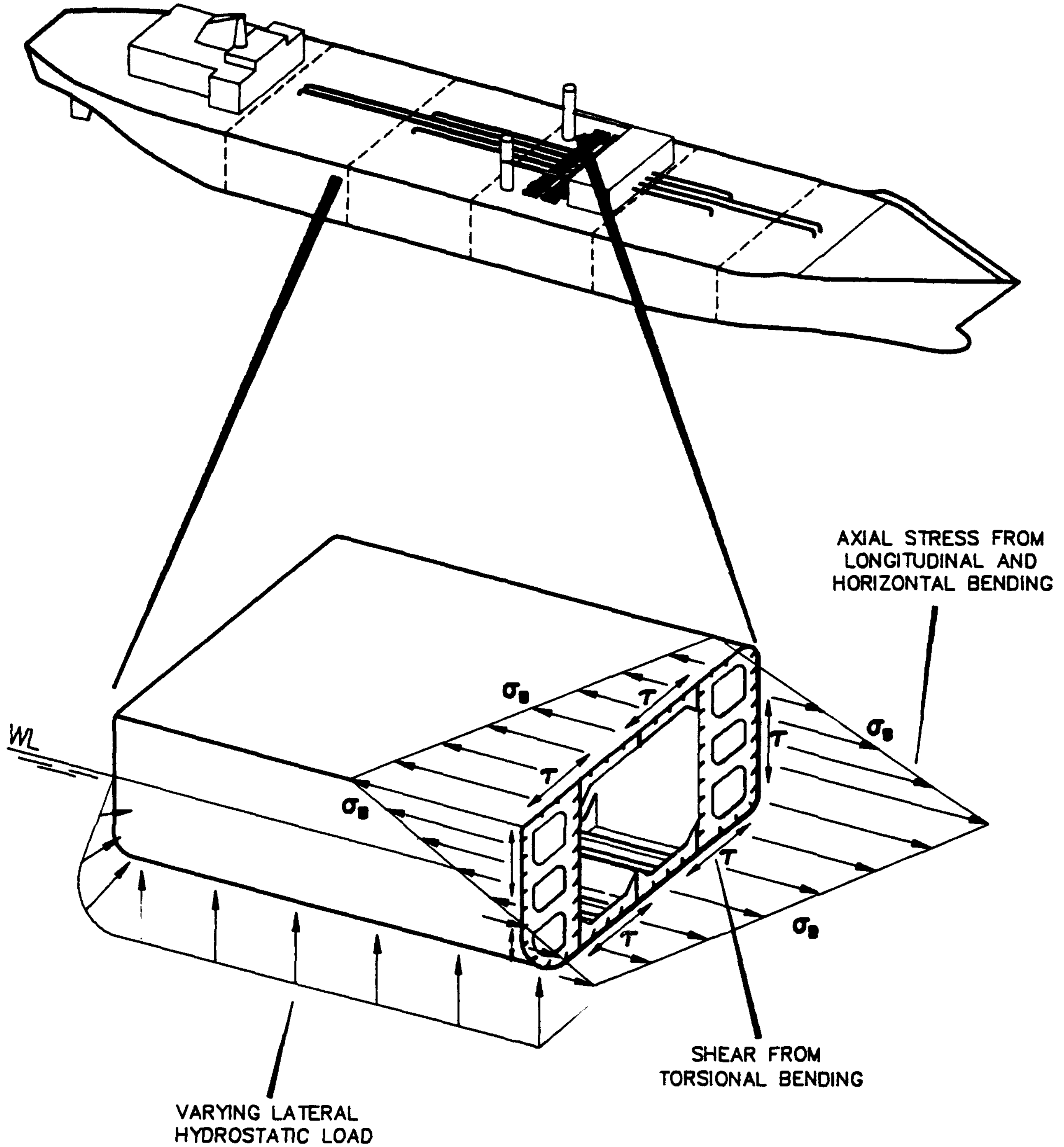

FIGURE 2-1: GLOBAL STRESSES DUE TO COMBINED VERTICAL AND LATERAL BENDING AND TORSION

dynamic effects, stresses from thermal differences in the girder, and residual stresses should be considered in the fatigue analysis.

Global loads are distributed through plates, girders, and panel stiffeners, all of which are connected by welded structural details that may concentrate stress.

2.1.2 Characterization of Stress for Fatigue Analysis

For the S-N curves in this report, stress is defined as the stress range (double amplitude) in the location of the weld in the absence of the weld. The overall geometry of the weld need not be considered unless there are discontinuities from overfill, undercutting, or gross variations in the weld geometry. The relevant stress range is the nominal stress range, which must include any local bending and stress concentrations caused by the geometry of the detail. In load-carrying fillet-welded joints or partial penetration joints, the maximum shear stress range may be used for the S-N curve that is developed using this definition. Finite element techniques predict stress in complex ship structural details that is compatible with the S-N curves presented here.

Stress associated with the physical geometry in structural details can be estimated by parametric approximations of stress concentration factors or for complex geometry associated with ship structures by finite element analysis as illustrated in Figure 2-2. The application of the finite element technique to ship structural details is described by Liu and Bakker (2-4).

Loading and resultant stresses are random and combine complexly. Because the nature of loading may vary with each detail of the same ship, a probabilistic approach is often used to characterize the long-term stress response distribution. The distribution is first developed by combining probabilities for each load and corresponding stress state. Then, the stress response transfer

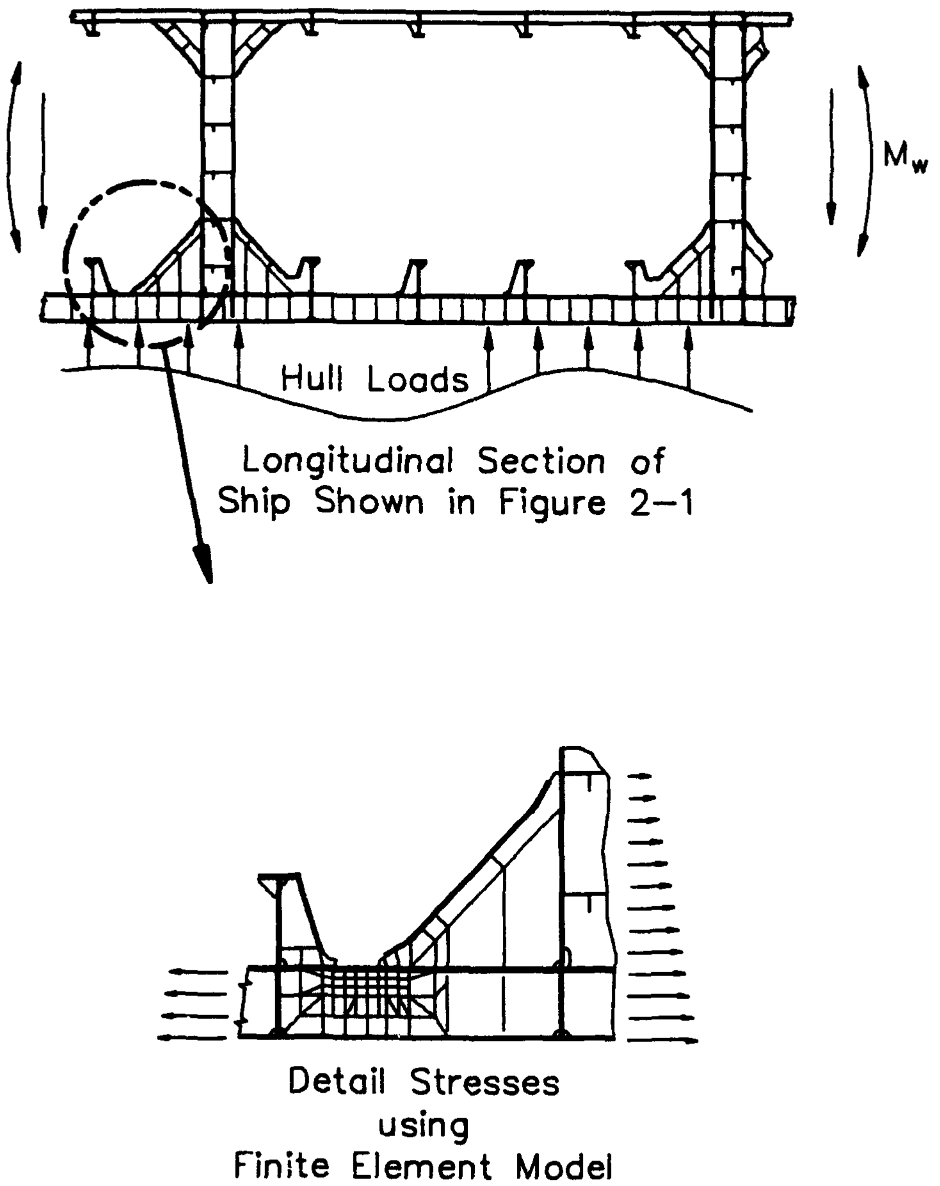

FIGURE 2-2: CHARACTERIZATION OF STRESS ON SHIP STRUCTURAL DETAILS

function is predicted for the individual load cases; and, finally, the distribution of joint probabilities are combined based on the probability of occurrence of each sea state. The long-term stress distribution is used in the cumulative damage analysis along with the S-N data applicable to the structural detail in question (see Figure 2-3).

Techniques for predicting long-term load and stress distribution and their development have been investigated extensively by Lewis (2-5), Sikora (2-6), Munse (2-7), White (2-8), Wirsching (2-9), and others but with little agreement as to the type of distribution that accounts for random load effects. The designer, therefore, must choose the dominant loads and combine them as they are expected to combine during the ship's service life.

2.2 FATIGUE LIFE PREDICTIONS USING S-N CURVES

The fatigue life of a structural detail is determined by the number of cycles required to initiate a fatigue crack and propagate it from subcritical to critical size. The cumulative damage approach, based on S-N curves, is a method used to predict and assess fatigue life. As developed by Miner (2-10), this approach requires knowledge of structural loading and the structure's capacity expressed as stress range and number of cycles to failure. Developed from test data (S-N curves), this method is based on the hypothesis that fatigue damage accumulates linearly and that damage due to any given cycle is independent of neighboring cycles. By this hypothesis, the total fatigue life under a variety of stress ranges is the weighted sum of the individual lives at constant S, as given by the S-N curves, with each being weighted according to the fractional exposure to that level of stress range. To apply this hypothesis, the long-term distribution of stress range is replaced by a stress histogram, consisting of a convenient number of constant amplitude stress range blocks, S_i, and a number of stress cycles, n_i. The

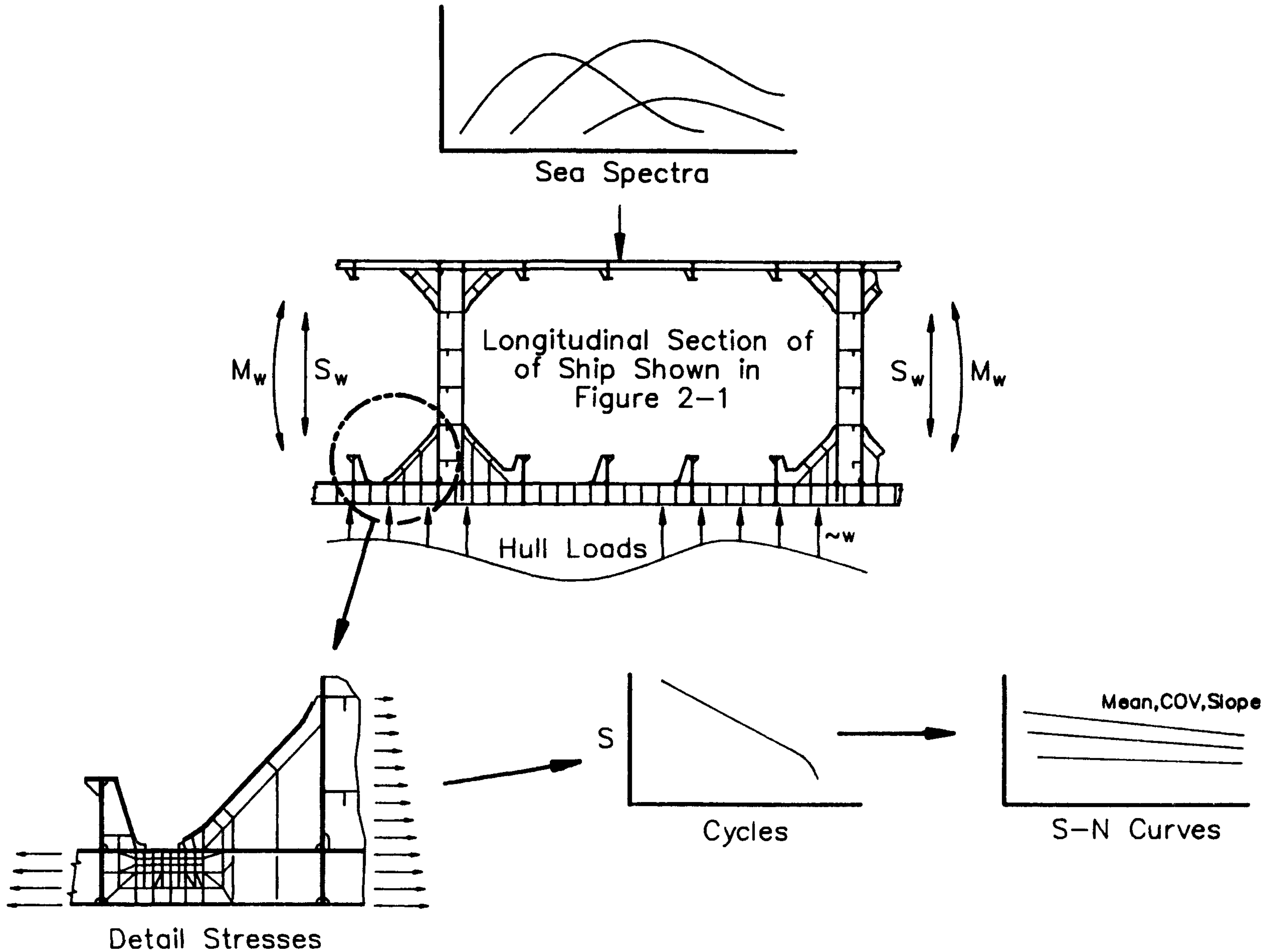

FIGURE 2–3: FATIGUE ANALYSIS OF STRUCTURAL DETAILS

constraint against fatigue fracture is then expressed in terms of a nondimensional damage ratio, η:

$$\sum_{i=1}^{\beta} \frac{n_i}{N_i} \leq \eta_L$$

where β = number of stress blocks

n_i = number of stress cycles in stress block i

N_i = number of cycles of failure at a constant stress range. S_i

η_L = limit damage ratio

The limit damage ratio η_L depends on maintainability, that is, the possibility for inspection and repair, and the fatigue characteristics of the particular detail. These factors also have probabilistic uncertainty associated with them.

Fatigue design, using the linear cumulative damage approach, ensures the safety or performance of a system for a given period of time and/or under a "specified" loading condition. But the absolute safety of the system cannot be guaranteed because of the number of uncertainties involved. In structural design, these uncertainties can be due to the random nature of loads, simplifying assumptions in the strength analysis, material properties, etc.

Two approaches, design code and reliability, have been proposed to account for the uncertainties not otherwise considered by the linear cumulative damage model of fatigue life prediction.

2.2.1 Design Code Approach

The design code uses qualitatively adjusted *S-N* curves or *S-N* curves that represent mean-minus-two standard deviations. The former approach is used by AWS (2-11) and AISC (2-12), and the latter by UK DOE (2-13). Both approaches have been used for buildings and bridges, for which design loads are specified and limited during operation. Results have been conservative yet acceptable.

The following design S-N curves are based on the mean-minus-two standard deviations for relevant experimental data. Their use therefore assumes a low but finite probability of failure at the calculated life. Thus, when using the curves an additional factor on life should be considered for cases of inadequate structural redundancy. In defining this factor, the accessibility of the joint, the proposed degree of repetition, and the consequences of failure should be considered. Because stress estimates are critical to calculated life, particular care should be taken to ensure that stresses are not underestimated.

2.2.2 Fatigue Reliability Approach

In contrast to design codes, the reliability approach accounts for the random nature of fatigue life data, stress in ship structure, and associated uncertainties. Munse (2-7), for example, proposes that the structural reliability problem be considered one of supply and demand; failure occurs when the supply (the resistance or strength of the system) is less than the demand (the loading on the system). For a structural system this can be stated as:

$$\text{Probability of Failure} = P_f = P\ (\text{Strength} < \text{Load})$$

If both load and strength are treated as random variables, then the reliability problem can be treated using probabilistic methods. To analyze reliability, a mathematical model that relates load and resistance needs to be derived. This relationship is expressed in the form of a limit-state equation. For the simple case cited above it would appear as:

$$g(x) = R - L$$

where R and L are the random variables of resistance and load-effect. While failure is represented by the region where g(x) is less than zero, the safe region is where g(x) is greater than zero. The line g(x) = 0 represents the boundary between these regions and is thus defined as the limit-state equation.

To use reliability-based design methods engineers and designers need not be deeply versed in probability theory. Rather, the design criteria they use should produce desirable levels of uniform safety among groups of structures. This can be accomplished without departing drastically from general practice. One of the more popular formats for probabilistic information in structural design is that of the Load and Resistance Factor Design (LRFD) recommended by the National Bureau of Standards (2-14). This approach uses load amplification factors and resistance reduction factors (partial safety factors) and can be expressed as:

$$\phi R \geq \sum_{i=1}^{n} \tau_i L_i$$

where R is the resistance, e.g., in flexural shear, fatigue, etc.; L_1 is the load-effect, e.g., due to dynamic, quasi-static, and static loads, etc.; ϕ is the resistance reduction factor: τ_i is the i^{th} partial load-effect amplification factor; and n is the total number of load-effects considered in the limit-state design equation.

For fatigue of structural details, resistance is usually expressed as the mean and standard deviation of the number of cycles to failure at a given stress range. This information typically derives from constant amplitude fatigue test data of the type of detail being investigated. A number of these tests are conducted and the results are provided in the form of stress range vs. life (S-N) curves. The data points at each stress range follow either a log-normal or Weibull distribution about the mean value of number of cycles to failure and can be represented by a probability density function (PDF). Resistance is then represented by a least-squares fit of the mean values of life at each stress range.

While the standard deviation of the fatigue life data can be found easily, the scatter of the data about the mean fatigue line is only one uncertainty in S-N analysis. A measure of the total uncertainty (coefficient of variation) in fatigue life, V_R, is usually developed to include the uncertainty in fatigue data, errors in the fatigue model, and any uncertainty in the individual stresses and stress effects. Ang and Munse (2-15) suggest that the total COV in terms of fatigue life could be given by:

$$V_R^2 = V_N^2 + V_F^2 + V_C^2 + (mv_s)^2$$

where

V_R = total COV of resistance in terms of cycles to failure

V_N = variation in fatigue test data about mean S-N line

V_F = variation due to errors in fatigue model and use of Miner's Rule

V_C = variation due to uncertainty in equivalent stress range (includes effects of fabrication, workmanship, and uncertainty in slope)

V_s = variation due to uncertainty in equivalent stress range (includes effects of error in stress analysis)

m = slope of mean S-N regression line

Values of m and V_n can be obtained from sets of S-N curves for the type of detail being investigated.

Although reasonable values for the remaining uncertainties are available in the literature (2-15, 2-16), much work remains to be done in this area. Typically V_s is assumed to be 0.1; V_C to be

0.4; and V_F to be 0.15. Recently, Wirsching (2-9) recommended adjustments to these values.

Reliability approaches help account for the random nature of ship loading and analytical uncertainties, but require more development to fully characterize the uncertainties described above.

3.0 S-N CURVES FOR SHIP STRUCTURAL DETAILS

The S-N curves and data presented in this section are derived from the same fatigue life data presented in SSC-318 (3-1). The data base was reanalyzed for steels with a yield strength, S_y<50ksi and one stress ratio, (R=0). The approach used to develop the S-N curves and data is discussed in Appendix A. The welded detail category, number, description, loading, and pictographs are presented in Table 3-1.

The S-N data are presented in two formats:

1. S-N curves are presented in Figures 3-1 and 3-2 for quick analysis by designers familiar with this format and the safety factors assumed by their use. These curves represent the mean-minus-two standard deviations as described in Appendix A.

2. Statistical data is presented in Table 3-2 for designers interested in performing a probabilistic analysis.

The basic design curves, which consist of linear relationships between log (ΔS_R) and log (N), are based on a statistical analysis of experimental data as described in Appendix A. Thus the basic
S-N curves are of the form:

$$\log(N) = \log C - m \cdot \log(\Delta S_R)$$

or in terms of stress range:

$$\Delta S_R = (C/N)^{1/m}$$

where:

N is the predicted number of cycles for failure under stress range ΔS_R

C is a constant relating to the mean S-N curve

m is the inverse slope of the S-N curve

Table 3-1
Welded Detail Classification

CATEGORY	DETAIL NUMBER	DESCRIPTION, LOADING	PICTOGRAPH
A	1	Plain plate, machined edges, Axial	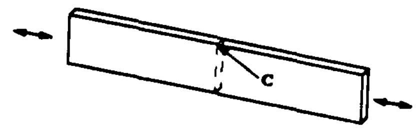
	2	Rolled I-Beam, Bending	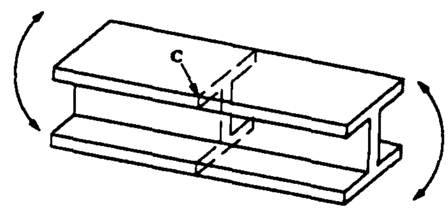
	8	Double shear bolted lap joint, Axial	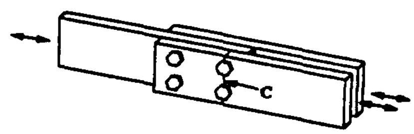
B	1(F)	Plain plate flame-cut edges, Axial	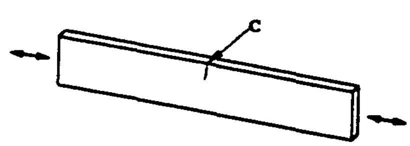

Key to symbols is presented on Page 3-15.

Table 3-1
Welded Detail Classification
(continued)

CATEGORY	DETAIL NUMBER	DESCRIPTION, LOADING	PICTOGRAPH
B	3	Longitudinally welded plate, as-welded, Axial	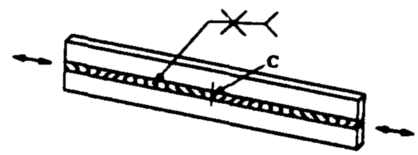 (As-welded)
	3(G)	Longitudinally welded plate, weld ground, Axial	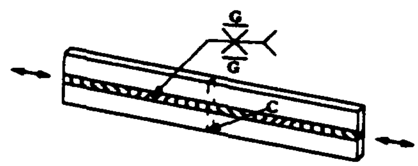 (Ground faces of the weld)
	10(G)	Transverse butt joint, weld ground, Axial	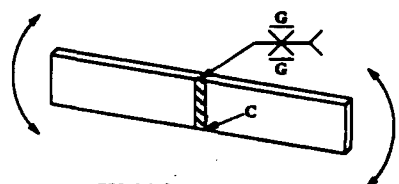 (Weld faces ground)
	10A	Transverse butt joint, as welded, In-plane bending	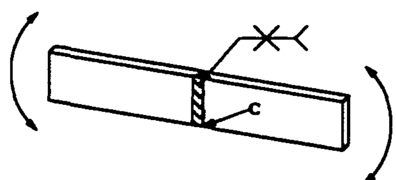 (As-welded)

Key to symbols is presented on Page 3-15.

Table 3-1
Welded Detail Classification
(continued)

CATEGORY	DETAIL NUMBER	DESCRIPTION, LOADING	PICTOGRAPH
B	25A	Lateral attachment to plate, Axial	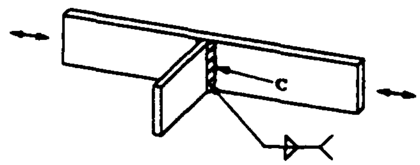
	13	Flange splice (unequal width), as-welded, Bending	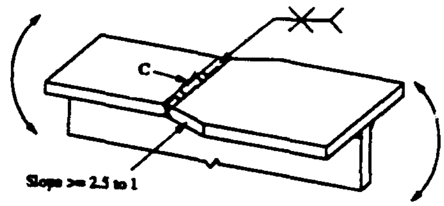 (As-welded)
	28	Plain plate with drilled hole, Axial	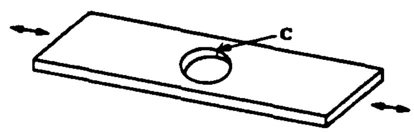 (Drilled hole)
C	12(G)	Flange splice (unequal thickness), weld ground, Bending	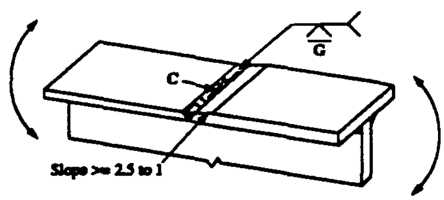 (Weld faces ground)

Key to symbols is presented on Page 3-15.

Table 3-1
Welded Detail Classification
(continued)

CATEGORY	DETAIL NUMBER	DESCRIPTION, LOADING	PICTOGRAPH
C	4	Welded I-beam continuous weld, Bending	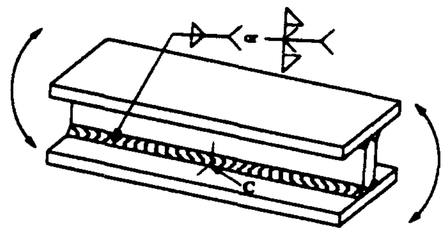
	6	Welded I-beam with longitudinal stiffeners welded to web, Bending	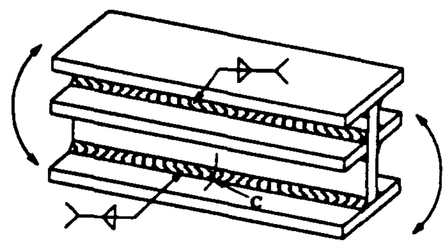
	9	Single shear riveted lap joint, Axial	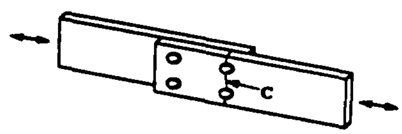 (Riveted)
	16(G)	Partial penetration butt weld, weld ground, Axial	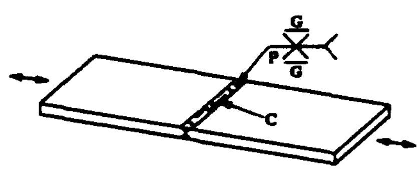 (Partial penetration - weld ground)

Key to symbols is presented on Page 3-15.

Table 3-1
Welded Detail Classification
(continued)

CATEGORY	DETAIL NUMBER	DESCRIPTION, LOADING	PICTOGRAPH
C	25	Lateral attachments to plate, Axial	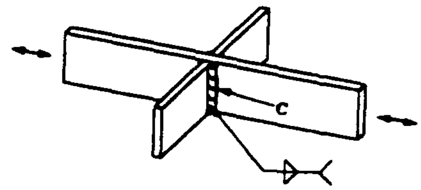
	7(B)	I-beam with welded stiffeners, Bending stress in web	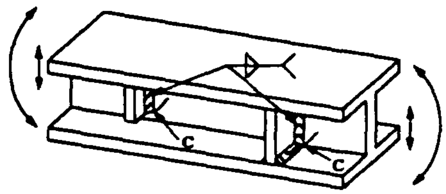
D	30A	Lateral attachments to plate, Bending	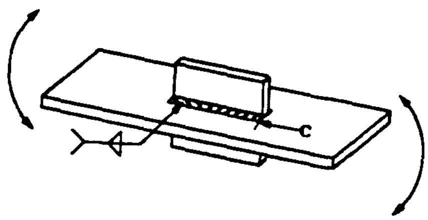
	26	Doubler plate welded to plate, Axial	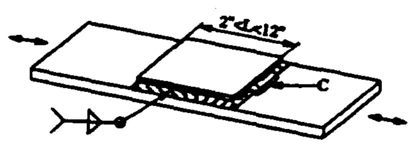

Key to symbols is presented on Page 3-15.

Table 3-1
Welded Detail Classification
(continued)

CATEGORY	DETAIL NUMBER	DESCRIPTION, LOADING	PICTOGRAPH
D	14	Cruciform joint, Axial	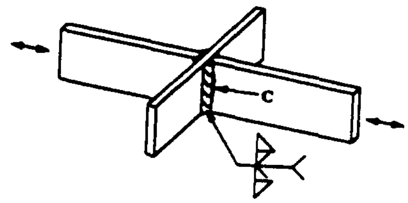
	11	Transverse butt welded I-beam, as-welded, Bending	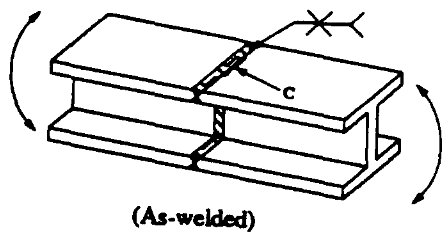
	21	Cruciform joint, 1/4" weld, In-plane bending stress at weld toe, C	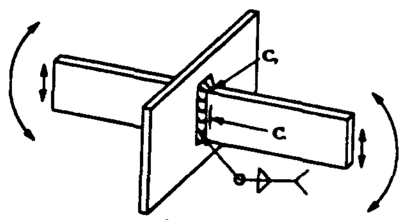
	7(P)	I-beam with welded stiffeners, Principal stress in web	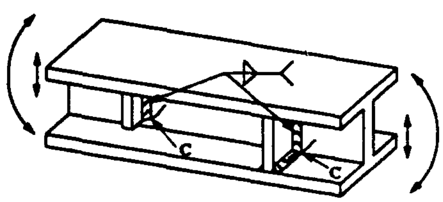

Key to symbols is presented on Page 3-15.

Table 3-1
Welded Detail Classification
(continued)

CATEGORY	DETAIL NUMBER	DESCRIPTION, LOADING	PICTOGRAPH
D	36	Welded beam with intermittent welds and cope hole in the web, Bending	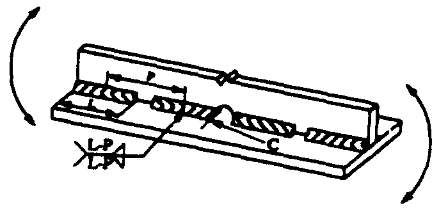
	25B	Lateral attachment to plate with stiffener, Axial	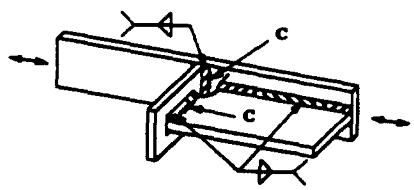
	12	Flange Splice (unequal thickness), as-welded, Bending	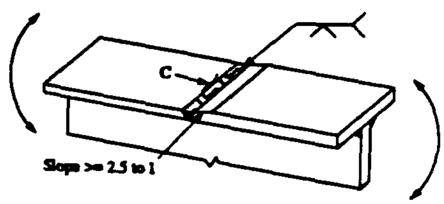 (As-welded)
	16	Partial penetration butt weld, as-welded, Axial	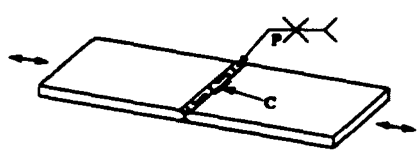 (Partial penetration - as-welded)

Key to symbols is presented on Page 3-15.

Table 3-1
Welded Detail Classification
(continued)

CATEGORY	DETAIL NUMBER	DESCRIPTION, LOADING	PICTOGRAPH
D	22	Attachment of stud to flange, Bending	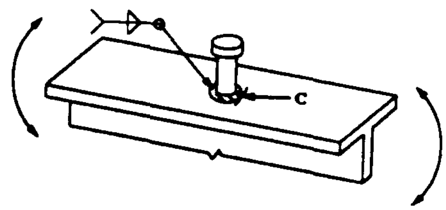
E	21(3/8")	Cruciform joint, 3/8" weld, Bending stress on throat weld	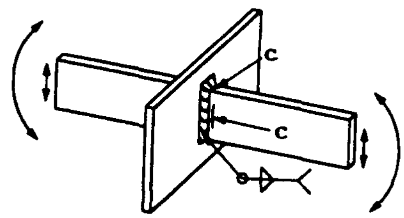
	20	Cruciform joint, Axial, Stress on plate at weld toe C	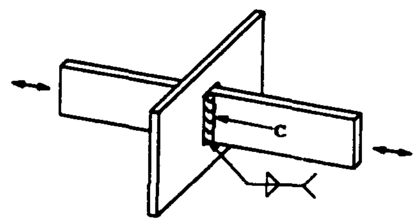
	23	Attachment of channel to flange, Bending	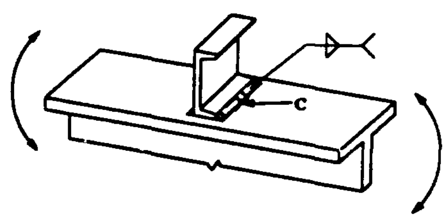

Key to symbols is presented on Page 3-15.

Table 3-1
Welded Detail Classification
(continued)

CATEGORY	DETAIL NUMBER	DESCRIPTION, LOADING	PICTOGRAPH
	24	Attachment of bar to flange (L<=2"), Bending	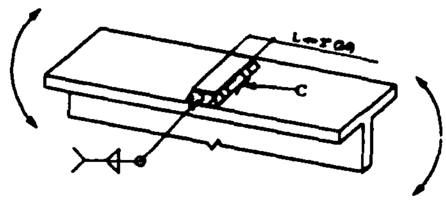
E	19	Flat bars welded to plate, lateral welds only, Axial	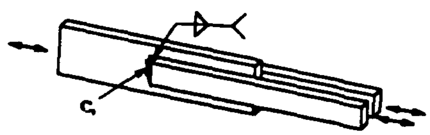
	30	Lateral attachments to plate, Axial	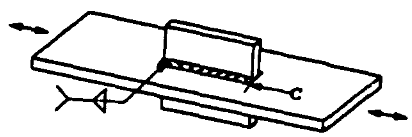
F	38	Beam connection with horizontal flanges, Bending	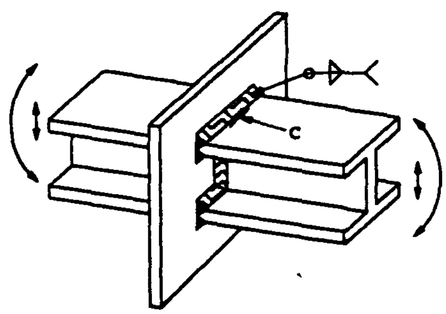

Key to symbols is presented on Page 3-15.

Table 3-1
Welded Detail Classification
(continued)

CATEGORY	DETAIL NUMBER	DESCRIPTION, LOADING	PICTOGRAPH
F	17A	Channel welded to plate, longitudinal weld only, Axial	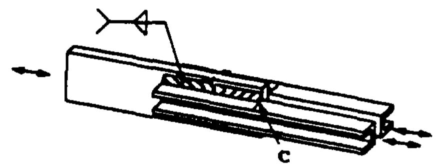
	31A	Attachments of plate to edge of flange, Bending	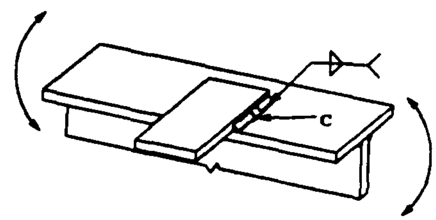
	17	Angles welded on plate, longitudinal welds only, Axial Stress in angle end of weld, C	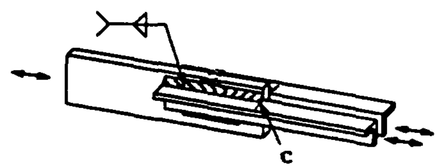
	18	Flat bars welded to plate, longitudinal weld only, Axial Stress in plate, C	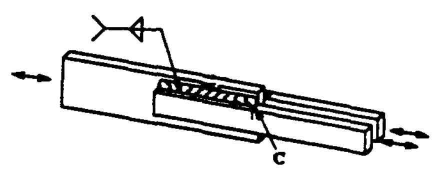

Key to symbols is presented on Page 3-15.

Table 3-1
Welded Detail Classification
(continued)

CATEGORY	DETAIL NUMBER	DESCRIPTION, LOADING	PICTOGRAPH
F	32A	Groove welded attachment of plate to edge of flange, Bending stress in flange at end of attachment, C	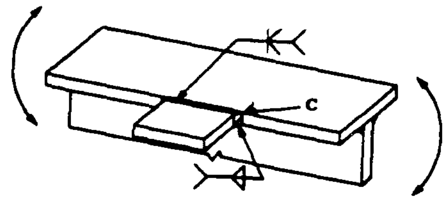
G	27	Slot or plug welded double lap joint, Axial	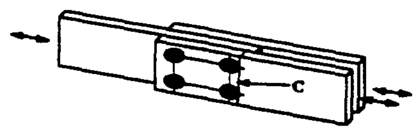 (Slot or Plug Welds)
	33	Flat bars welded to plate, lateral and longitudinal welds, Axial	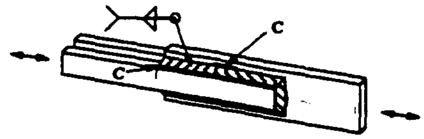
	46	Triangular gusset attachments to plate, Axial	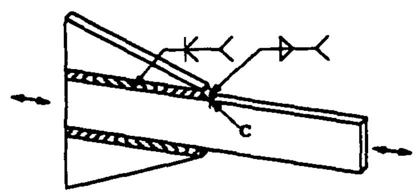

Key to symbols is presented on Page 3-15.

Table 3-1
Welded Detail Classification
(continued)

CATEGORY	DETAIL NUMBER	DESCRIPTION, LOADING	PICTOGRAPH
G	40	Interconnecting beams, Bending in perpendicular directions	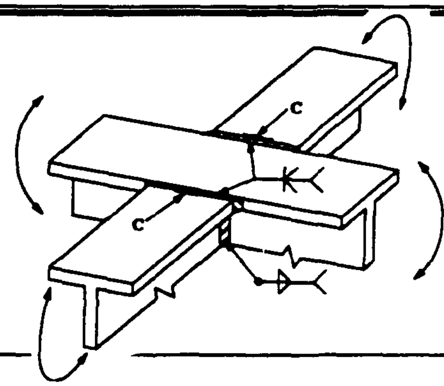
	32B	Butt welded flange (unequal width), Bending	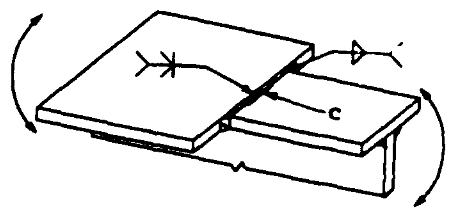
S	21(S)	Cruciform joint, In-plane bending, Shear stress on the weld, C_s	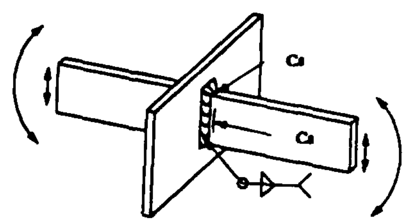
	18(S)	Flat bars welded to plate, longitudinal weld only, Axial, Shear stress on weld, C_s	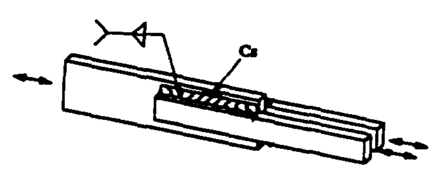

Key to symbols is presented on Page 3-15.

Table 3-1
Welded Detail Classification
(continued)

CATEGORY	DETAIL NUMBER	DESCRIPTION, LOADING	PICTOGRAPH
S	33(S)	Flat bars welded to plate, lateral and longitudinal welds, Axial, Shear stress on weld, C_s	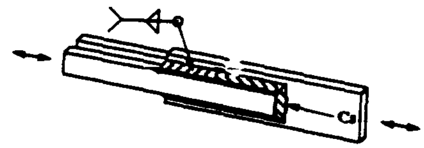
	17(S)	Angle welded to plate, longitudinal weld only, Axial, Shear stress on weld, C_s	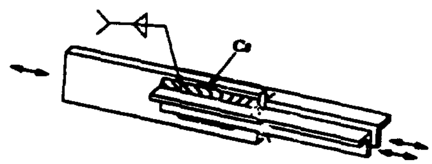
	17A(S)	Channel welded to plate, longitudinal weld only, Axial, Shear stress on weld, C_s	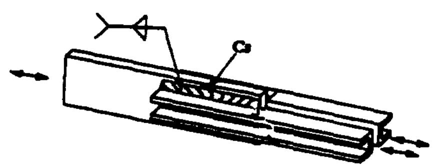
	20(S)	Cruciform joint, Axial, Shear stress on weld, C_s	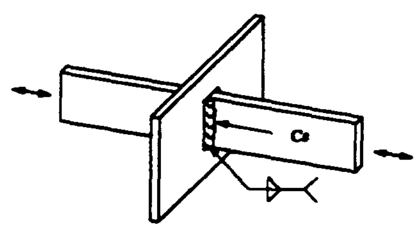

Key to symbols is presented on Page 3-15.

Table 3-1
Welded Detail Classification
(continued)

CATEGORY	DETAIL NUMBER	DESCRIPTION, LOADING	PICTOGRAPH
S	19(S)	Flat bars welded to plate, lateral welds only, Axial, Shear stress on weld, C_s	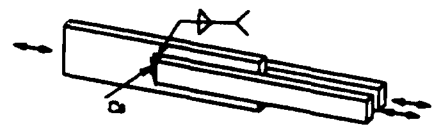
	38(S)	Beam connection with horizontal flanges, Shear stress on weld, C_s	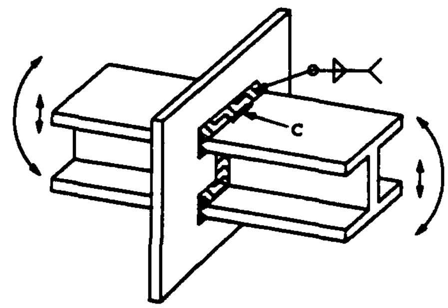

Key to Symbols

(F) - Flame cut edges
(G) - Weld ground
(B) - Bending stresses
(P) - Principal stresses
(S) - Shear stresses
A,B,C, .. Additional description within the same detail number
C→ - Crack initiation site due to tensile stresses
C_s→ - Crack initiation site due to shear stresses
L - Length of intermittent weld
P - Pitch between to intermittent welds
R - Radius
t - Thickness of plate

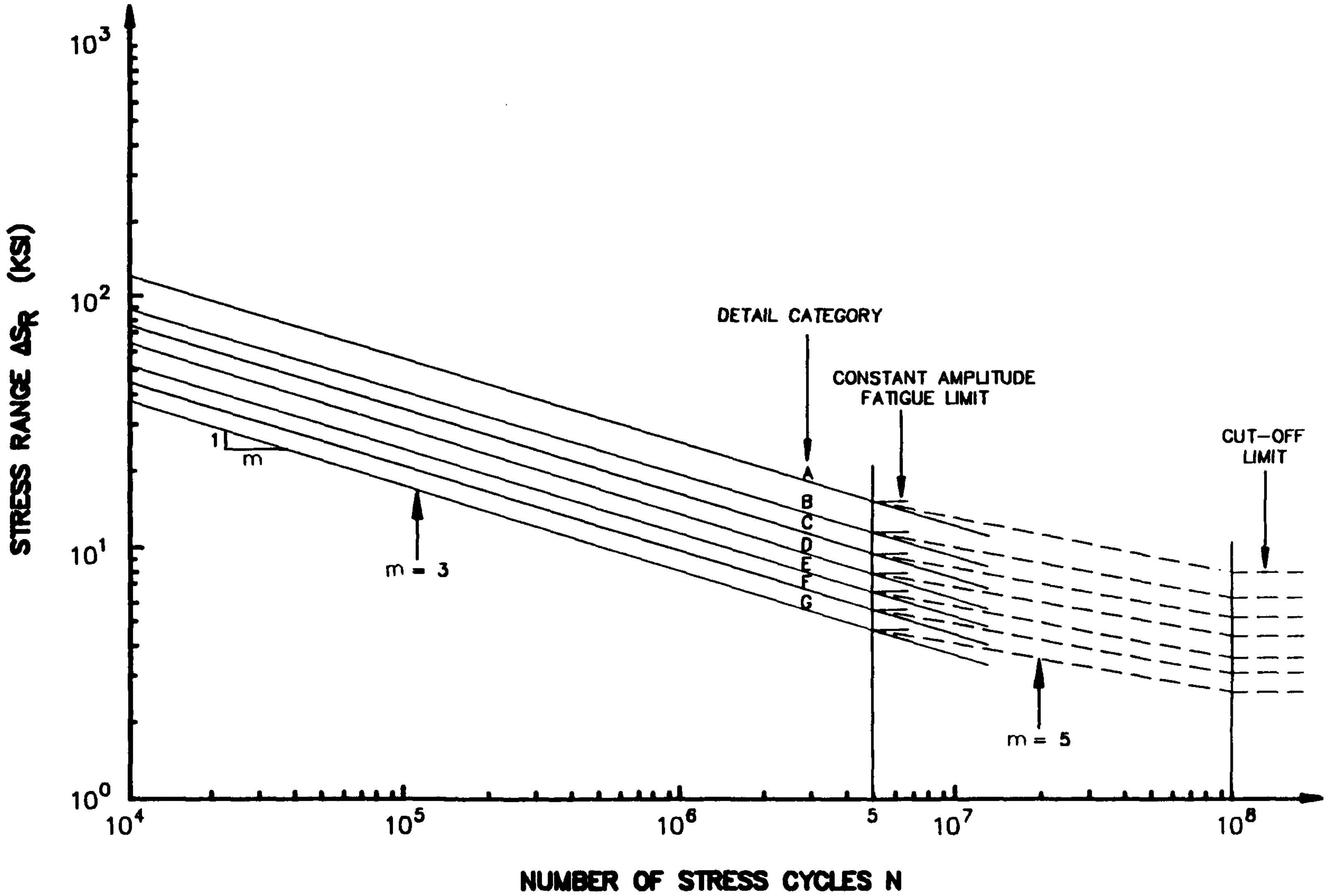

FIGURE 3-1: SHIP DESIGN FATIGUE STRESS CURVES

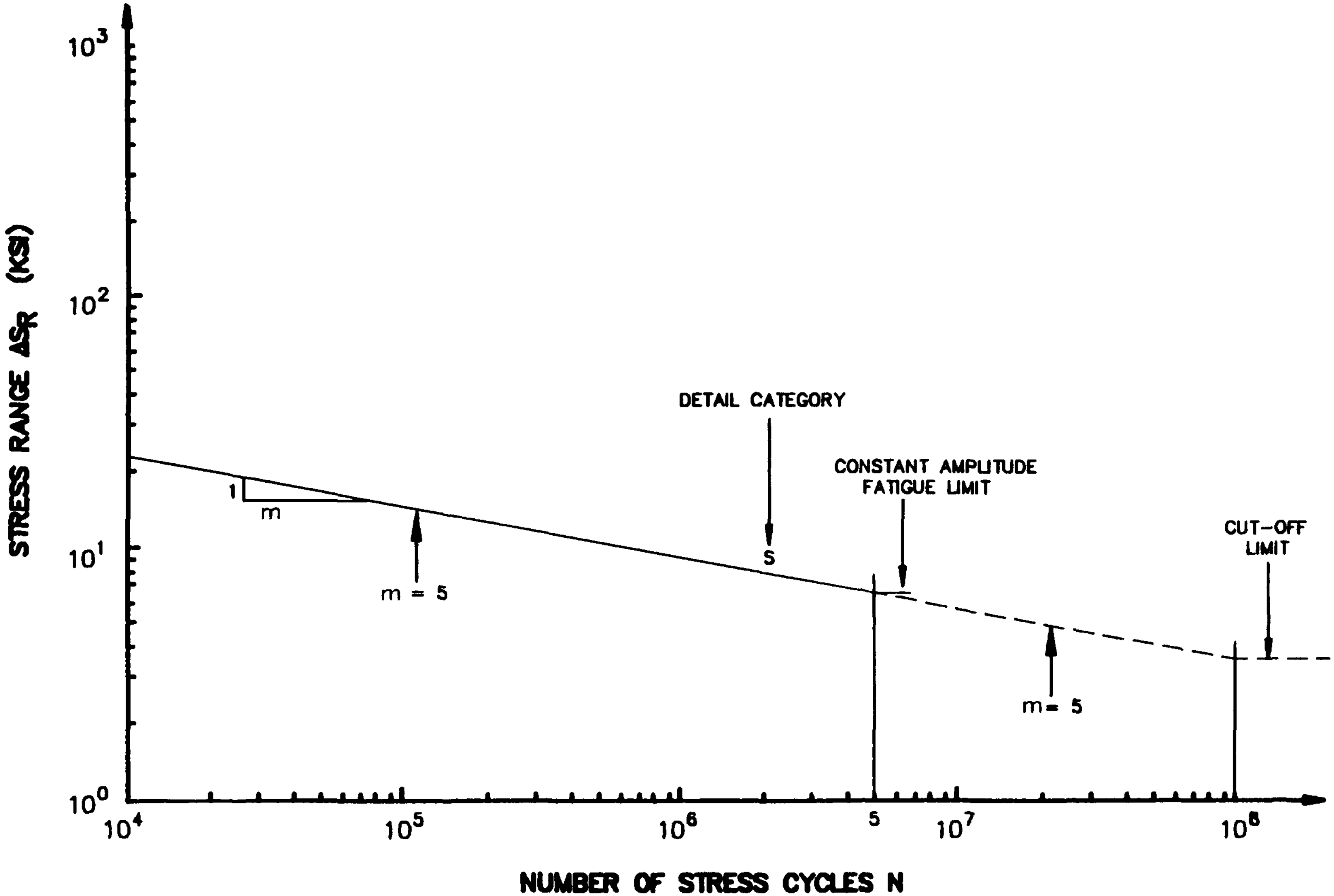

FIGURE 3-2: SHIP DESIGN FATIGUE SHEAR STRESS RANGE

Table 3-2
S-N Curve Statistics

Category	Design Stress Range* 10^6 Cycles ksi	Fatigue Constant log C	Inverse Slope m		Standard Deviation log ΔS_R at $n=10^6$
			$n<5x10^6$	$n<5x10^6$	
A	24	10.14	3.0	5.0	.083
B	19	9.84	3.0	5.0	.083
C	16	9.61	3.0	5.0	.083
D	13	9.34	3.0	5.0	.083
E	11	9.12	3.0	5.0	.083
F	9.5	8.93	3.0	5.0	.083
G	8	8.71	3.0	5.0	.083
S	7.2	10.30	5.0	5.0	.083

*Design stress range is the regression mean minus two standard deviations

The relevant statistics, including the standard deviation of the log of ΔS_R, are shown in Table 3-2.

The slopes of the S-N curves are bi-linear to account for the constant amplitude fatigue limit. This limit begins at $5 \cdot 10^6$ cycles. When all nominal stress ranges are less than the constant amplitude fatigue limit for the particular detail, no fatigue assessment is required.

The S-N curves have a cut off limit at 10^8 cycles. This limit is calculated by assuming a slope corresponding to m=5 below the constant amplitude fatigue limit. All stress cycles in the design spectrum below the cut off limit may be ignored when the structure is adequately protected against corrosion.

Other than as described above, no qualitative adjustments are included in this S-N Data set, which is typical of many other structural design codes. Adjustments required to account for other factors influencing fatigue response are left to the designer, who should find the research described in the following sections helpful.

4.0 FACTORS INFLUENCING FATIGUE RESPONSE

Designers of a ship's structural details must be aware of deviations from the data base used to develop the S-N curves. Recommended adjustments are presented where differences may exist.

4.1 MATERIAL

The strength of typical ship steels (Sy<50ksi) does not change the S-N curve of a welded joint appreciably. Experiments (4-1) show that higher tensile strength steels used in shipbuilding do not have a higher fatigue strength than mild steels, in the case of welded joints. In fatigue critical locations, therefore, the use at stronger steels to increase allowable stress should be approached with caution.

4.2 WELD FABRICATION AND INSPECTION

Welding processes (*e.g. automatic submerged arc or manual*) can significantly influence fatigue response and are noted in the descriptive information for the structural detail presented in Section 3.0 of this report.

Joint misalignments can significantly affect fatigue response. S-N curves are developed assuming that weld quality is free of critical defects and meets the requirements of regulatory and classification societies for (4-2). Any deviations from these requirements should put the detail in the lowest category G.

Weld profile changes by grinding and planing affect fatigue response as noted in the UK DOE (4-3) design code, and have been included as part of the data base evaluated here. Grinding butt weld reinforcement was evaluated, but no difference in response was noted.

4.3 COMBINED STRESSES

Predicting stress and its corollary S-N category are very important factors when determining fatigue life. As described earlier, the designer must account for the geometric stress concentration and stress conditions at the weld. The state of stress in a ship's structural details is often more complex than that indicated by the relatively simple details presented here. Combined axial, bending, and shear stress are present in most of a ship's structural details. Equivalent stress techniques have been reviewed by Stambaugh and Munse (4-4). The equivalent shear stress, maximum principal stress, and maximum octahedral stress may characterize the state of stress in a structural detail, depending on the characteristics of the principal stress field in the joint.

4.4 MEAN STRESS

The correction for mean stress ratios other than R=O is based on work by Yung and Lawrence (4-5), who propose an equation to calculate the mean fatigue strength of weldments at long lives.

$$\frac{\Delta S_R}{\Delta S_{R=0}} = \frac{1+(2N)^b}{1+\frac{1+R}{1-R}(2N)^b}$$

Based on this equation, we can predict the mean fatigue strength at any R value at 10^6 cycles from the R=0 fatigue strength at 10^6 cycles. Fatigue strength exponent b is estimated by:

$$b = -\frac{1}{6}\ log2\ (1 + \frac{50}{1.5S_u})$$

where S_u is the ultimate strength of base metal. The derivation of this correction is presented in Appendix A along with its validation using the UIUC fatigue data bank.

4.5 CORROSION

Salt water can seriously affect the fatigue life of structural details. The data available (4-6), (4-7), (4-8) indicate that corrosion decreases fatigue life where details are uncoated or do not have cathodic protection. When no consistent protection is provided, evidence suggests that fatigue life should be reduced by a factor of two for all categories. Corrosion also affects fatigue limit, which becomes non-existent when corrosion is present. As noted by UK DOE (4-2), the S-N curve must be continued without a change in slope.

4.6 THICKNESS

At present, most agree that for geometrically similar welds larger weldments will sustain shorter fatigue lives. Theoretical (4-9) and experimental (4-10) evidence confirm the existence of a size effect, but there is much scatter in the data. Thus, the magnitude of the thickness effect remains in question. Lawrence (4-5), Gurney (4-11), and Smith (4-12) recommend the following relationship:

$$\left[\frac{S_1}{S_2}\right] = \left[\frac{t_2}{t_1}\right]^m$$

where t_2 is taken to be 25mm (1 inch)
t_1 is the thickness of plate (mm)
S_1 is the design stress at the thickness in question
S_2 is the design stress for the referenced thickness
m is 1/4 as recommended by Lawrence (4-5) for the S-N curves given in Appendix B.

The one inch thickness cited is greater than most structural details constructed of steel plate and shapes.

5.0 EXAMPLE CORRELATION BETWEEN SHIP STRUCTURAL DETAILS AND S-N CATEGORIES

Structural details transfer loads between structural members in ships. The types of details vary greatly with the kind of ship, loading on the ship, structural connection, economic considerations, or even shipyard practice. The thousands of possible configurations are presented by Jordan, et al. in SSC-292 (5-1) and SSC-294 (5-2).

Designers must carefully consider this variety when selecting categories. Geometric configuration, loading, type of weld, fabrication and inspection procedures, and type of stress must be reviewed carefully so a ship's structural detail is correlated with the appropriate S-N category. If a detail significantly differs from the category description, a review of Appendix A and of SSC-318 (5-3) details may be appropriate. In some instances, more tests must be conducted. As illustrated in the following examples, however, the detail categories presented in this report are sufficient to correlate with most of a ship's structural details.

5.1 WEB FRAME CUTOUT

The web frame cutout used here to illustrate the relationship between S-N categories and structural details has many fatigue critical locations. Variables affecting these locations include the structural detail, geometry, weld type, stress type, and stress magnitude.

In the example, the cut out radius is equivalent in geometry to detail 28(F). Here the "F" represents flame cut. Stress in the detail must be equated to the axial stress indicated in the pictographs, using the maximum shear stress depending on the characteristics predicted for the detail's location in the ship. The flatbar attachment is fillet welded to the side shell stiffener. The detail geometry and applied stress are similar to detail 21. The shear stress in the throat of the fillet weld will correlate to detail 21(s). The local stress field is characterized by combined stresses between the web frame and side shell stiffener and varies in magnitude as the loading changes in the seaway. The web frame attachment to the side shell is similar to the weld ending associated with detail 36. Bending stress dominates the stress field in the web frame. The stress concentrates at the weld ending. The correlation between the fatigue critical area and the related S-N curve detail is shown in Figure 5-1. The equivalent S-N categories are as follows:

Local Detail	Equivalent Detail	S-N Category
Flatbar stiffener connection to tee longitudinal	21	D
Side shell plating at cutout	36	D
Radius of cutout	1(F)*	A

*With appropriate geometric stress concentration factor.

5.2 CENTER VERTICAL KEEL

Our second example (Figure 5-2) pertains to fatigue cracking on a Center Vertical Keel (CVK). The CVK bracket, the transition between the CVK and the bulkhead girder, experiences sheer stress from external loading on the ship hull. The hull girder stress and stresses induced by cargo and ballast are superimposed on the local loading. This combined stress field must be simplified to equal the state of stress associated with the S-N detail. The upper end of the bracket geometry correlates to detail 14 and 20 for full penetration and fillet welds, respectively. the lower bracket end correlates to detail 21(s) in geometry and stress characteristics. Detail 30 correlates to the structural detail at the top of the CVK bracket. In both types of details,

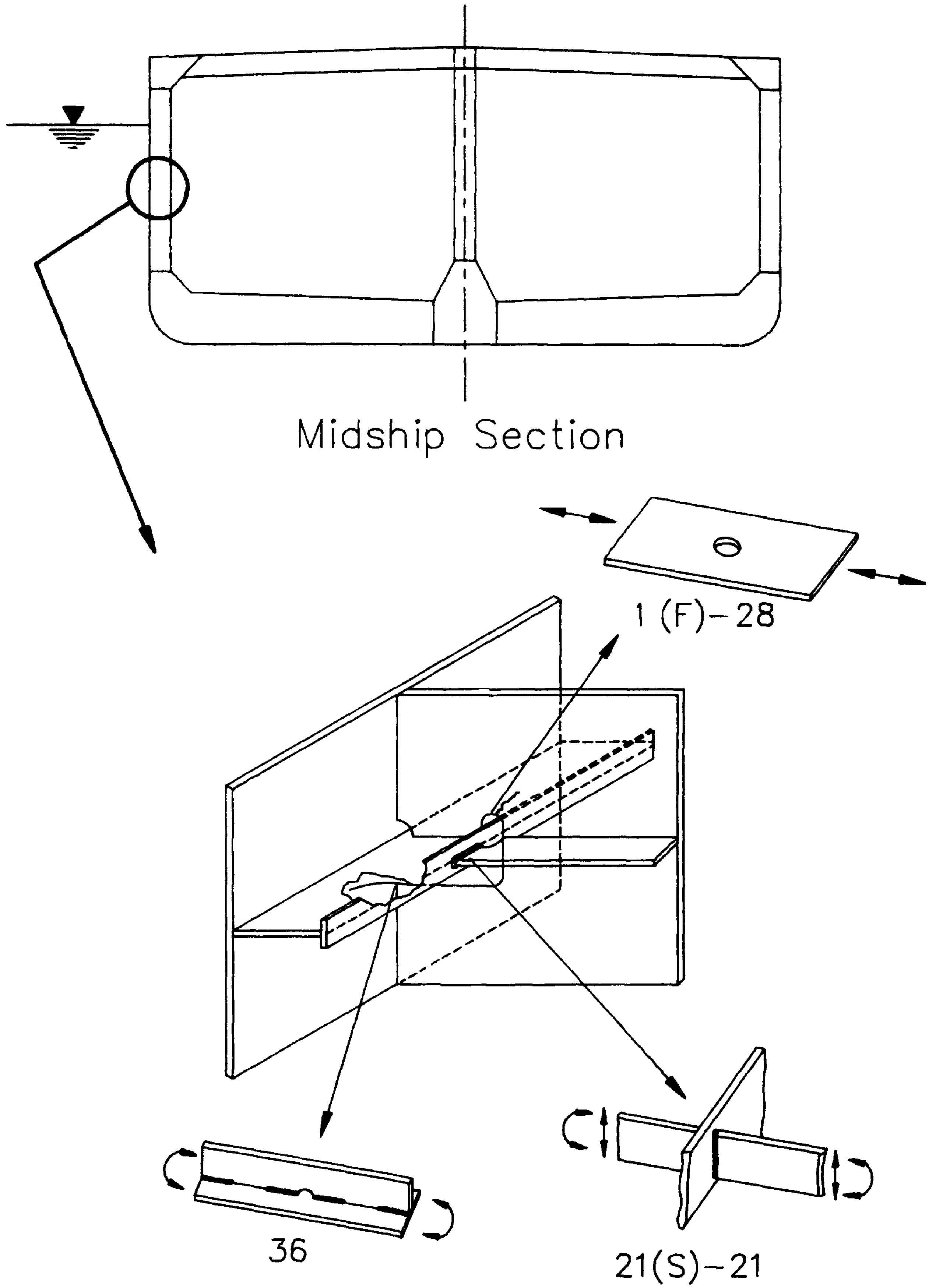

FIGURE 5-1: FATIGUE IN WEB FRAME BRACKET

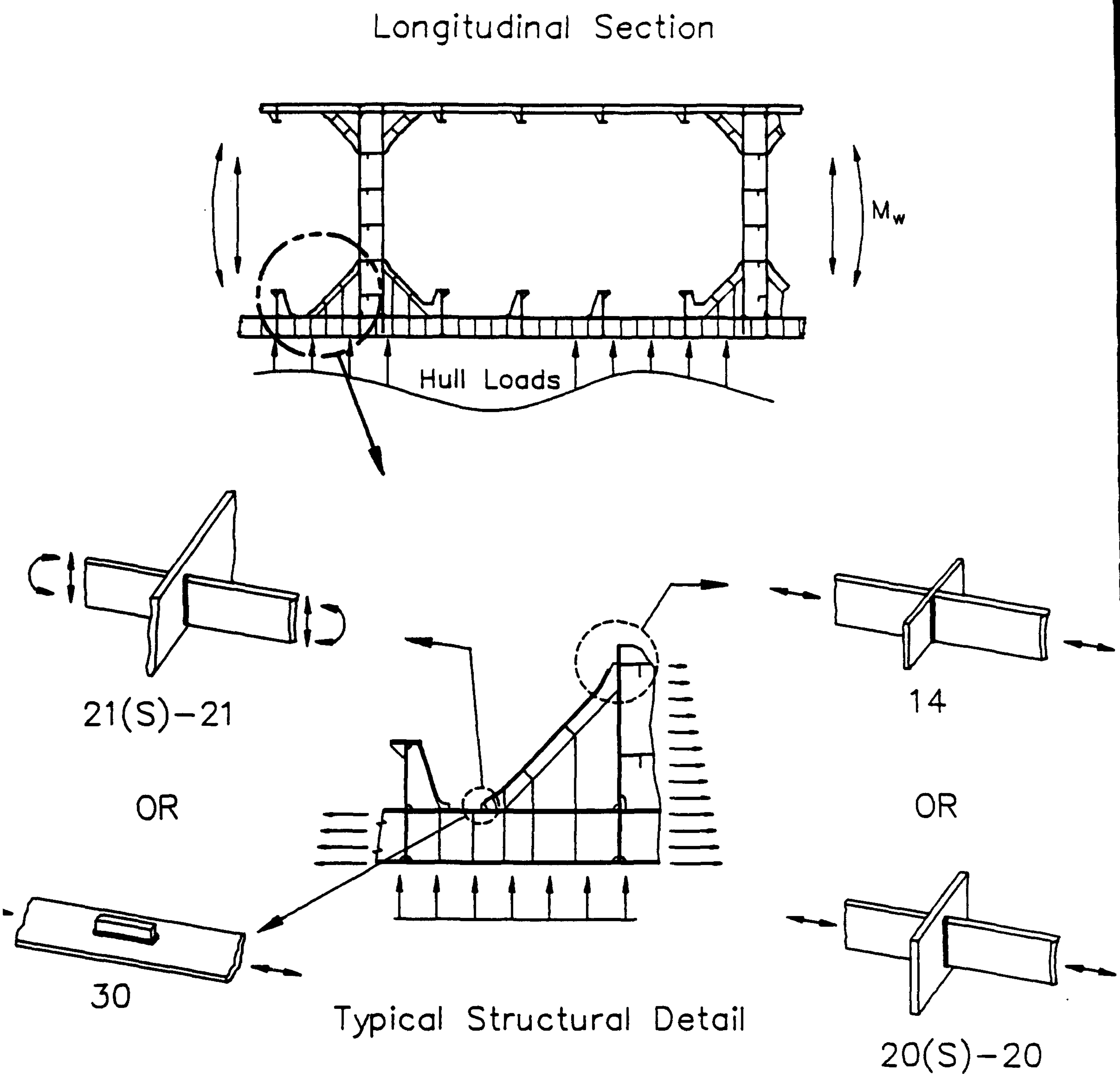

FIGURE 5-2: FATIGUE IN A CENTER VERTICAL KEEL (CVK)

stresses combine in a complex manner. Sheer and bending stress are applied to details 30 and 21(s). The correlation between the fatigue critical locations and the S-N categories for the CVK are as follows:

Ship Detail	Equivalent Detail	S-N Category
Base of bracket on CVK	21(s) or 30	S or E
Top of bracket on vertical bulkhead girder	14 or 20(s)	D or S

As discussed earlier, the designer must review the geometric stress concentrations, weld type, loading, and stress state very carefully. The designer is also encouraged to review the cited literature and other fatigue life approaches for ship structures. In any application of S-N curves, the designer's knowledge and judgement are required to correlate the S-N curve results to complex applications associated with a ship's structural details.

6.0 CONCLUSIONS

1. The S-N curves presented in SSC-318 were analyzed using R=0 and S_y<50ksi to reduce scatter in the mean fatigue strength at 10^6 cycles. A consistent ranking of details resulted from this analysis.

2. The standard deviations of the log of fatigue strength at 10^6 cycles did not correlate with weldment severity nor with the type of fatigue initiating notch. The standard deviations of the log of fatigue strength at 10^6 did vary with sample size. Sample sizes less than 8 were excluded from consideration. This limitation excluded details from the SSC-318 data base, SR-1298, and other sources. An average standard deviation for the data base was used to develop the fatigue strength categories.

3. Correlations are provided for details subject to R ratios other than 0 and members sized greater than 1 inch thick.

4. The reanalyzed data base was ordered according to strength at 10^6 cycles; and categories were assigned to produce uniform groups of approximately 1.21 times the fatigue strength, which is approximately three times the fatigue life.

5. The details characterized by shear stress in the weld throat were separated into a unique S-N curve with inverse slope (m)=5.

7.0 RECOMMENDATIONS

1. The initial efforts of this project indicate a dominating effect of weld type in detail classification, with other variables and factors influencing the fatigue strength. Additional research should be conducted to correlate the details according to weld type and configuration using the detailed stress predicted by finite element analysis.

2. Additional fatigue testing is recommended to include the type of details unique to ship structures and detail loading more characteristic of ship structural experience.

3. The coefficient of variation for each detail category did not correlate to parameters of sample size or K_f. Further investigation is required to refine the definition of coefficient of variation for probabilistic design applications.

REFERENCES

1-1 Munse, W.H., T.W. Wilbur, M.L. Tellalian, K. Nicoll and K. Wilson, "Fatigue Characterization of Fabricated Ship Details for Design," Report No. SSC-318, Department of Civil Engineering, University of Illinois at Urbana-Champaign, sponsored by the Ship Structure Committee, 1983.

1-2 Lawrence, F.W., "Fatigue Characterization of Fabricated Ship Details -- Phase II," Ship Structure Committee Project SR-1298, University of Illinois, Urbana, Illinois (awaiting publication).

2-1 Jordan, C.R. and Cochran, C.S. "In-Service Performance of Structural Details," SSC-272, 1978.

2-2 Jordan, C.R. and Knight, L.T. "Further Survey of In-Service Performance of Structural Details," SSC-294, 1980.

2-3 Stambaugh, K. and W. Wood, "Ship Fracture Mechanisms Investigation," Final Report for ISSC, March 1987.

2-4 Liu, D. and A. Bakker, "Practical Procedures for Technical and Economic Investigations of Ship Structural Details," Marine Technology, January 1981.

2-5 Lewis, E.V., Van Hoof, R., Hoffman, D. Zubaly, R.B. and Maclean, W.M. "Load Criteria for Ship Design," SSC-240, 1973.

2-6 Sikora, J.P., A. Dinsenbacher and J.E. Beach, "A Method for Estimating Lifetime Loads and Fatigue Lives for SWATH and Conventional Monohull Ships," Naval Engineers Journal, ASNE, May 1983, pp. 63-85.

2-7 Munse, W.H., T.W. Wilbur, M.L. Tellalian, K. Nicoll and K. Wilson, "Fatigue Characterization of Fabricated Ship Details for Design," Report No. SSC-318, Department of Civil Engineering, University of Illinois at Urbana-Champaign, sponsored by the Ship Structure Committee, 1983.

2-8 White, G.J. and B.M. Ayyub, "Reliability Based Fatigue Design for Ship Structures," ASNE Journal, May 1985.

2-9 Wirsching P.H., Chen Y.-N., "Considerations of Probability-Based Fatigue Design for Ship Structures," ASNE Journal, May 1985.

2-10 Miner, M.A., "Cumulative Damage in Fatigue," Journal of Applied Mechanics, Vol. 12, 1945.

2-11 AWS - American Welding Society, "Structural Welding Code, Steel," AWS D1.1-90.

2-12 AISC. "Specification for the Design, Fabrication and Erection of Structural Steel for Buildings," American Institute of Steel Construction, 1990.

2-13 British Department of Energy (UK DOE), "Fatigue Design Guidance for Steel Welded Joints in Offshore Structures," London HMSO, 1984.

2-14 Ellingwood, B.R., T.V. Galambos, J.L. MacGregor and A.C. Corwell, "Development of a Probability Based Load Criteria for American National Standard A58," National Bureau of Standards, special publication No. 577, June 1980.

2-15 Ang, A. H-S., and Munse W.H., "Practical Reliability Basis for Structural Fatigue, "Meeting Reprint 2492, ASCE National Structural Engineering Conference, April 14-18, 1975.

2-16 Thayamballi, A., Y-K Chen and D. Liu, "Fracture Mechanics Based Assessment of Fatigue Reliability in Ship Structures Symposium, 1984.

3-1 Munse, W.H., T.W. Wilbur, M.L. Tellalian, K. Nicoll and K. Wilson, "Fatigue Characterization of Fabricated Ship Details for Design," Report No. SSC-318, Department of Civil Engineering, University of Illinois at Urbana-Champaign, sponsored by the Ship Structure Committee, 1983.

3-2 Lawrence, F.W., "Fatigue Characterization of Fabricated Ship Details -- Phase II," Ship Structure Committee Project SR-1298, University of Illinois, Urbana, Illinois (awaiting publication).

4-1 Munse, W.H., T.W. Wilbur, M.L. Tellalian, K. Nicoll and K. Wilson, "Fatigue Characterization of Fabricated Ship Details for Design," Report No. SSC-318, Department of Civil Engineering, University of Illinois at Urbana-Champaign, sponsored by the Ship Structure Committee, 1983.

4-2 American Bureau of Shipping, "Rules for Building and Classing Steel Vessels," 1990. Paramus, New Jersey.

4-3 British Department of Energy (UK DOE), "Fatigue Design Guidance for Steel Welded Joints in Offshore Structures," London HMSO, 1984.

4-4 Stambaugh, K., Munse, W.H., "Fatigue Performance under Multiaxial Loading Conditions," Ship Structure Committee Project SR-1324, Columbia Research Corporation, 1990.

4-5 Yung, J.-Y. and F.V. Lawrence, Jr., "Analytical and Graphical Aids for the Fatigue Design of Weldments," Fatigue Pract. Engineering Mater. Struct., Vol. 8, No. 3, pp. 223-241, November 1985.

4-6 Marshall, P., "Basic Considerations for Tubular Joint Design in Offshore Construction," Welding Research Council Bulletin 193, April 1974.

4-7 Burnside, O.H., S.J. Hudak, Jr., E. Oelkers, K. Chen, and Dexter R.J., "Long-Term Corrosion Fatigue of Welded Marine Steels, "SSC-326, 1984.

4-8 Albrecht, P., Sidani M., "Fatigue Strength of Weathering Steel for Bridges," University of Maryland Department of Civil Engineering, October 1987.

4-9 Gurney, T.R., "The Influence of Thickness on the Fatigue Strength of Welded Joints," Proceedings 2nd International Conference on Behaviour of Offshore Structures (BOSS), London, 1979.

4-10 Maddox, S.J., "The Effect of Plate Thickness on the Fatigue Strength of Fillet Welded Joints," The Welding Institute, 1987.

4-11 Gurney, T.R., "Revised Fatigue Design Rules," Metal Construction 15, 1983.

4-12 Smith, I.J., "The Effect of Geometry Change Upon the Predicted Fatigue Strength of Welded Joints," Proc. 3rd Int. Conf. on Numerical Methods in Fract. Mech., pp. 561-574.

5-1 Jordan, C.R. and Cochran, C.S. "In-Service Performance of Structural Details," SSC-272, 1978.

5-2 Jordan, C.R. and Knight, L.T. "Further Survey of In-Service Performance of Structural Details," SSC-294, 1980.

APPENDIX A

Reanalysis of SSC-318 Data
and
Development of the S-N Curves

A-1 INTRODUCTION AND SUMMARY

A-1.1 The University of Illinois Fatigue Data Bank

The University of Illinois Fatigue Data Bank was developed by W. H. Munse and his co-workers over the last 20 years. The basic structure of the data bank is described by Radziminiski (A-1). In its current form, the data bank contains results for over 25,000 tests of steel weldments for 100 of types of details from over 2,500 references. The descriptor identifying a given data set allows the user to discriminate between different materials, loading conditions, welding procedures, etc. Standard statistical techniques can be used to estimate the mean and standard deviations of data in the collection. The development of this resource for steel weldment fatigue data is described in detail in Reference (A-1) and (A-2).

A-1.2 Data Analysis Summary

The allowable stress ranges for AISC weldment categories A - F were reanalyzed using the UIUC Fatigue Data Bank. The data bank was originally set-up on an IBM main-frame computer and operated via punched cards. At the outset of the current project, the UIUC Fatigue Data Bank was transferred to a Mac IIcx computer and converted for use with the data base software FoxBASE +/ Mac version 2.00.

As part of the work performed, Lawrence and Banas (A-3) separated the data into the AISC A - G weldment categories, for which they generated category S-N curves and the 95% survival levels based on stress range. Regression analysis was performed only on the data representing actual failures. No attempt was made to rationalize the data base, that is, to exclude the potential effects of differing load ratios (R), different material yield strengths (S_y), and the effects of weldment size that result from the indiscriminate collection of fatigue data without noting these effects.

Thus, all data in the UIUC data bank were included for all load ratios, steel strengths, and thicknesses. The large scatter observed may have resulted in part from grouping the weldment fatigue data into broad categories without attempting to exclude the uncertainty produced by the known effects of load ratio, material strength, and weldment size.

A-1.3 Edited Data Base Summary

The authors further analyzed the UIUC Fatigue Data Bank's information for the 53 weldments considered in SSC-318. The main goal here was to edit the data sets so that the information reflects principally the effects of loading condition and the severity of the weldment geometry. The effects of load ratio, base metal yield strength, and weldment size are thus minimized or excluded.

First, the authors created an edited data base which considers only zero-to-tension test results (R=0) and only base metal yield tensile strengths below 50 ksi. Generally reducing the amount of scatter in each data set, this strategy frequently led to different average fatigue strengths at 10^6 cycles than had been calculated using the unedited data (see Tables A-1 to A-4 and Figures A-1 and A-3).

After this editing procedure was established, the standard deviations(s) of the fatigue strength at 10^6 cycles for each of the 53 details were compared to see if they correlated with the mean value of their fatigue strength at 10^6 cycles (ΔS) or their estimated value of fatigue notch factor (K_f). No correlation was found between K_f and the standard deviation, although the standard deviation was found to be a function of sample size (n) (see Figures A-4 and A-5). Consequently, in the subsequent estimation of design fatigue (ΔS), the constant <u>average</u> standard deviation shown in Figure A-5 was applied to <u>all</u> 53 weld details, there being no rational basis for any other procedure based on the information at our disposal.

Table A-1
Regression analysis Paremeters for SSC-318 Weldments
Using only R=0 and Sy <50KSI Data

SSC - 318 Weldment Details	Mean Fatigue Strength at 1E+06 Cycles (ksi)	Regression Analysis Parameters	
	R = 0 , Sy < 50 ksi	log C	m
1Q	----	----	----
1H	39.3	2.262	0.111
1.All	38.2	2.097	0.086
1M	36.2	2.246	0.115
8	35.4	1.899	0.058
2	35	1.795	0.042
10Q	----	----	----
10(G)	31.6	2.185	0.114
3(G)	31	2.45	0.16
1(F)	30.5	1.814	0.055
21(S)	30.5	2.53	0.174
10A	29.7	2.084	0.102
25A	29.6	2.229	0.126
3	29.2	2.214	0.125
13	28.5	3.182	0.288
28	28.1	1.709	0.044
12(G)	27.2	2.495	0.177
10H	25.8	2.199	0.131
4	25.7	1.698	0.048
6	25.7	1.698	0.048
9	25.5	1.668	0.044
10M	24.5	2.123	0.122
16(G)	24.5	2.243	0.142
25	24.5	1.919	0.088
7(B)	24.4	2.347	0.16
30A	23	3.143	0.297
26	23	1.79	0.072
14	22.9	2.025	0.111
11	22.1	2.246	0.15
21	21.8	1.714	0.063
7(P)	----	----	----
18(S)	21	1.98	0.11
33(S)	20.7	2.25	0.156
36	20	2.175	0.144
25B	20	2.175	0.144
12	19.7	2.658	0.227
17(S)	19.6	1.919	0.105
17A(S)	19.6	1.919	0.105
16	19.6	2.688	0.232
22	19.4	2.912	0.271
21(3/8")	17.9	1.622	0.062
20	17.5	2.511	0.211
20(S)	17.3	1.756	0.087
23	----	----	----
24	----	----	----
19	----	----	----
30	16.7	3.126	0.317
38	16	2.938	0.289
17A	15.8	2.536	0.223
31A	----	----	----
19(S)	15.4	2.138	0.158
17	14.6	2.824	0.277
18	14.5	2.202	0.173
32A	14.1	2.579	0.238
27	13.5	2.254	0.188
38(S)	13.5	1.6	0.078
33	12.9	2.539	0.238
46	----	----	----
40	----	----	----
32B	----	----	----

Table A-2
Mean Fatigue Strength and Standard Deviation for SSC-318 Weldments Using only R=0 and S_y<50ksi Data

SSC - 318 Weldment Details	Mean Fatigue Strength (ΔS) at 1E+06 Cycles (ksi)				Standard Deviation of Log ΔS (ksi units)		Kf	Fatigue Crack Initiation Sites
	SSC - 318	All R , All Sy	R = 0	R = 0 , Sy < 50 ksi	R = 0	R = 0 , Sy < 50 ksi		
1Q	51	51.8	51	----	0.074	----	1.43*	----
1H	48.5	48.2	45.6	39.3	0.06	0.04	1.43*	----
1.All	46.5	44.9	42.1	38.2	0.104	0.042	1.43*	----
1M	38.3	37.1	36.2	36.2	0.04	0.04	1.43*	----
8	39.2	39.8	39.1	35.4	0.094	0.079	1.54	----
2	42	42.1	41	35	0.076	0.017	1.43*	----
10(G)	36.1	35.2	32.8	31.6	0.136	0.127	1.82	Weld
10Q	31.2	31.5	32.7	----	0.114	----	1.84	Toe
3(G)	31.3	31.2	31	31	0.084	0.081	1.94	Weld
1(F)	41.5	38.4	38.4	30.5	0.117	0.057	1.43*	----
10A	30.9	31.1	28.8	29.7	0.115	0.066	2.04	Toe
25A	38.1	35.8	29.3	29.6	0.109	0.12	2.05	Toe
3	30.3	29	29.1	29.2	0.049	0.044	2.07	Ripple
13	28	27.8	27.3	28.5	0.055	0.057	2.15	Toe
28	29.8	29.8	28.4	28.1	0.097	0.045	2.11	----
12(G)	27.2	27.2	27.2	27.2	0.072	0.072	2.16	Weld
10H	34	35.2	33.1	25.8	0.102	0.101	1.84	Toe
4	28.3	27.3	26.8	25.7	0.092	0.095	2.19	Ripple
6	28.3	27.3	26.8	25.7	0.092	0.095	2.19	Ripple
9	25.7	25.7	25.8	25.5	0.079	0.085	2.33	----
10M	25.2	26.4	24.5	24.5	0.093	0.093	2.46	Toe
16(G)	23.6	22.7	24.5	24.5	0.215	0.215	2.46	Root
25	24	24.1	23.9	24.5	0.09	0.08	2.52	Toe
7(B)	24.3	23.8	23.8	24.4	0.083	0.11	2.46	Toe or D. T.**
19	17	23.2	23.1	----	0.157	----	2.61	Toe
30A	23	23	23	23	0.014	0.014	2.62	D. T.
26	17.1	17.4	23	23	0.054	0.054	2.62	Toe
14	29.8	25.9	22.9	22.9	0.115	0.109	2.63	Toe
11	22.3	22.7	22.7	22.1	0.078	0.08	2.58	Toe
21	21.8	21.8	21.8	21.8	0.117	0.117	2.69	Toe
7(P)	20.4	21.5	21.5	----	0.075	----	2.73	Toe or D. T.
36	20.6	20	20	20	0.062	0.062	3.01	D. T.
25B	20.6	20	20	20	0.062	0.062	2.93	Toe or D. T.
12	19.6	19.7	19.7	19.7	0.055	0.055	2.98	Toe
16	19.9	19.6	19.6	19.6	0.104	0.104	3.07	Toe or Root
22	19.2	19.1	19.5	19.4	0.045	0.044	3.01	Toe
21(3/8")	18.1	17.9	17.9	17.9	0.037	0.037	3.28	Toe
20	16.1	17.5	17.5	17.5	0.099	0.099	3.44	Toe
23	17.2	18.3	----	----	----	----	----	Toe
24	17.2	18.3	----	----	----	----	----	Toe
30	16.7	16.7	16.7	16.7	0.051	0.051	3.6	D. T.
38	16	16	16	16	0.058	0.058	3.66	Toe
17A	15.6	16.2	15.8	15.8	0.051	0.051	3.81	D. T.
17	15	14.6	14.6	14.6	0.046	0.046	4.26	D. T.
18	11.5	12.2	12.8	14.5	0.107	0.148	4.7	D. T.
32A	14.1	14.1	14.1	14.1	0.055	0.055	4.16	D. T.
27	12	12.8	13.5	13.5	0.101	0.101	4.46	----
33	11.4	11.6	12.9	12.9	0.055	0.055	4.67	Toe at C.T. or D. T.**
31A	15.7	15.6	15.8	----	0.12	----	3.71	Toe
46	11.9	11.9	----	----	----	----	----	D.T.
40	11.2	11.2	----	----	----	----	----	Toe and D. T.
32B	11.2	11.2	----	----	----	----	----	Toe and D. T.

*Plain Plate
* C. T. - Continuous Termination , D. T. - Discontinuous Termination

Table A-3
Mean Fatigue Strength and Standard Deviation for SSC-318 Weldments Loaded in Shear Using only R=0 and Sy<50KSI Data

SSC - 318 Weldment Details	Mean Fatigue Strength (ΔS) at 1E+06 Cycles (ksi)				Standard Deviation of Log ΔS (ksi units)		Kf	Fatigue Crack Initiation Sites
	SSC - 318	All R , All Sy	R = 0	R = 0 , Sy < 50 ksi	R = 0	R = 0 , Sy < 50 ksi		
21(S)	31	31	30.5	30.5	0.031	0.031	1.97	Toe
18(S)	20	20	21	21	0.042	0.042	2.87	Toe and D. T.
33(S)	20.5	20.5	20.7	20.7	0.06	0.06	2.91	Toe
17(S)	21	21	19.6	19.6	0.041	0.041	3.07	Toe
17A(S)	21	21	19.6	19.6	0.041	0.041	3.07	Toe
20(S)	19.6	21.2	16.9	17.3	0.159	0.168	3.56	Toe
19(S)	20.3	18.2	15.4	15.4	0.124	0.124	3.91	Toe
38(S)	13	13.3	13.5	13.5	0.113	0.113	4.46	Toe

Table A-4
Average Standard Deviation for SSC-318 Weldments
Calculated Using Various Editing Conditions

Condition	Mean of s	Standard Deviation of s
All R , All Sy	0.092	0.036
R = 0	0.08	0.033
R = 0 , Sy < 50 ksi	0.077	0.034
R = 0 , Sy < 50 ksi , n > 8	0.08	0.035

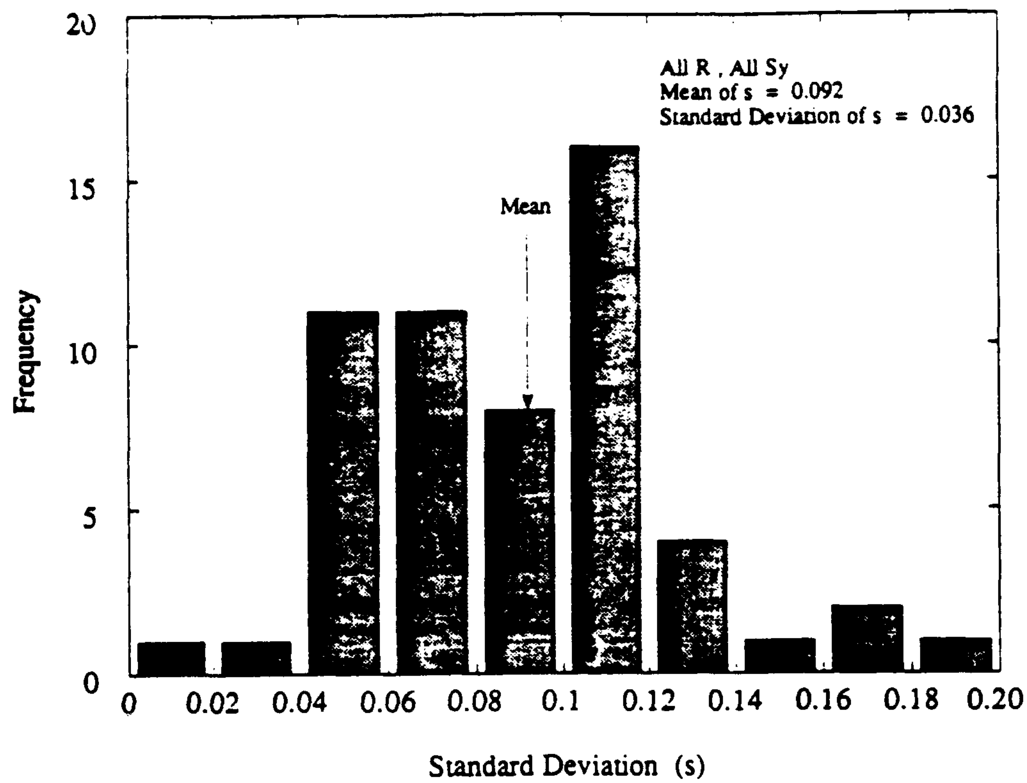

Fig. A-1 Histogram of standard deviations on the log of fatigue strength for all R ratios and all values of base metal yield strength

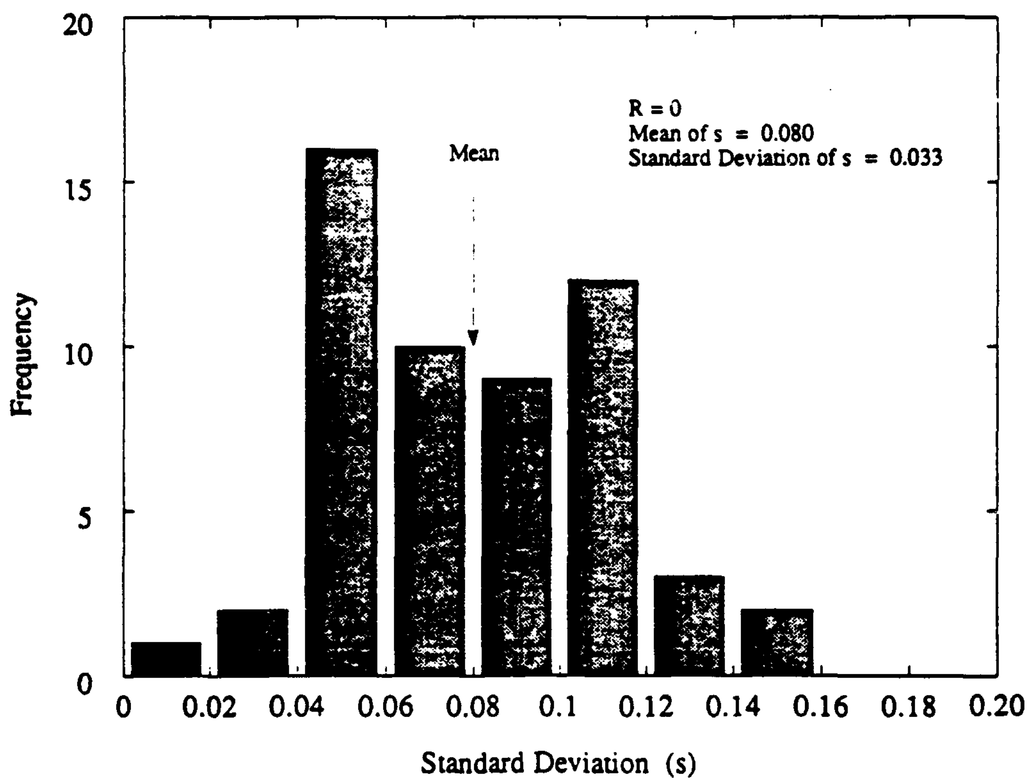

Fig. A-2 Histogram of standard deviation in the log of fatigue strength for R=0 and all values of base metal yield strength

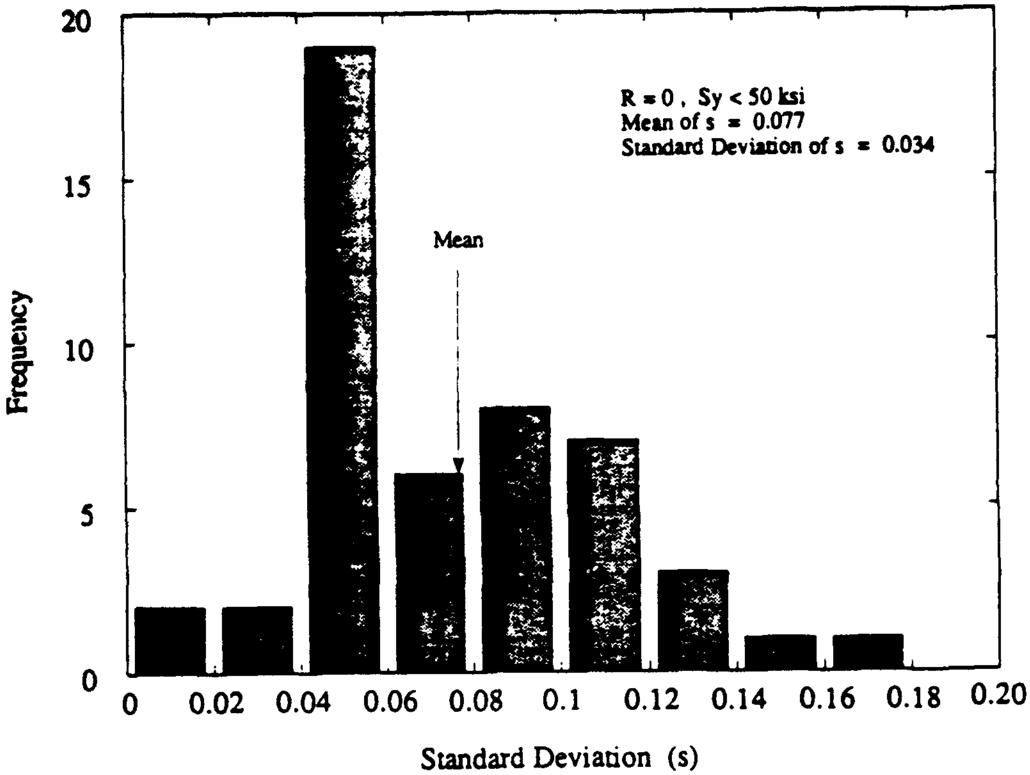

Fig. A-3 Histogram of standard deviation in the log of fatigue strength for R=0 and all values of base metal yield strength

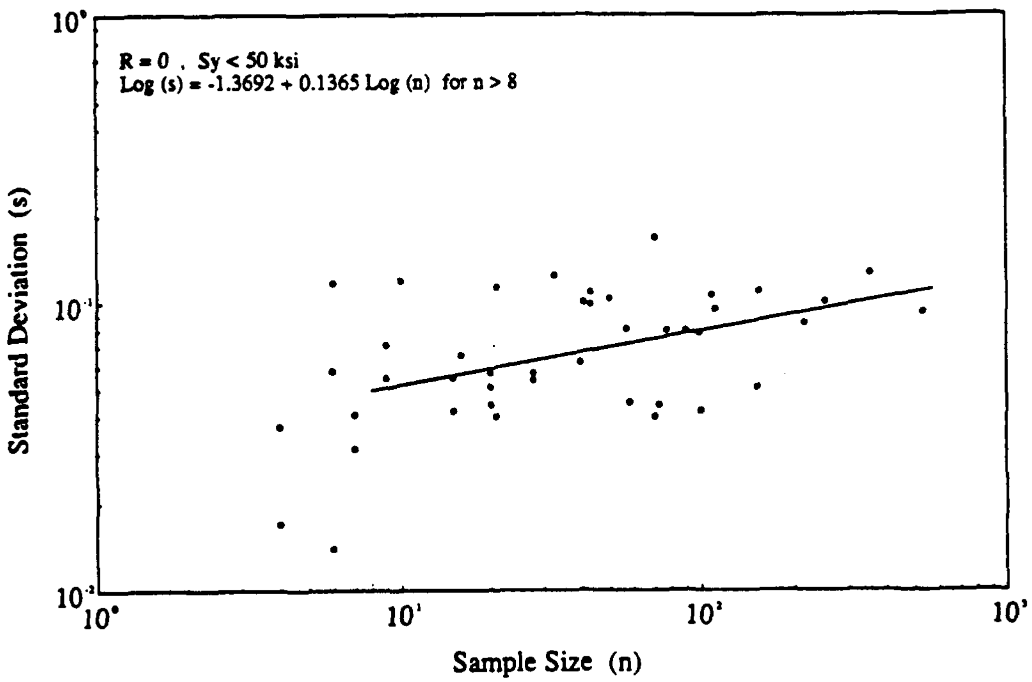

Fig. A-4 Variation in standard deviation in the log of fatigue strength with sample size

Table A-5
Design Fatigue Strength for SSC-318 Weldments Estimated Using the Average Standard Deviation in the Log in Fatigue Strength

SSC - 318 Weldment Details	Fatigue Strength (ksi)			Weldment Category	Category Shift
	Mean Fatigue Strength (ΔS) at 1E+06 Cycles		Design Fatigue Strength $\Delta Sd = 10^{(\log\Delta S - 2*0.08)}$		
	All R , All Sy	R = 0 , Sy < 50 ksi	R = 0 , Sy < 50 ksi		
1Q	51.8	----	----		
1H	48.2	39.3	26.8		
1.All	44.9	38.2	26.1	A	
1M	37.1	36.2	24.7		
8	39.8	35.4	24.2		
2	42.1	35	23.9		
10Q	31.5	----	----		
10(G)	35.2	31.6	21.6		
3(G)	31.2	31	21.2		
1(F)	38.4	30.5	20.8		-1
21(S)	31	30.5	20.8	B	
10A	31.1	29.7	20.3		
25A	35.8	29.6	20.2		-1
3	29	29.2	19.9		
13	27.8	28.5	19.4		1
28	29.8	28.1	19.2		
12(G)	27.2	27.2	18.6		
10H	35.2	25.8	17.6		-1
4	27.3	25.7	17.5		
6	27.3	25.7	17.5		
9	25.7	25.5	17.4	C	
10M	26.4	24.5	16.7		
16(G)	22.7	24.5	16.7		1
25	24.1	24.5	16.7		1
7(B)	23.8	24.4	16.6		1
30A	23	23	15.7		
26	17.4	23	15.7		1
14	25.9	22.9	15.6		-1
11	22.7	22.1	15.1	D	
21	21.8	21.8	14.9		
7(P)	21.5	----	----		
18(S)	20	21	14.3		
33(S)	20.5	20.7	14.1		
36	20	20	13.6		
25B	20	20	13.6		
12	19.7	19.7	13.4		
17(S)	21	19.6	13.4	D	
17A(S)	21	19.6	13.4		
16	19.6	19.6	13.4		
22	19.1	19.4	13.2		
21(3/8")	17.9	17.9	12.2		
20	17.5	17.5	11.9		1
20(S)	21.2	17.3	11.8		
23	18.3	----	----	E	
24	18.3	----	----		
19	23.2	----	----		1
30	16.7	16.7	11.4		
38	16	16	10.9		
17A	16.2	15.8	10.8		
31A	15.6	----	----		
19(S)	18.2	15.4	10.5	F	
17	14.6	14.6	10		
18	12.2	14.5	9.9		1
32A	14.1	14.1	9.6		
27	12.8	13.5	9.2		
38(S)	13.3	13.5	9.2		
33	11.6	12.9	8.8	G	
46	11.9	----	----		
40	11.2	----	----		
32B	11.2	----	----		

1 Detail shifts from lower one category to a higher one category according to new categorization.
-1 Detail shifts from a higher one category to a lower one category according to new categorization.

Using the mean fatigue strength at 10^6 cycles of each detail less two (average) standard deviations, the 53 details were ranked and arranged in the weld categories A through G which have the stress range boundaries suggested by Stambaugh (A-4) (see Table A-5).

Thus we have demonstrateu (1) that weldment fatigue data bases should be edited to include only standard values of R ratios, material strength, and weldment size and (2) that appropriate design values for other R ratios, strengths, and weldment sizes can be analytically estimated from this standard data.

A-2 PROCEDURES AND RESULTS

A-2.1 Data Analysis Procedures

The least-squares method was used to generate new S-N curves for each of the 53 details using only R=0 and S_y<50ksi test data. The regression line is:

$$\log C = m\log\Delta S - \log N \tag{1}$$

where:

N	=	Fatigue life
ΔS	=	Stress range
C, m	=	Regression constants

Values of log C and m obtained for each detail are listed in Table A-1. The standard deviations of the regression lines (based on log of the stress range or fatigue strength) were also calculated:

$$s^2 = \frac{\sum_{i=1}^{n} [\log\Delta S_i - (\log C - m\log N_1)]^2}{n-2} \tag{2}$$

where:

n = Sample size

s = Standard deviation in the Log of the stress range or fatigue strength

The calculated standard deviation for each detail is listed in Tables A-2 and A-3 together with their mean fatigue strength at 10^6 cycles. The fatigue notch factor K_f for each detail was estimated from UIUC fatigue data bank information in the following manner. At a given fatigue life, the fatigue notch factor K_f is defined as:

$$K_f' = \frac{\Delta S smooth\ specimen}{\Delta S weldment} \tag{3}$$

From the work of Chang (A-5), the ratio of mean fatigue strength at 10^6 cycles of smooth specimen to that of plain plate is 1.43. Therefore, the K_f can be written as:

$$K_f = 1.43 \frac{\Delta S plain\ plate}{\Delta S weldment} \tag{4}$$

$$K_f = 1.43 \frac{\Delta S plain\ plate}{\Delta S weldment} \qquad at\ 10^6\ cycles\ and\ for\ R=0 \tag{5}$$

Values of ΔS plane plate and ΔS weldment were taken from the UIUC data bank at a life of 10^6 cycles to obtain the K_f values listed for each detail in Tables A-2 and A-3.

A-3 DISCUSSION

A-3.1 Mean Fatigue Strength

Tables A-2 and A-3 give calculated mean fatigue strength at 10^6 cycles (ΔS). The values calculated in this study based on R=0 and S_y<50ksi are entered in bold type. For comparison, other values of mean fatigue strength are listed including the actual values listed in SSC-318, based on all R ratios and all material strengths. The comparison also includes values for all strengths and R=0. The values for all R ratios and all strength values more-or-less reproduce the values given in SSC-318. However, restricting the data base both in terms of R ratio and material strength leads to quite different values of ΔS. The difference between these values is generally least for details with the lowest fatigue strengths.

A-3.2 Fatigue Notch Factor K_f and Crack Initiation Sites

For each detail, the fatigue notch factor and the fatigue crack initiation sites are listed in Tables A-2 and A-3. The fatigue crack initiation sites have been grouped into four main categories: weld bead ripple, weld toes, continuous weld terminations (wrap-around welds), and discontinuous terminations (stops). Details in which cracks initiate at the weld ripple have the lowest values of K_f. Details in which fatigue cracks initiate at weld toes and discontinuous terminations (stops) have the highest value of K_f.

A-3.3 Relationship Between Standard Deviation and Weldment Notch Severity

Figures A-1 to A-3 are histograms of the standard deviation of the log ΔS (s) of the 53 details with different conditions of data base editing. Fewer details were considered because some, such as 16(G), contained a partial penetration of unknown and presumably variable dimensions. Others were eliminated because they contained only high strength data (1Q, 10Q, 23, 24, 31A) or because we could not reproduce the SSC-318 data set (19, 7P) or because there was an absence of data in their data sets (46, 40, 32B). Also, as seen in Figure A-5, the standard deviation(s) is a function of sample size. Sample sizes less than 8 were considered unreliable and were excluded from consideration in Figures A-1 - A-3. The histogram of $s_{R=0,}$ S_y<50ksi (Figure A-4) has less scatter than other conditions and the smallest mean value (see Table A-4).

Figure A-5's values of $s_{R=0}$, S_y<50ksi for SSC-318 details are plotted as a function of their fatigue notch factor K_f. It seems that there is no correlation between $s_{R=0}$, S_y<50ksi K_f or the nature of the discontinuity initiating the fatigue failure. The COV of fatigue life at a given stress level reported in SSC-318 for each of the 53 details is plotted as a function of K_f in Figure A-6. Figure A-6 also suggests that the uncertainty in fatigue life is not a strong function of K_f.

It is possible that the results shown in Figure A-5 indicate that details with terminations have lesser values of $s_{R=0}$, S_y<50ksi. The $s_{R=0,}$ S_y<50ksi, however, seemed not to be a strong function of K_f or fatigue crack initiation site, but rather of sample size. A t-test was performed to see whether the weld terminations have less values or standard deviation than those of other crack initiation sites. The results indicate that there is no correlation between standard deviation and weld terminations. Therefore, the average value of $s_{R=0}$, S_y<50ksi = 0.083 is recommended for all detail categories. Future research should be conducted in this important area.

A-3.4 New Ranking of Weldments by Categories

The mean value of standard deviations of $s_{R=0}$, S_y<50ksi for sample size n > 8 was calculated to be 0.083. This value was used to calculate the design mean fatigue strength ΔS_d at a fatigue life 10^6 cycles. The ΔS_d is defined as:

$$\Delta S_d = 10^{\log \Delta s - (2 \times 0.083)} \quad \textit{at a fatigue life } 10^6 \textit{ cycles} \tag{6}$$

Using the mean fatigue strength at 10^6 cycles of each detail less two (average) standard deviations, the 53 details were ranked and arranged in the weld categories A through G which have the stress range boundaries following the ECCS model (A-4) (see Table A-5). If a detail's weldment category changed after the data base was edited, the shift is indicated in a column in Table A-5 as either +1 or -1.

A-3.5 Design Strengths for Load Ratios other than R=0

From Basquin's Law, Yung and Lawrence (A-6) propose an equation to calculate the mean fatigue strength of weldments at long lives:

$$\Delta S = \frac{(\sigma_f' - \sigma_r)\ (2N)^b}{K_f\ (1 + \frac{1+R}{1-R}(2N)^b)} \tag{7}$$

where:

σ_f' = Fatigue strength coefficient
σ_r = Residual stress
b = Fatigue strength exponent

For a certain weldment, when R=0 Eq. 7 can be written as:

$$\Delta S_{R=0} = \frac{(\sigma_f' - \sigma_r)\ (2N)^b}{K_f\ (1+(2N)^b)} \tag{8}$$

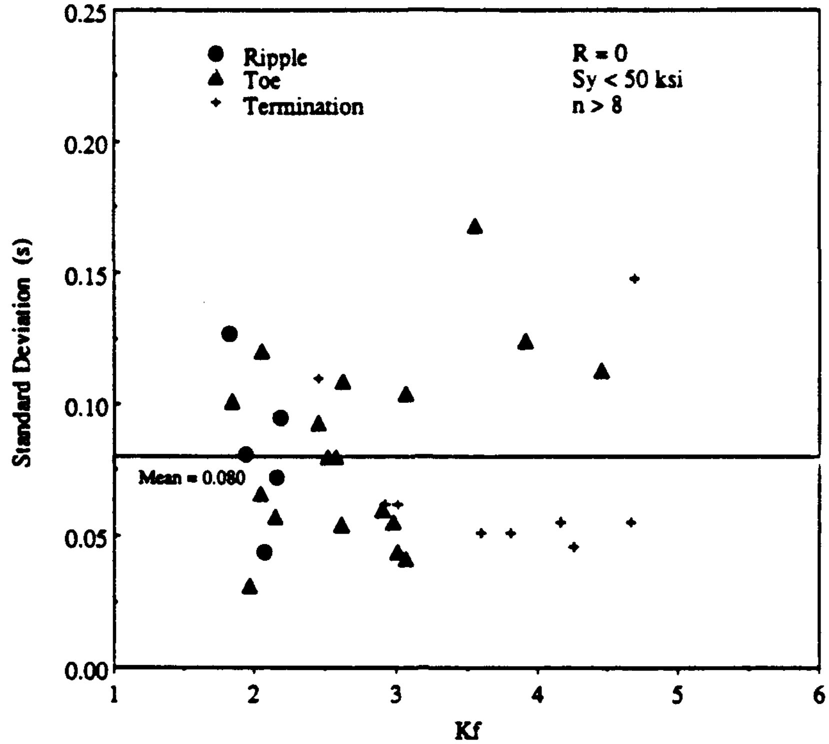

Fig. A-5 Variation in standard deviations in the Log of fatigue strength with K_f

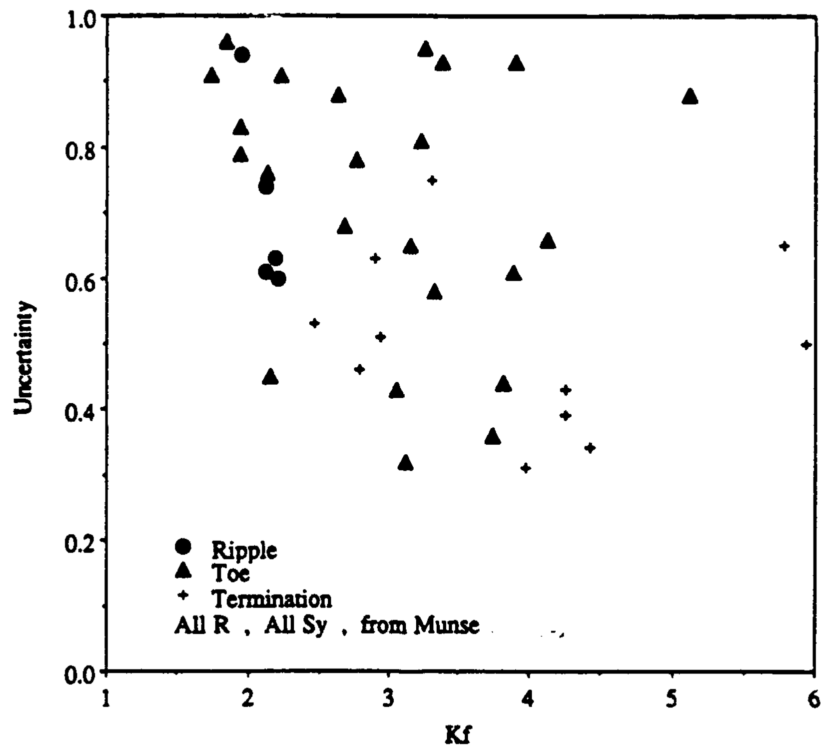

Fig. A-6 Variation in standard deviation in the log of fatigue life with K_f

Dividing Eq. 7 by Eq. 8, the ratio of the mean fatigue strength ratio at any R value to R=0 is:

$$\frac{\Delta S_R}{\Delta S_{R=0}} = \frac{1+(2N)^b}{1+\frac{1+R}{1-R}(2N)^b} \tag{9}$$

Based on Eq. 9, we can predict the fatigue strength at any R value at 10^6 cycles by the mean fatigue strength of R=0 at fatigue life 10^6 cycles. Eq. 11 was used to predict the allowable stress ranges of different R ratios at 10^6 cycles based on the ΔS of R=0. Fatigue strength exponent b is estimated by:

$$b = -\frac{1}{6}\ log2\ (1 + \frac{50}{1.5S_u}) \tag{10}$$

where S_u is the ultimate strength of base metal. A value of 80 ksi was used as a rough value of S_u.

The predicted results for R=-1 and R=0.5 are shown in Figures A-7 and A-8. The predicted mean stress ranges for R=-1 and R=0.5 are in good agreement with the values of the UIUC fatigue data bank; therefore, fatigue data banks based on R=0 information can be used to predict behavior at other R ratios.

A-4 SUMMARY OF FINDINGS

Editing the UIUC data base to include only R=0 and S_y<50ksi reduced the scatter in the mean fatigue strength at 10^6 cycles for the 53 details of SSC-318.

The standard deviations of the log of fatigue strength at 10^6 cycles did not correlate with weldment severity nor with the type of fatigue initiating notch. The standard deviations of the log of fatigue strength at 10^6 did vary with sample size. Sample sizes of less than 8 were not considered. An average standard deviation was estimated from the results for selected weldments.

The design fatigue strength at 10^6 cycles was estimated using mean fatigue strength at 10^6 cycles for a given detail minus two (average) standard deviations.

The mean fatigue strength at 10^6 cycles at other R ratios can be analytically estimated from UIUC data bank values at R=0 and an analytical model based on the theories of fatigue crack initiations. The resulting S-N curves for each detail are presented in Figures A-9 through A-65.

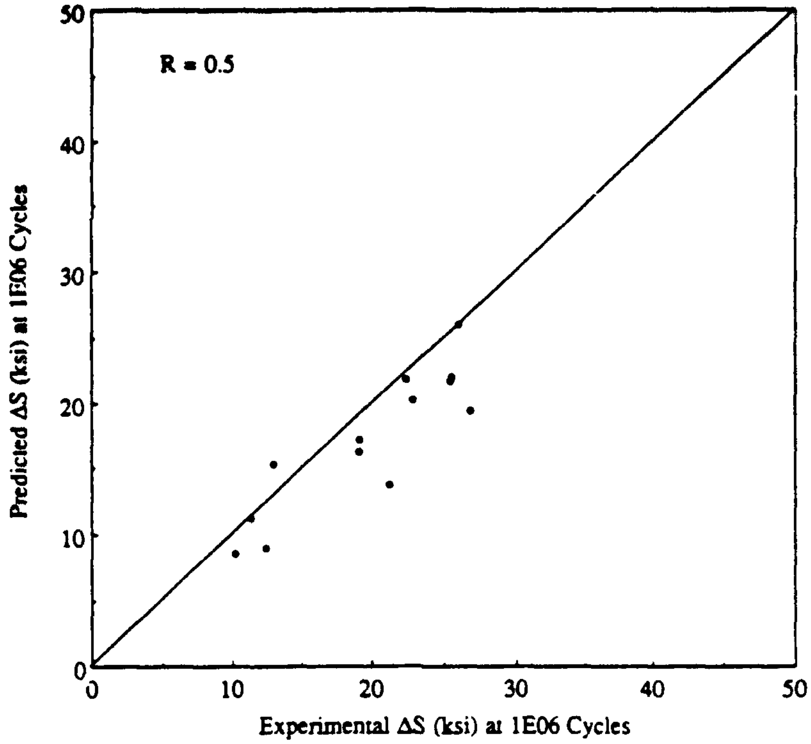

Fig. A-7 Predicted and estimated mean fatigue strength at 10^6 cycles for R=0.5

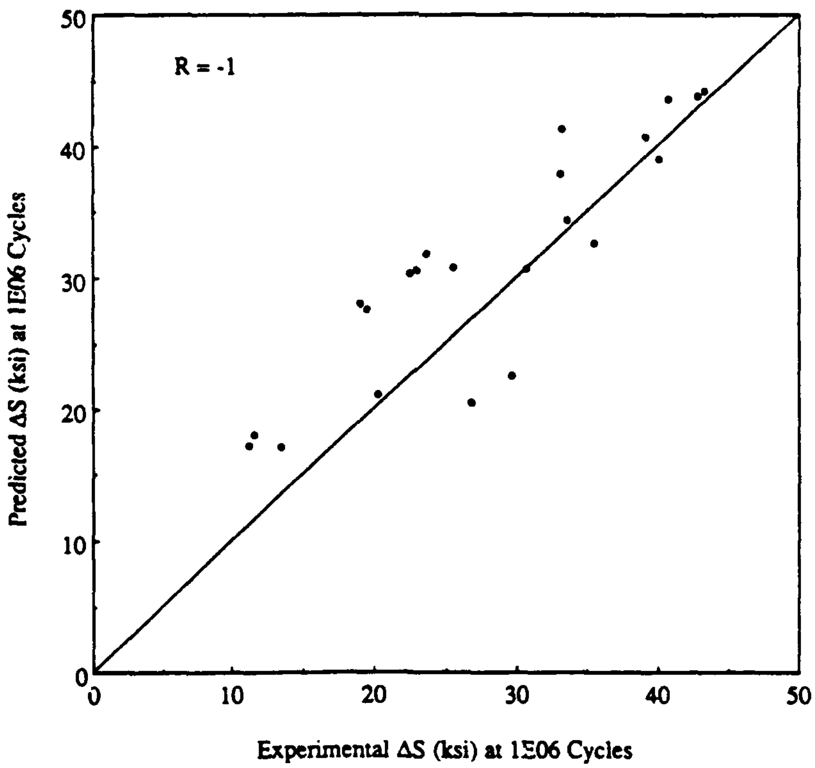

Fig. A-8 Predicted and estimated mean fatigue strength at 10^6 cycles for R=-1

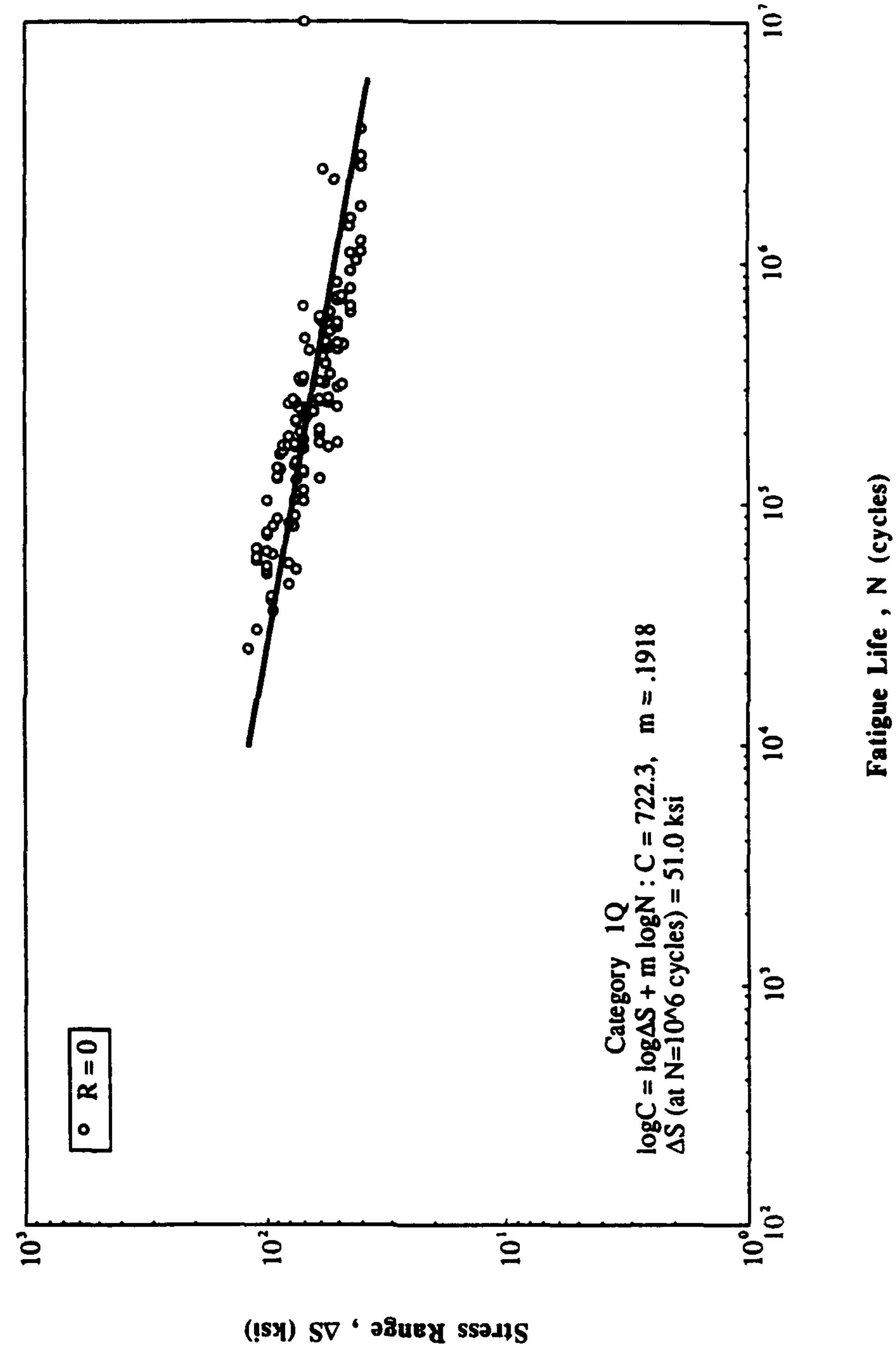

Fig. A-9 Detail Category 1Q

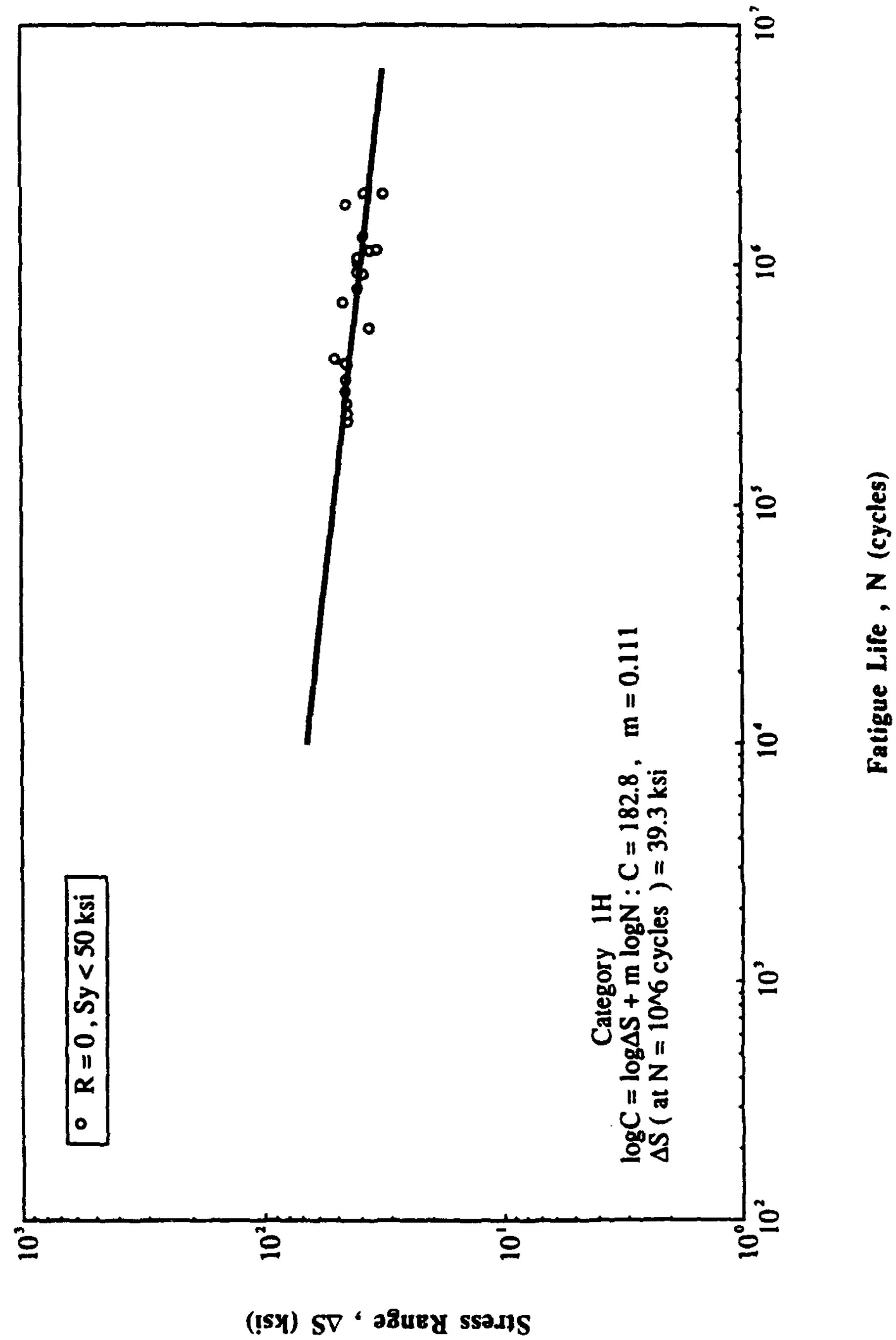

Fig. A-10 Detail Category 1H

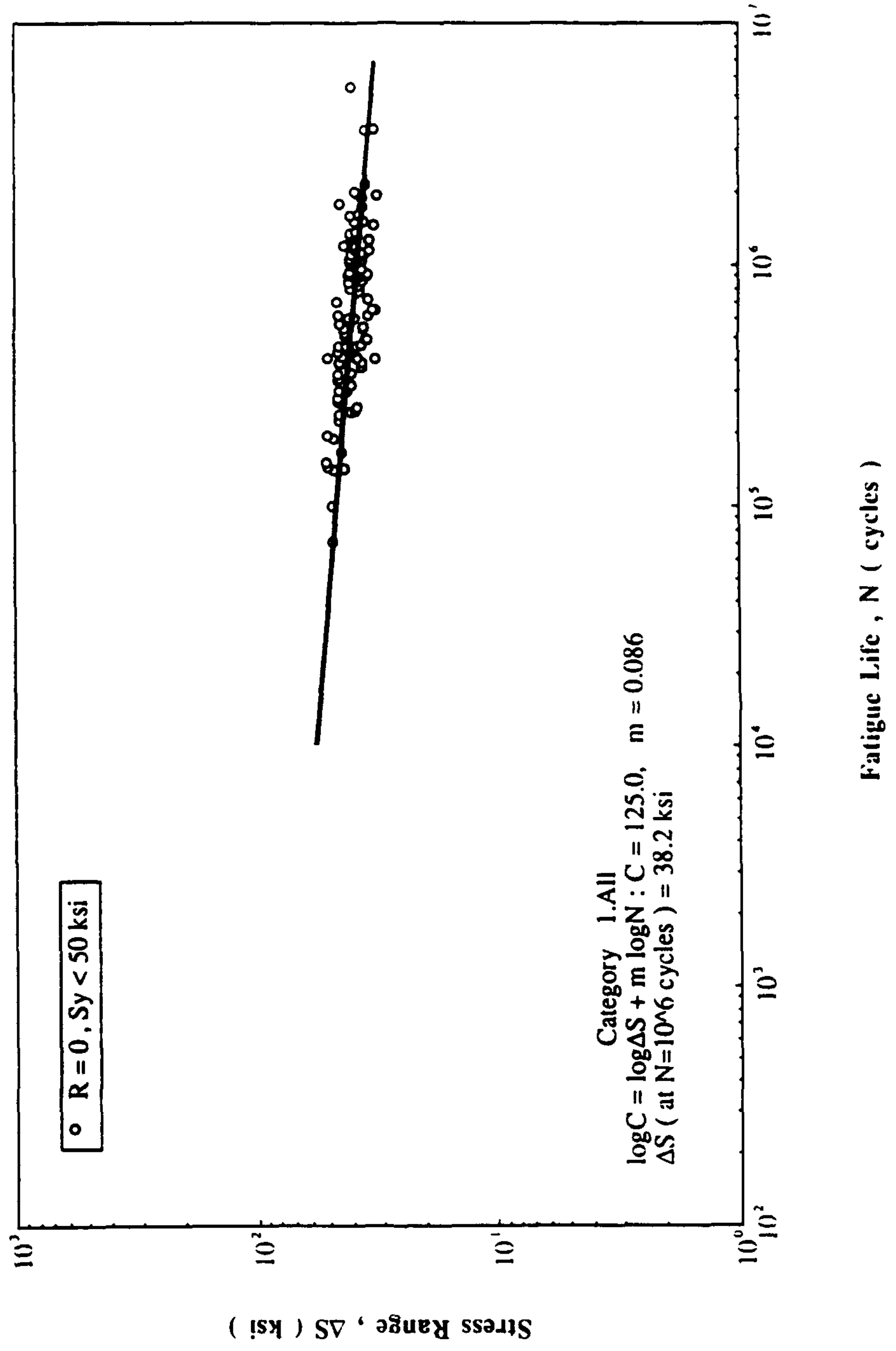

Fig. A-11 Detail Category 1.All

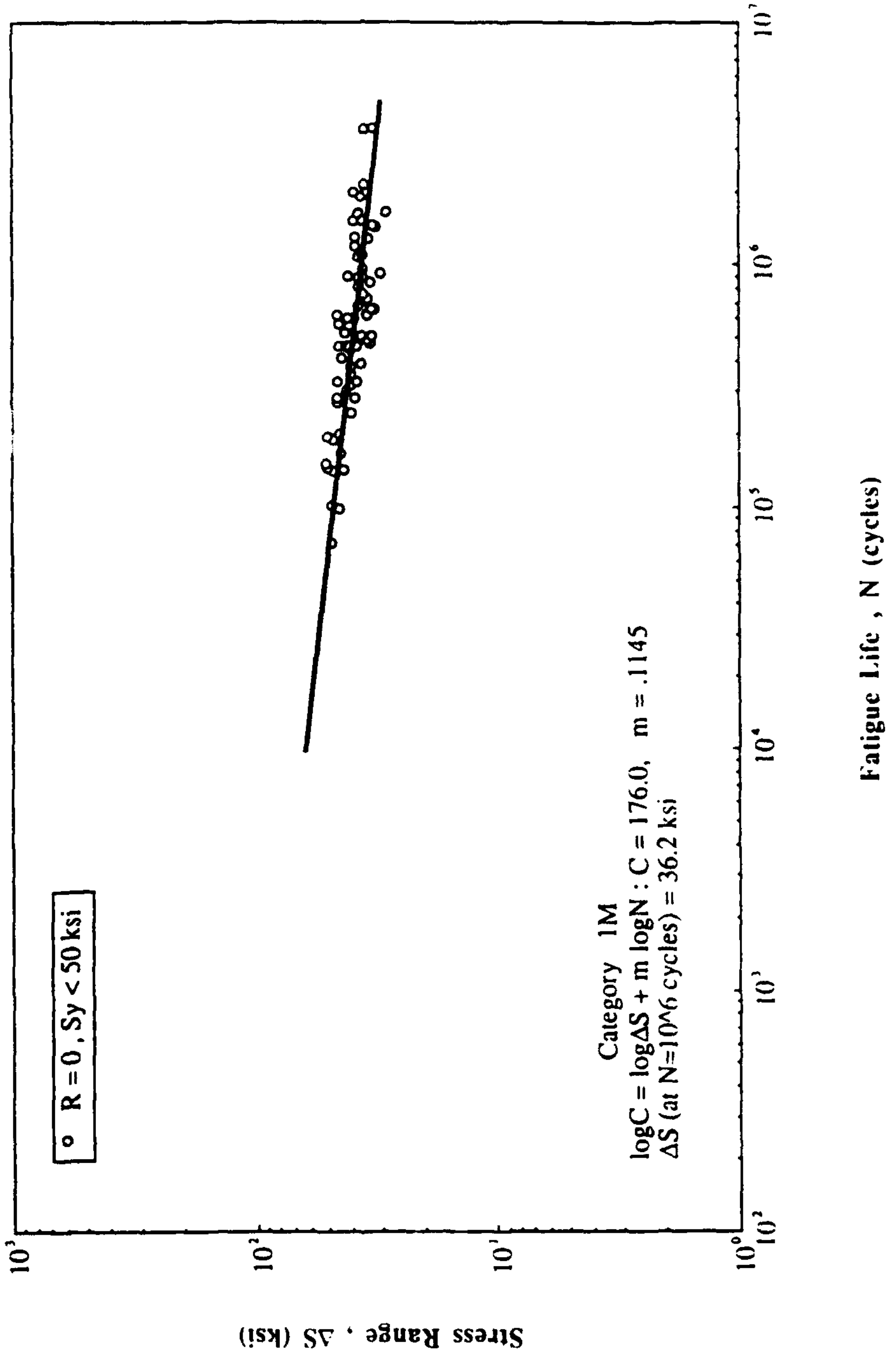

Fig. A-12 Detail Category 1M

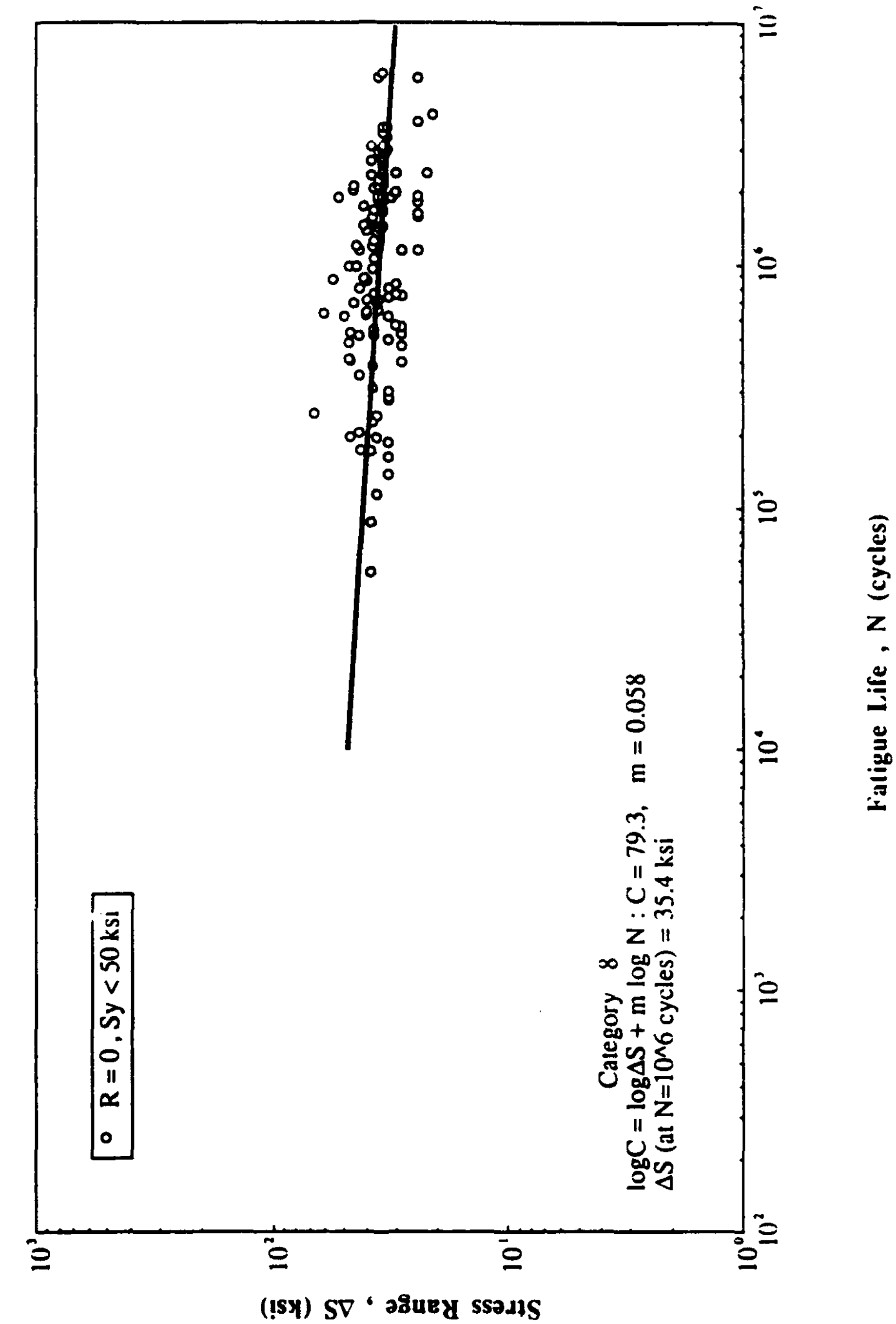

Fig. A-13 Detail Category 8

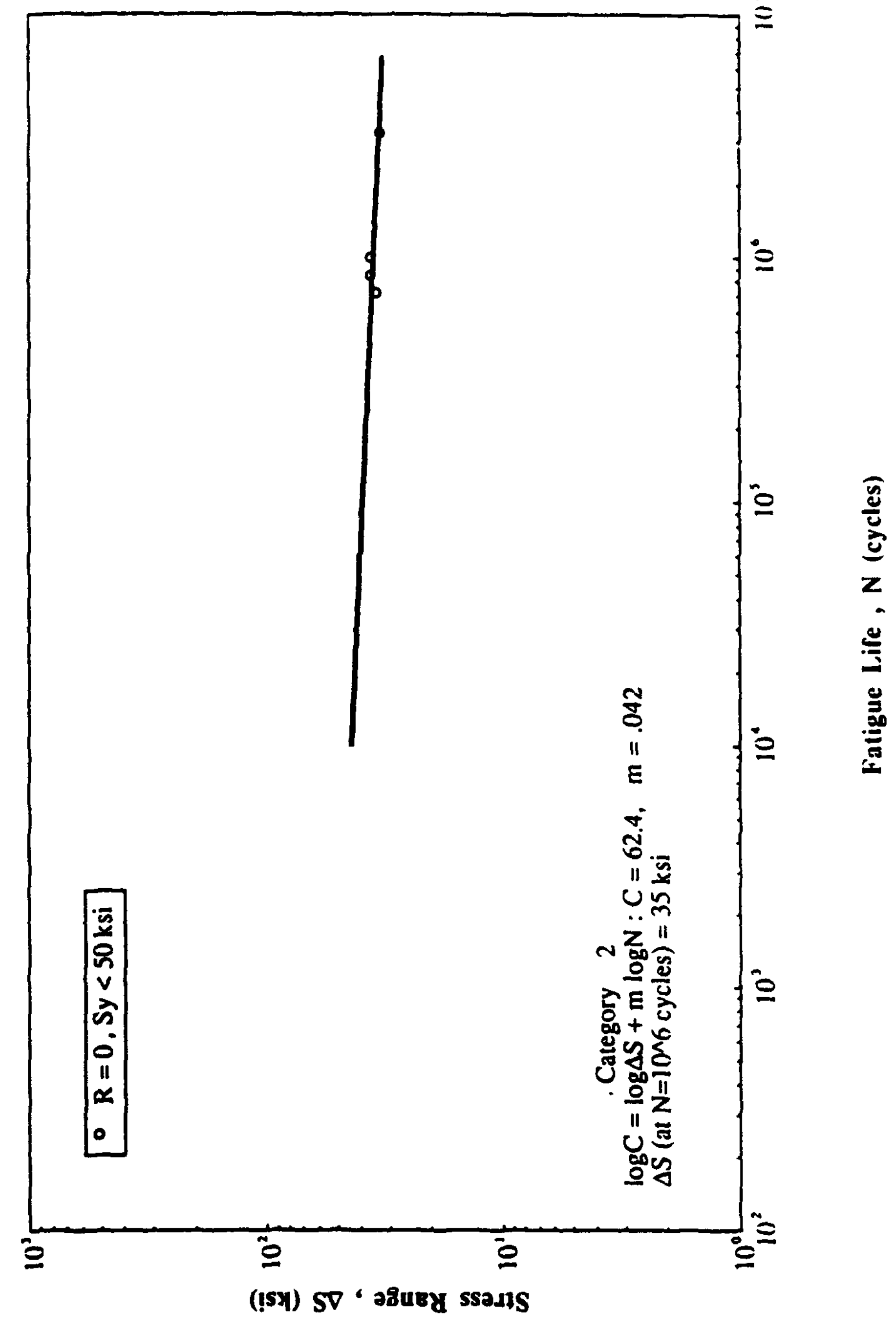

Fig. A-14 Detail Category 2

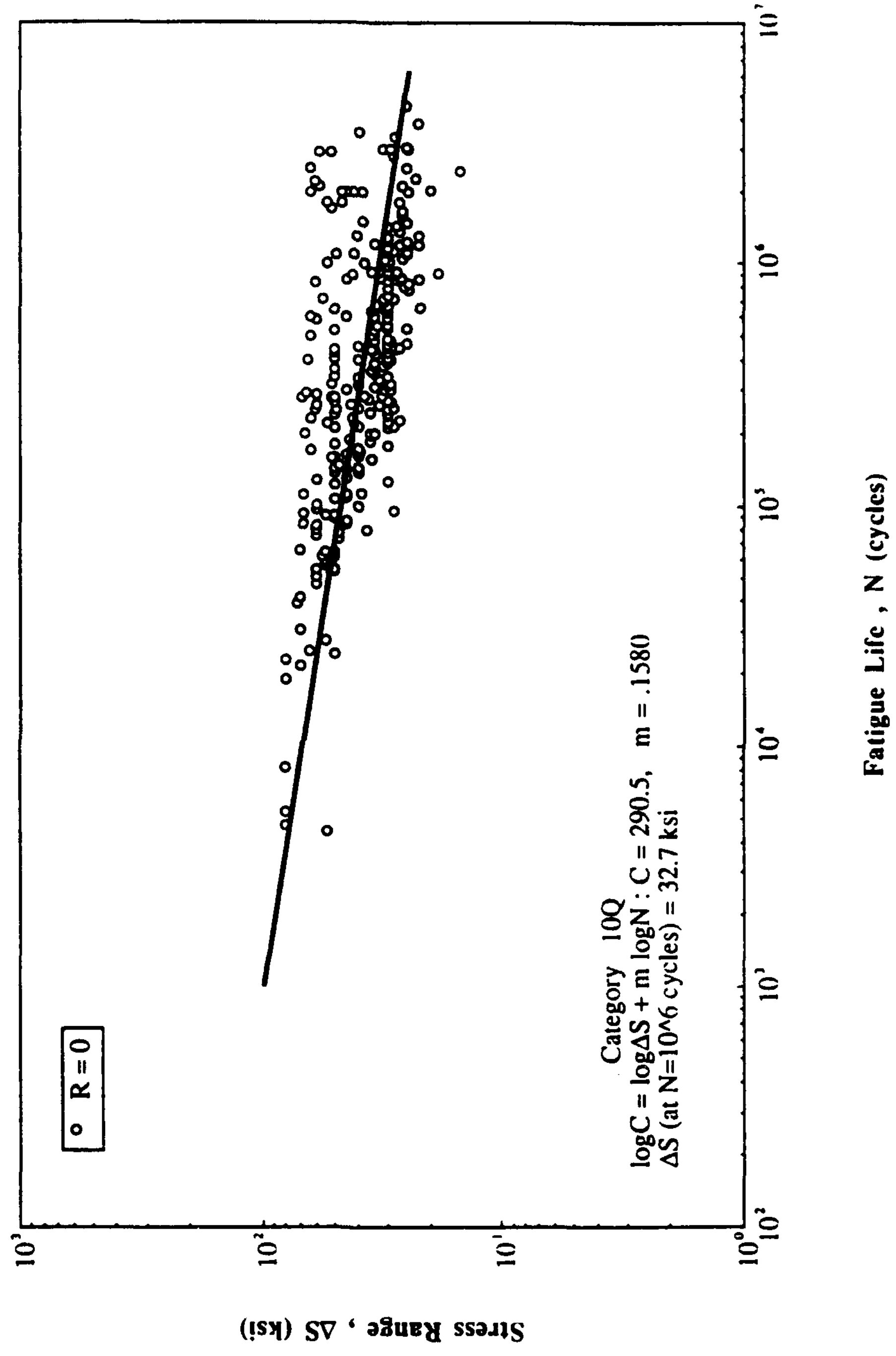

Fig. A-15 Detail Category 10Q

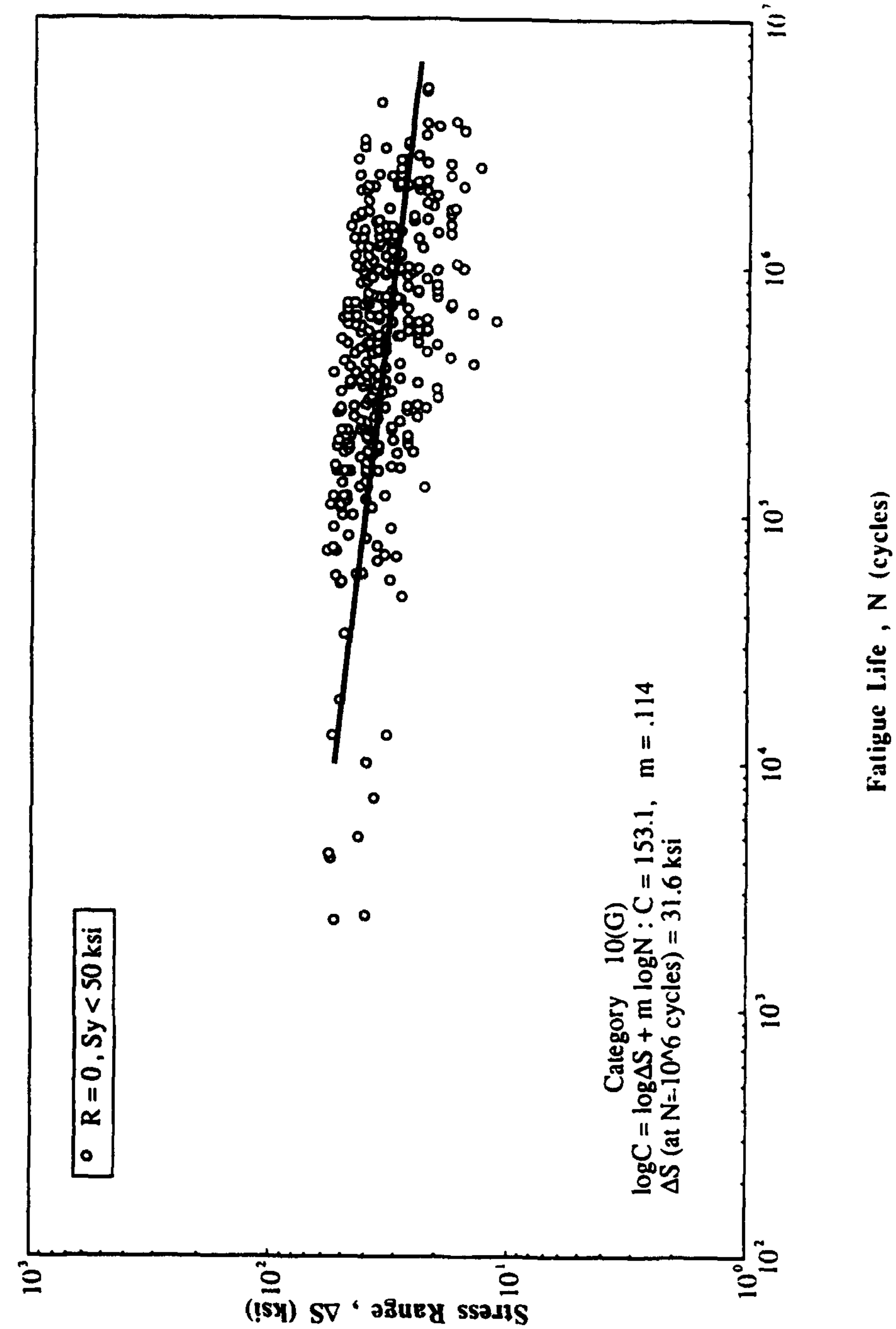

Fig. A-16 Detail Category 10(G)

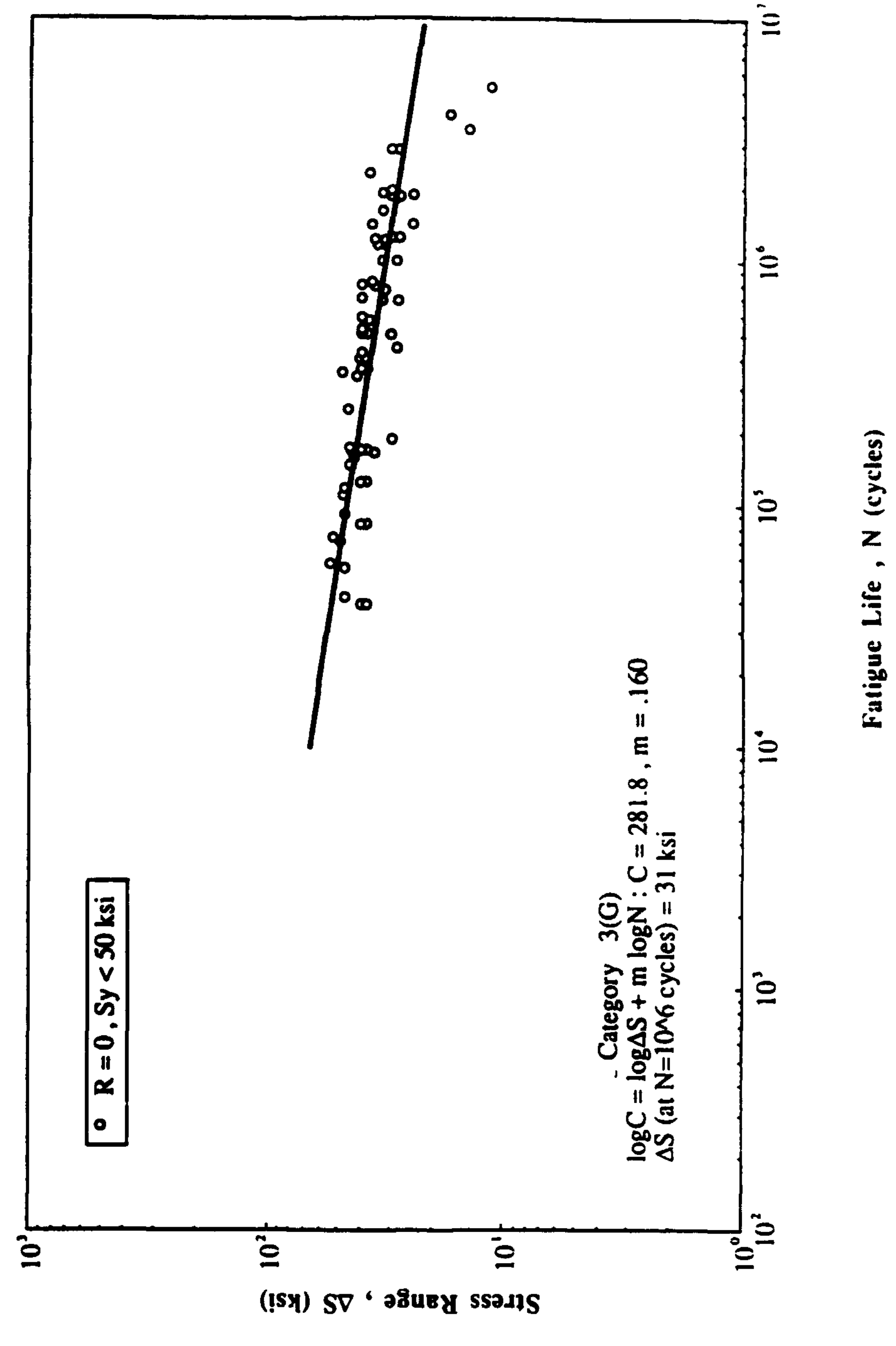

Fig. A-17 Detail Category 3(G)

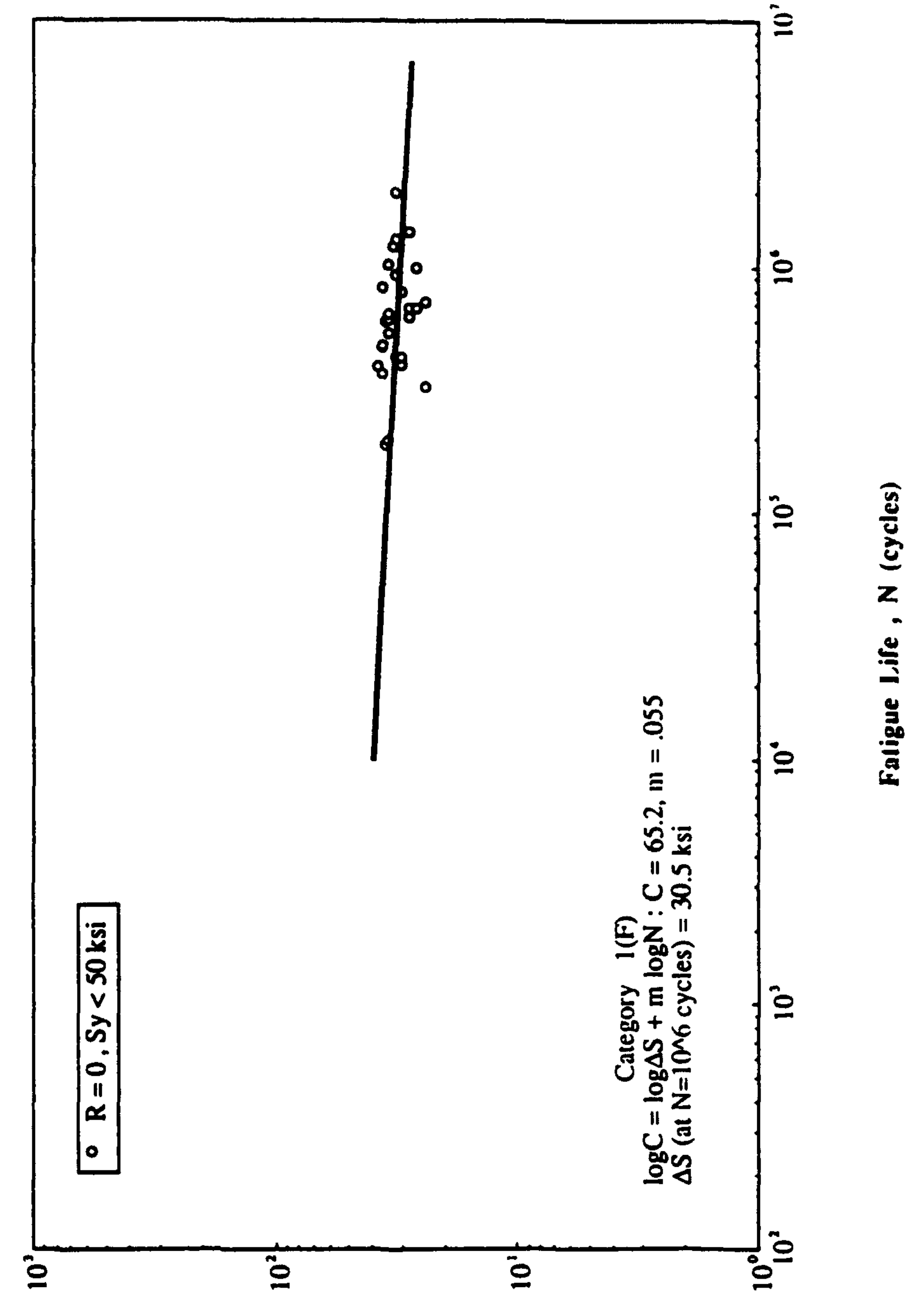

Fig. A-18 Detail Category 1(F)

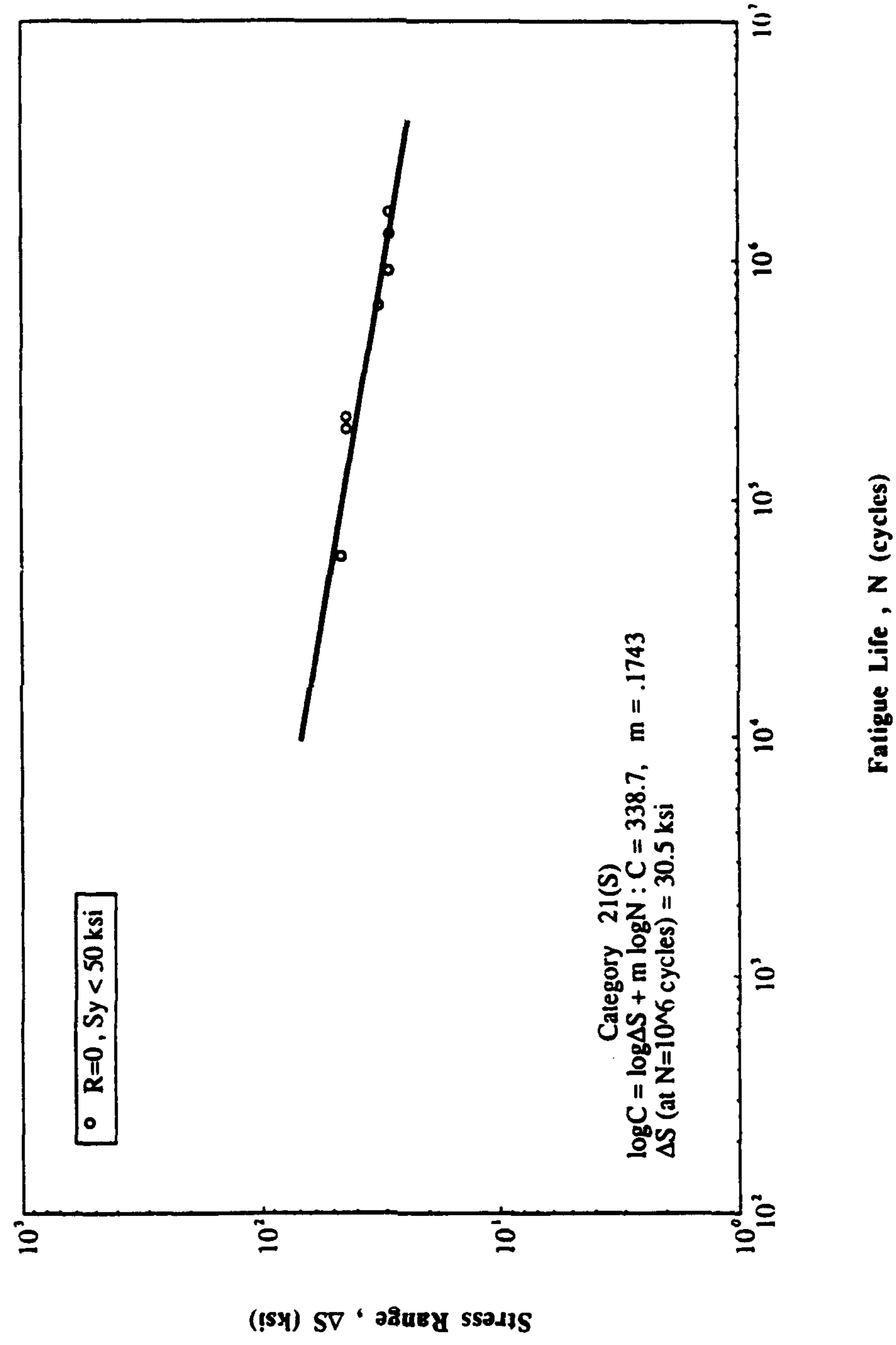

Fig. A-19 Detail Category 21(S)

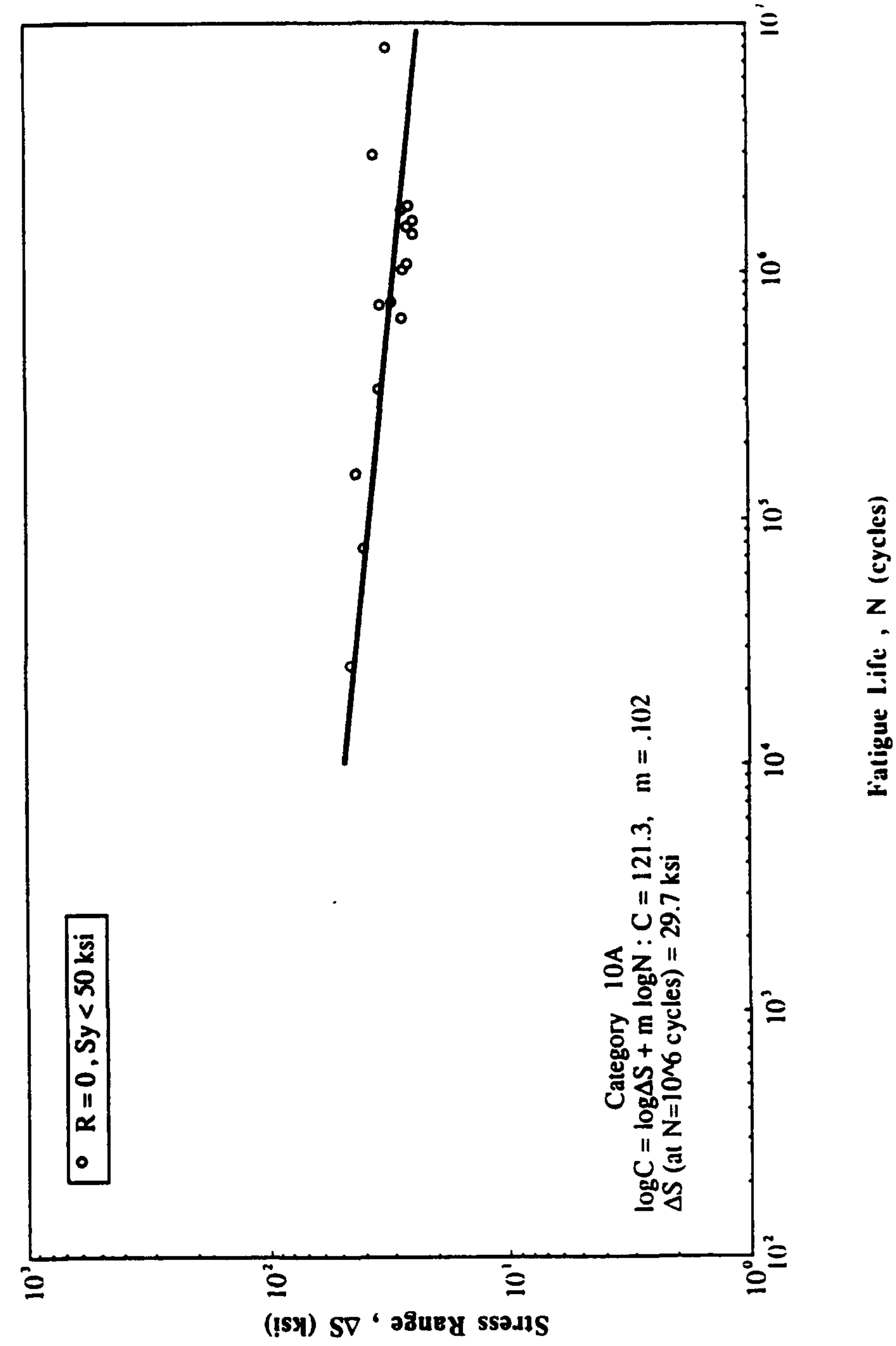

Fig. A-20 Detail Category 10A

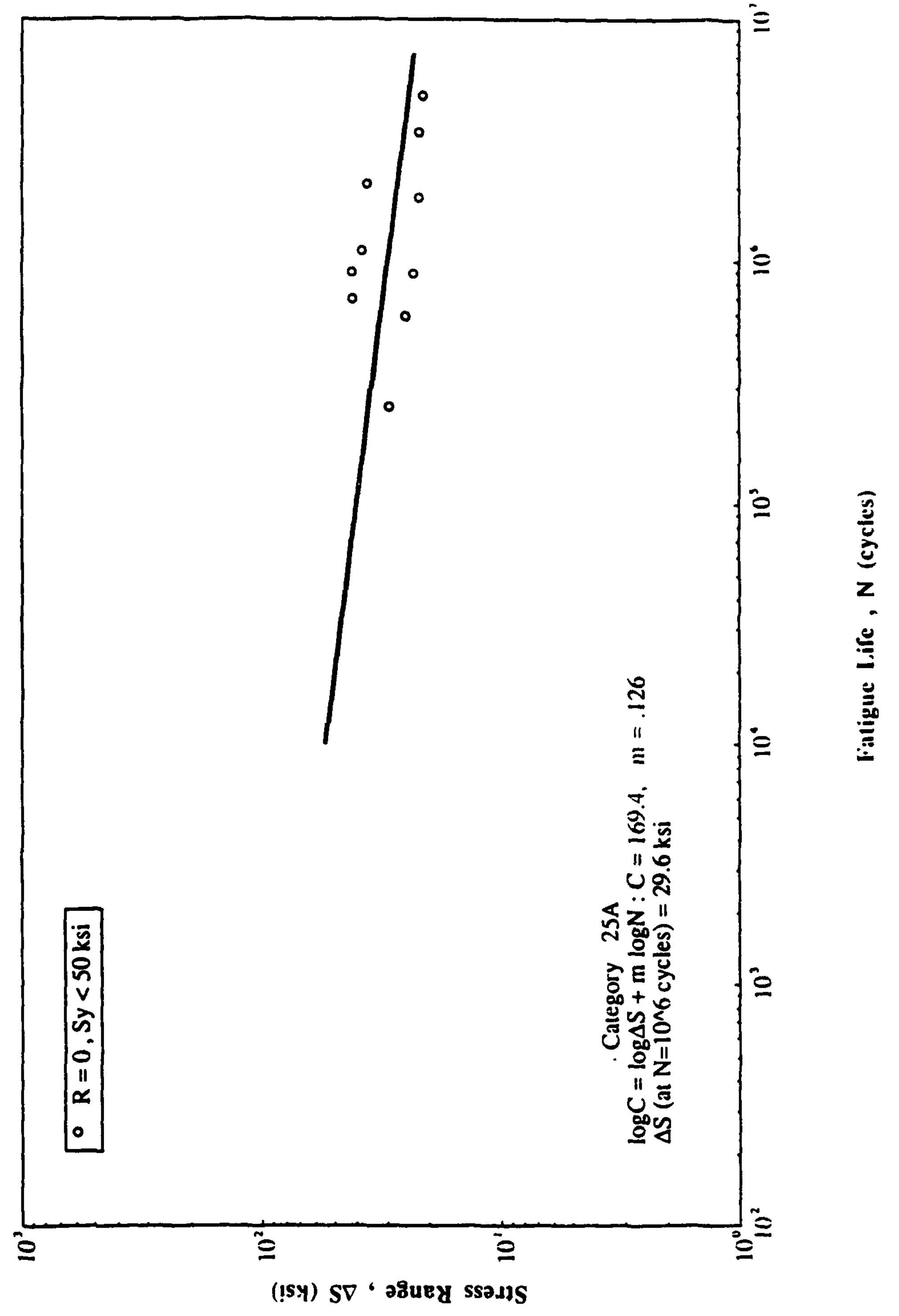

Fig. A-21 Detail Category 25A

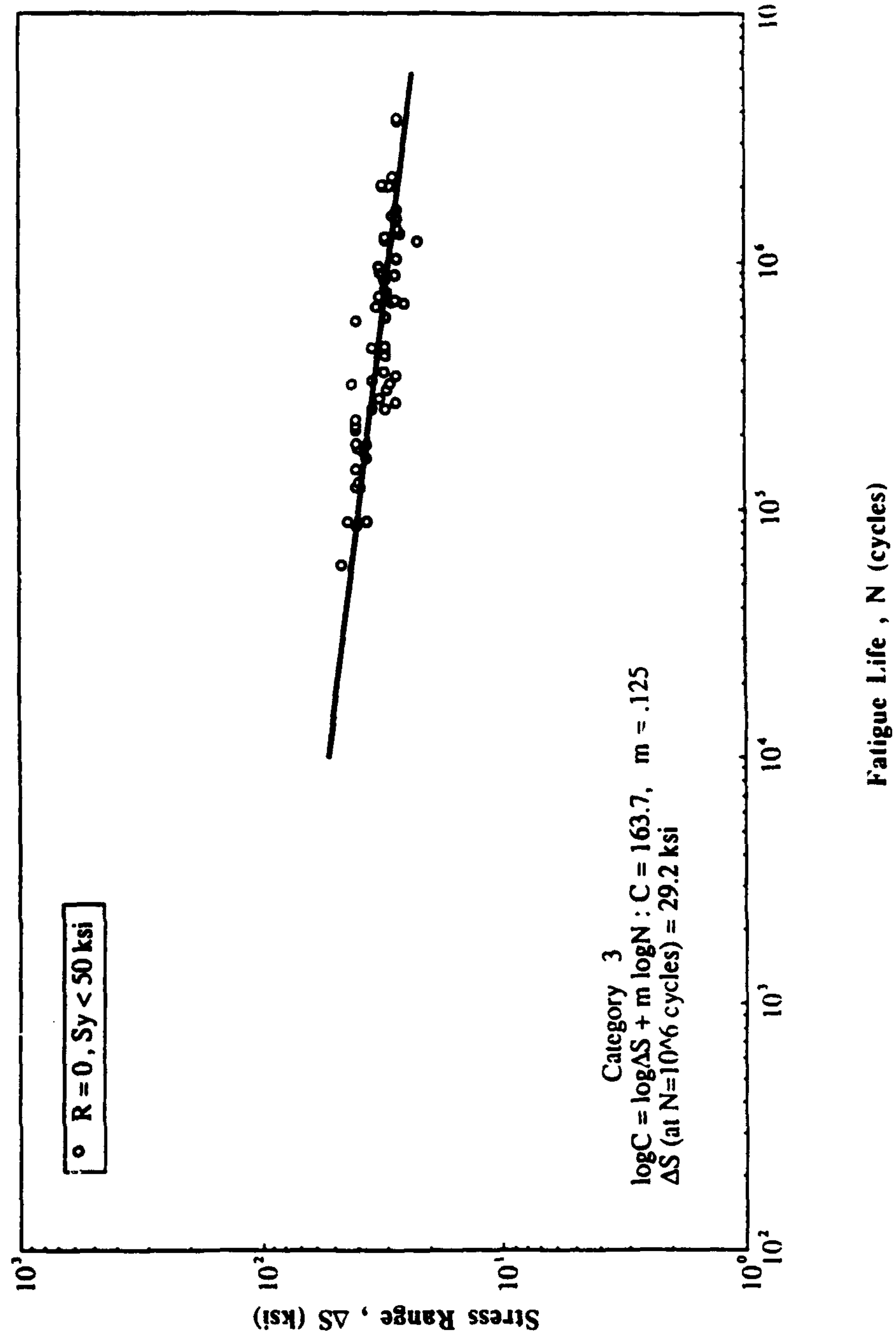

Fig. A-22 Detail Category 3

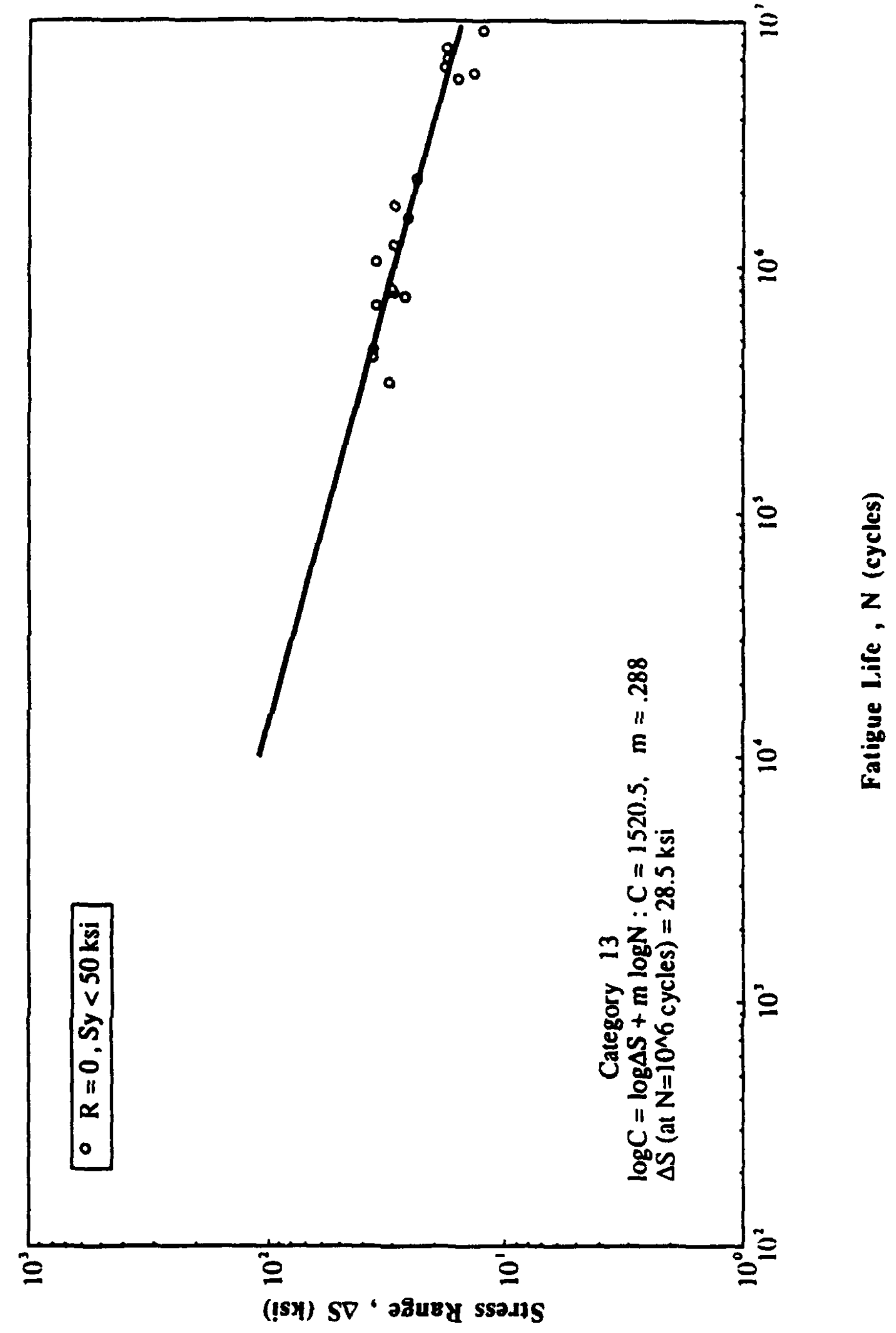

Fig. A-23 Detail Category 13

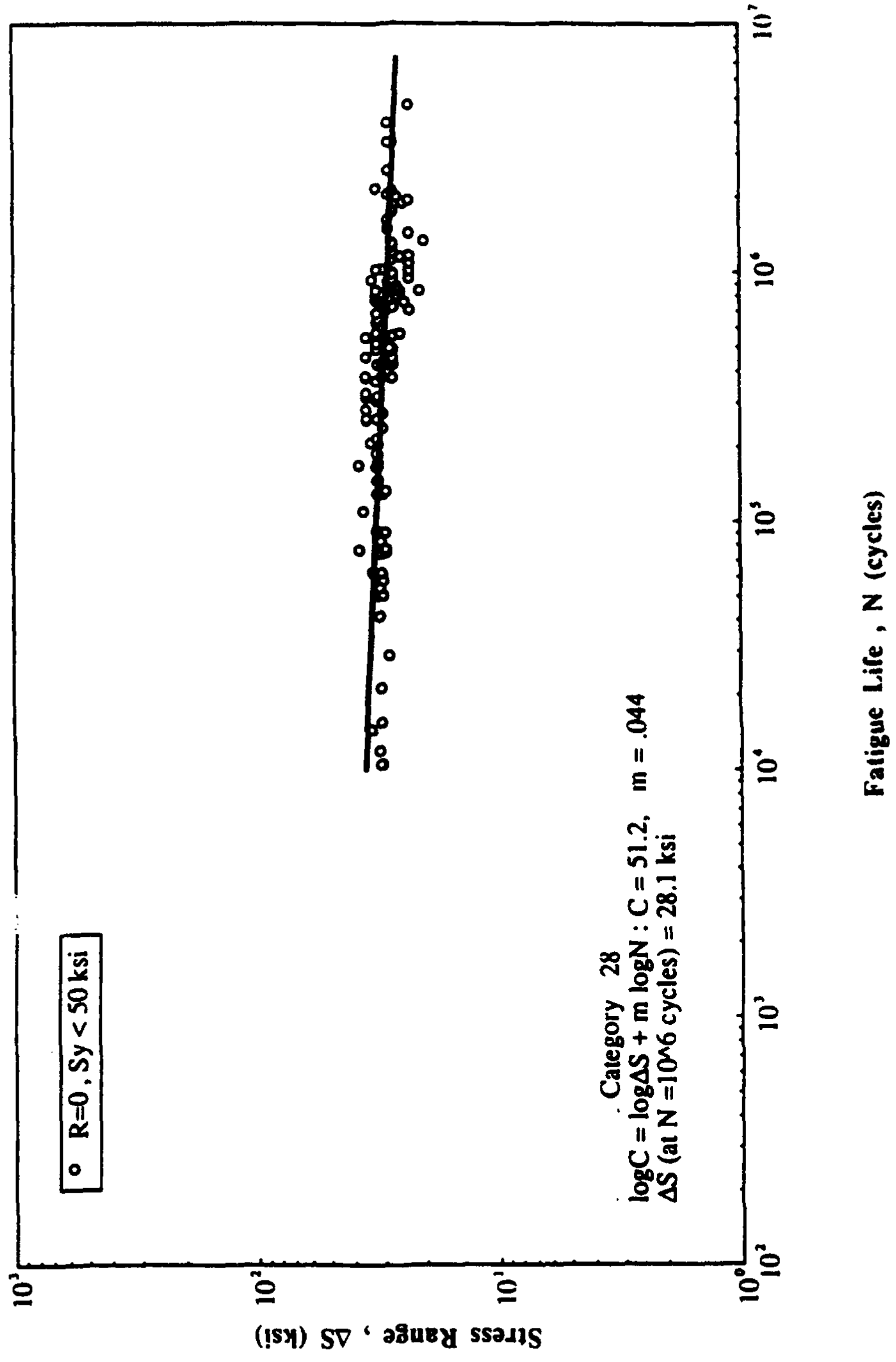

Fig. A-24 Detail Category 28

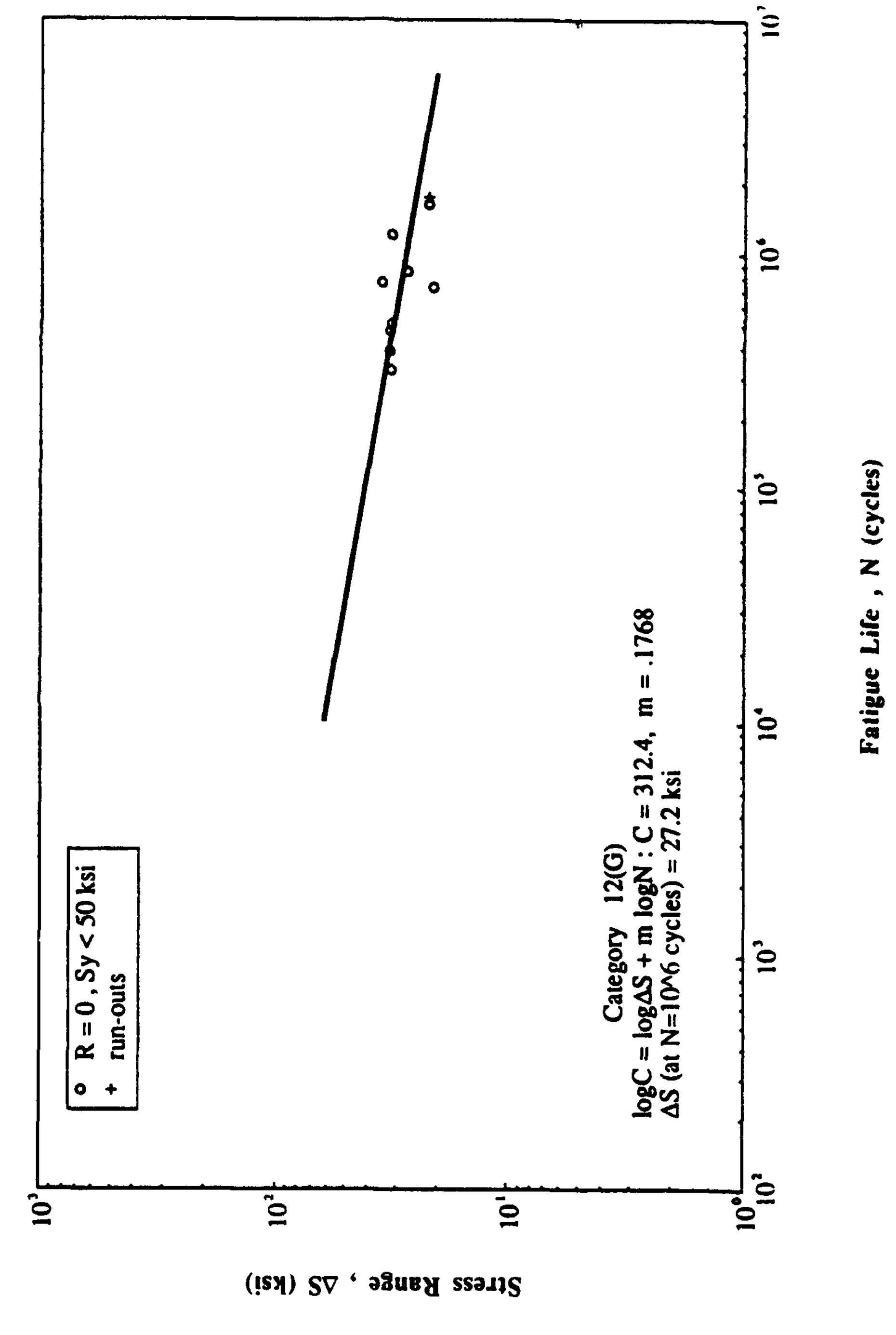

Fig. A-25 Detail Category 12(G)

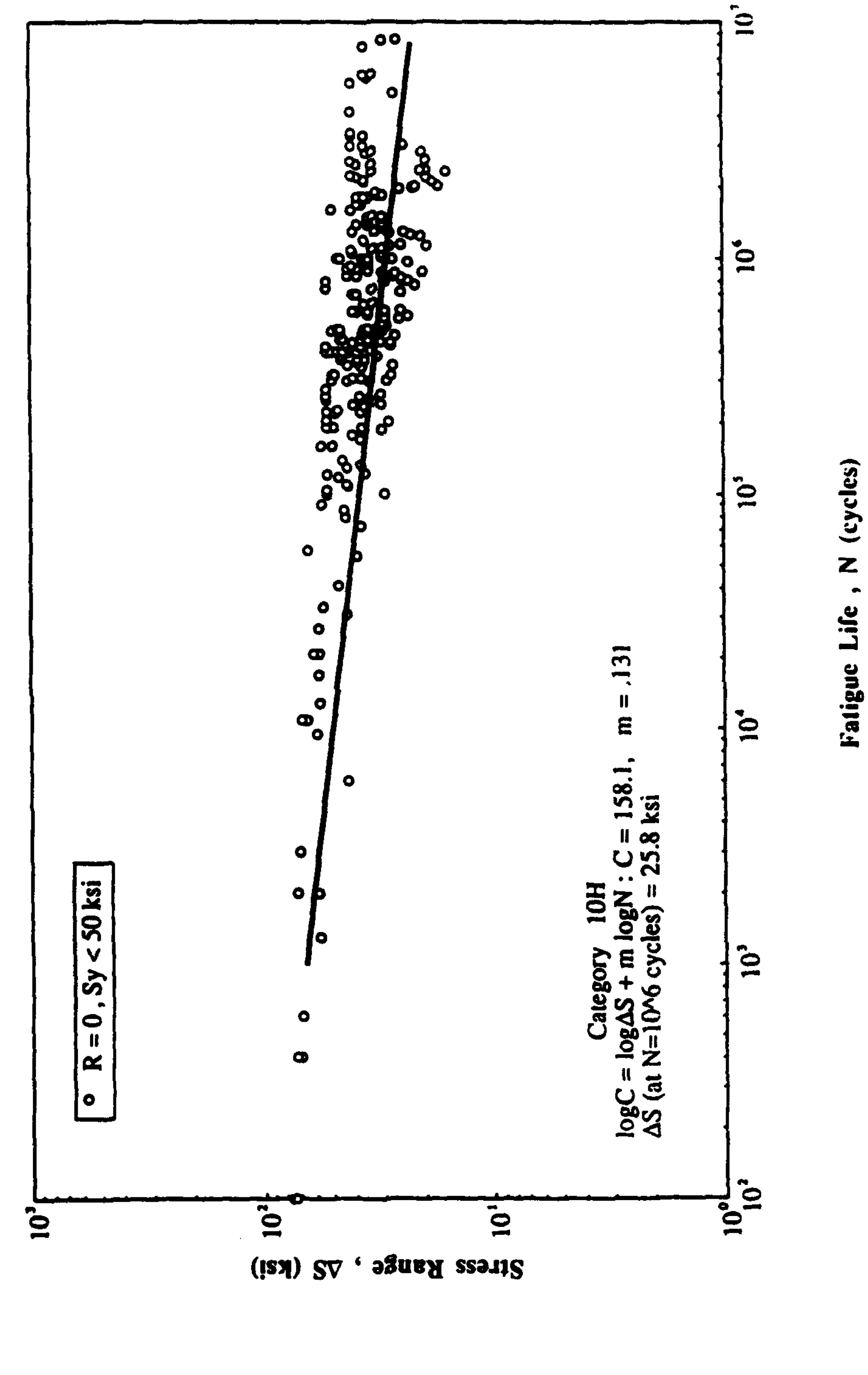

Fig. A-26 Detail Category 10H

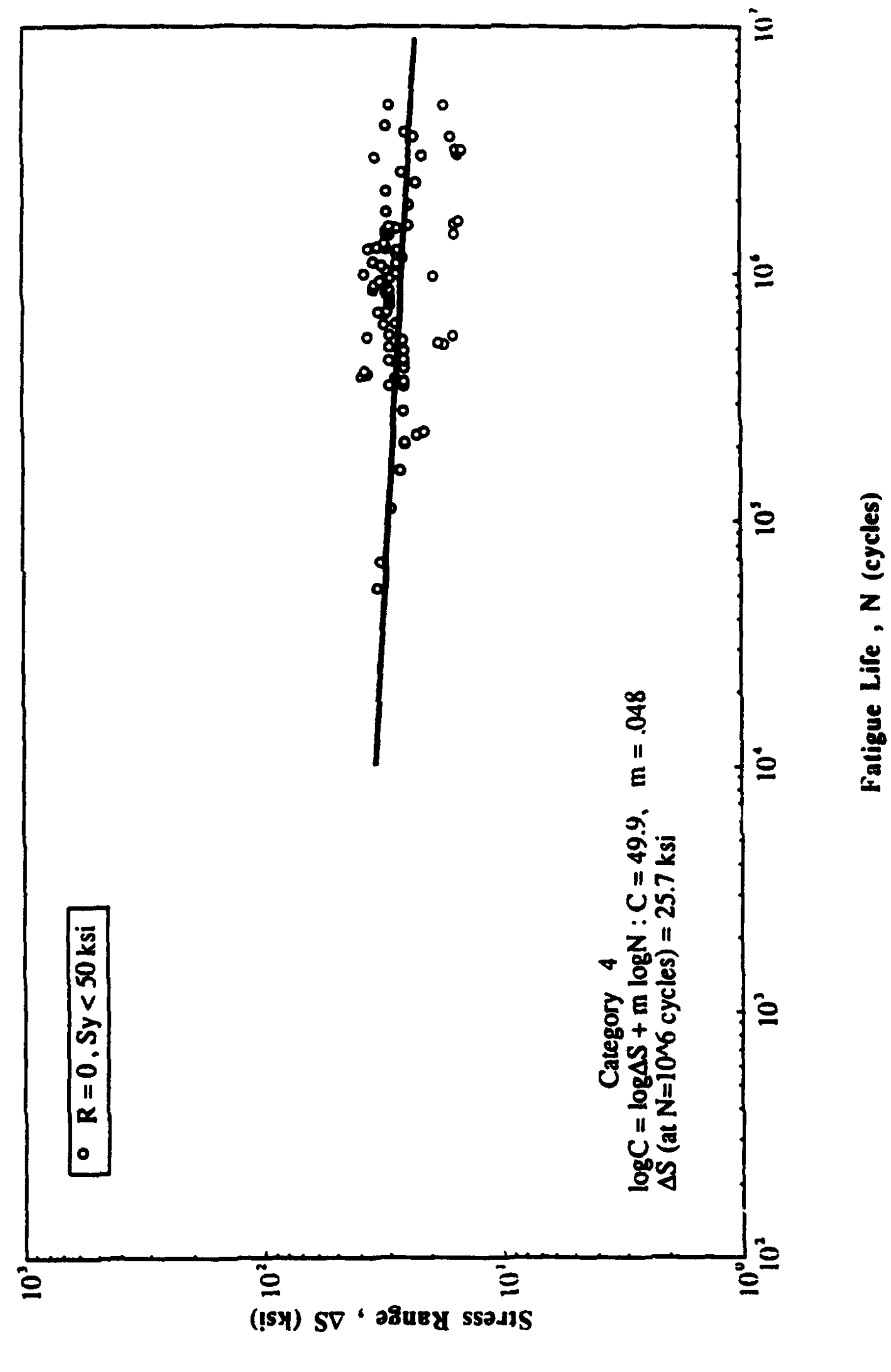

Fig. A-27 Detail Category 4

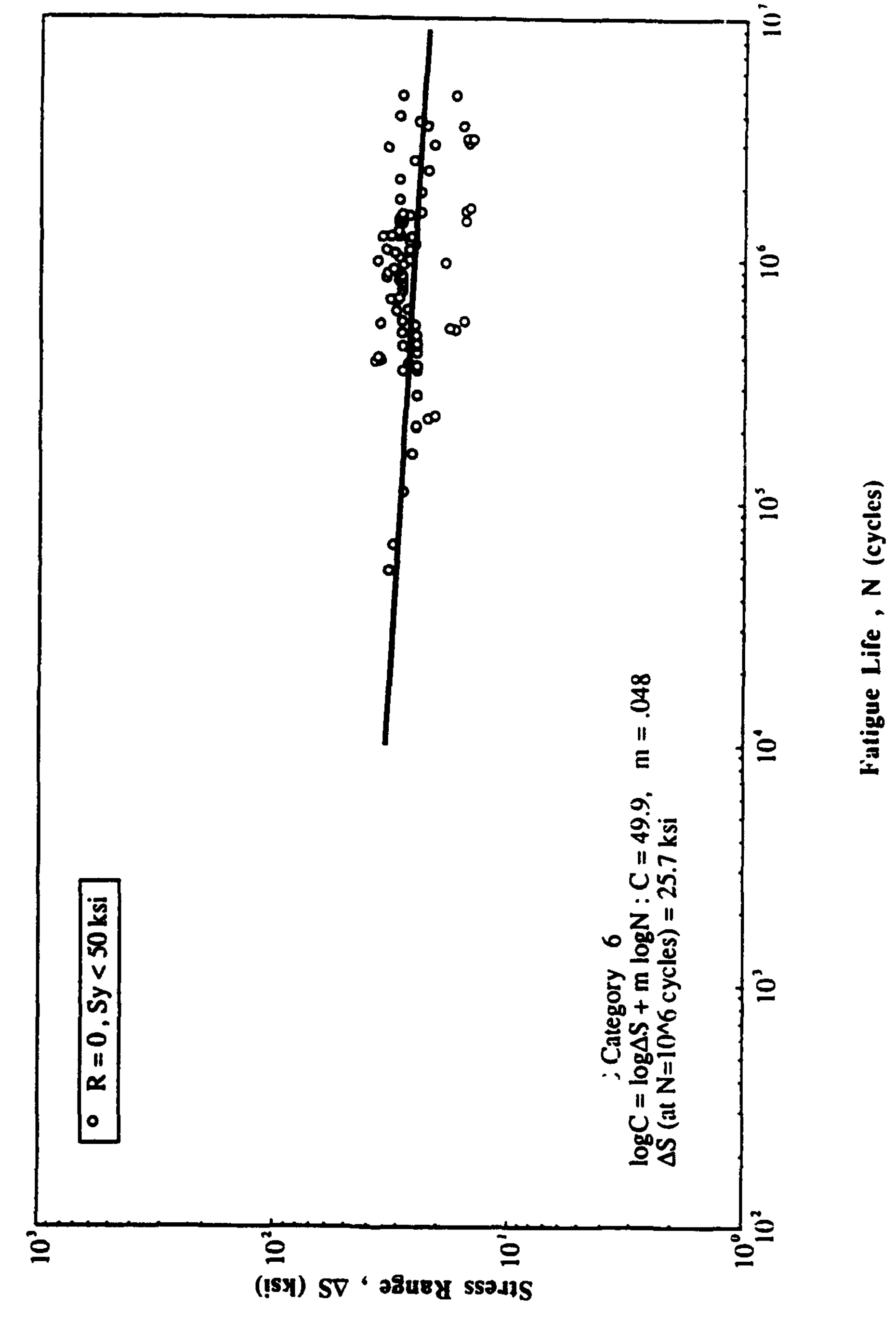

Fig. A-28 Detail Category 6

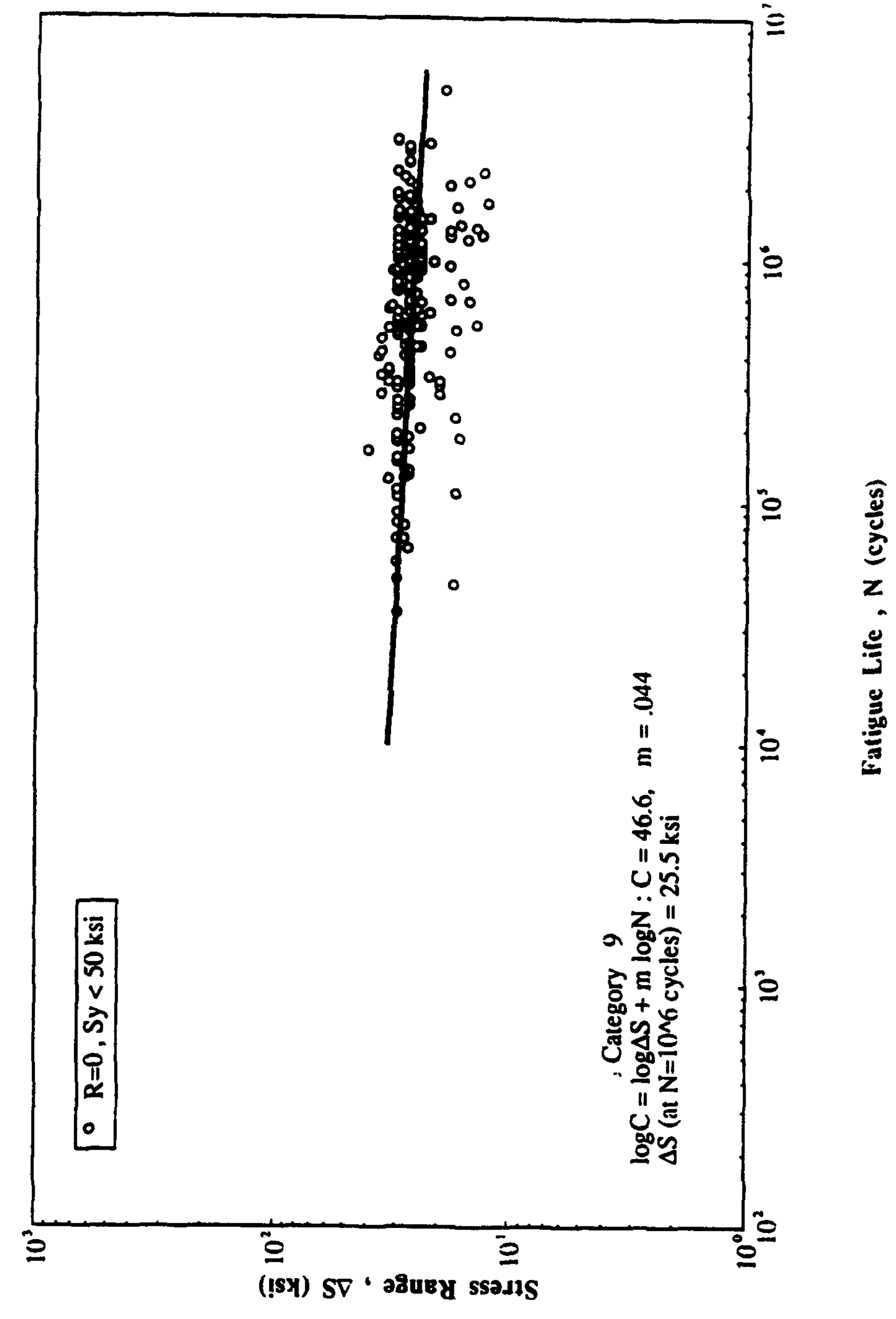

Fig. A-29 Detail Category 9

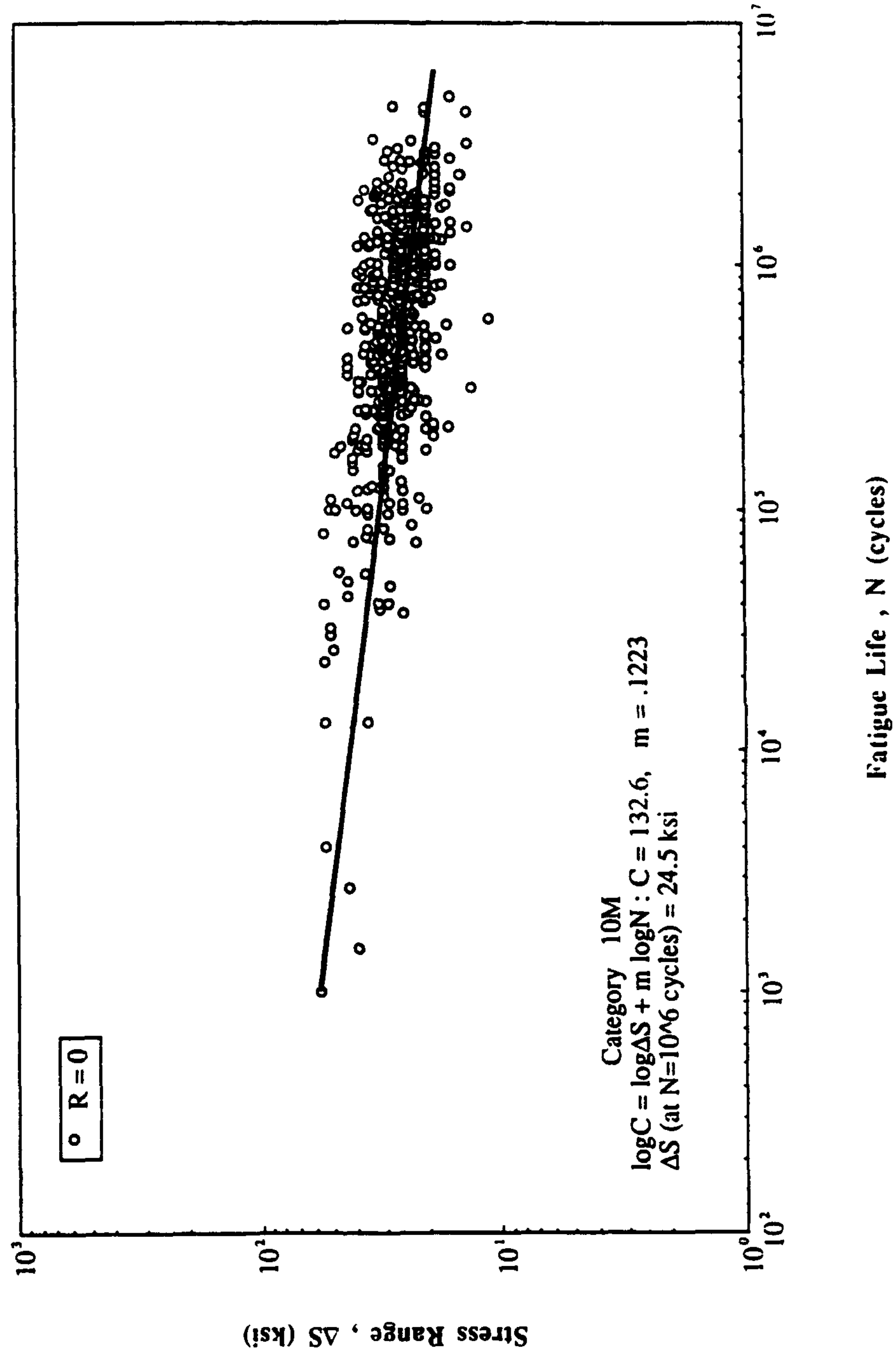

Fig. A-30 Detail Category 10M

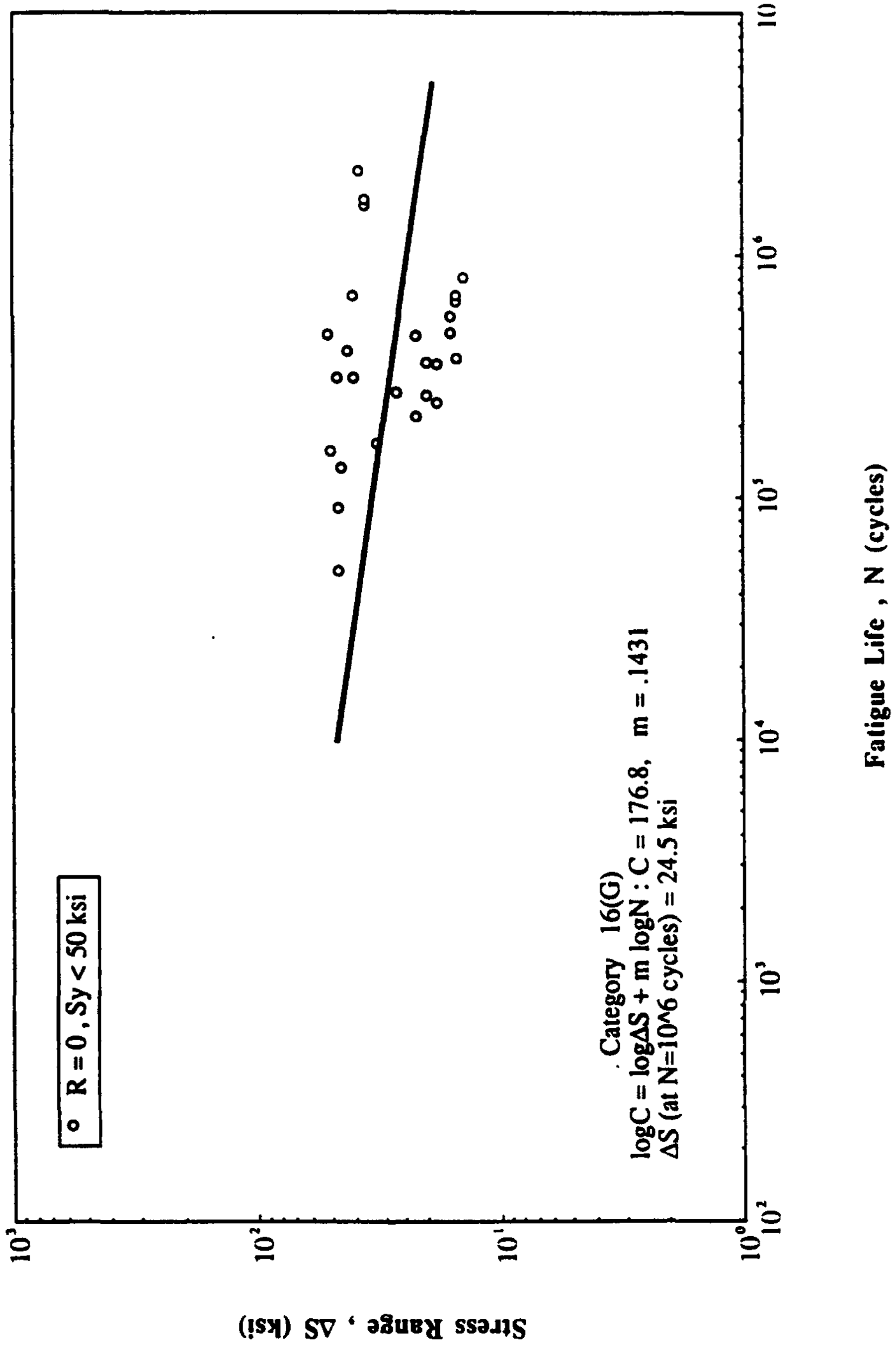

Fig. A-31 Detail Category 16(G)

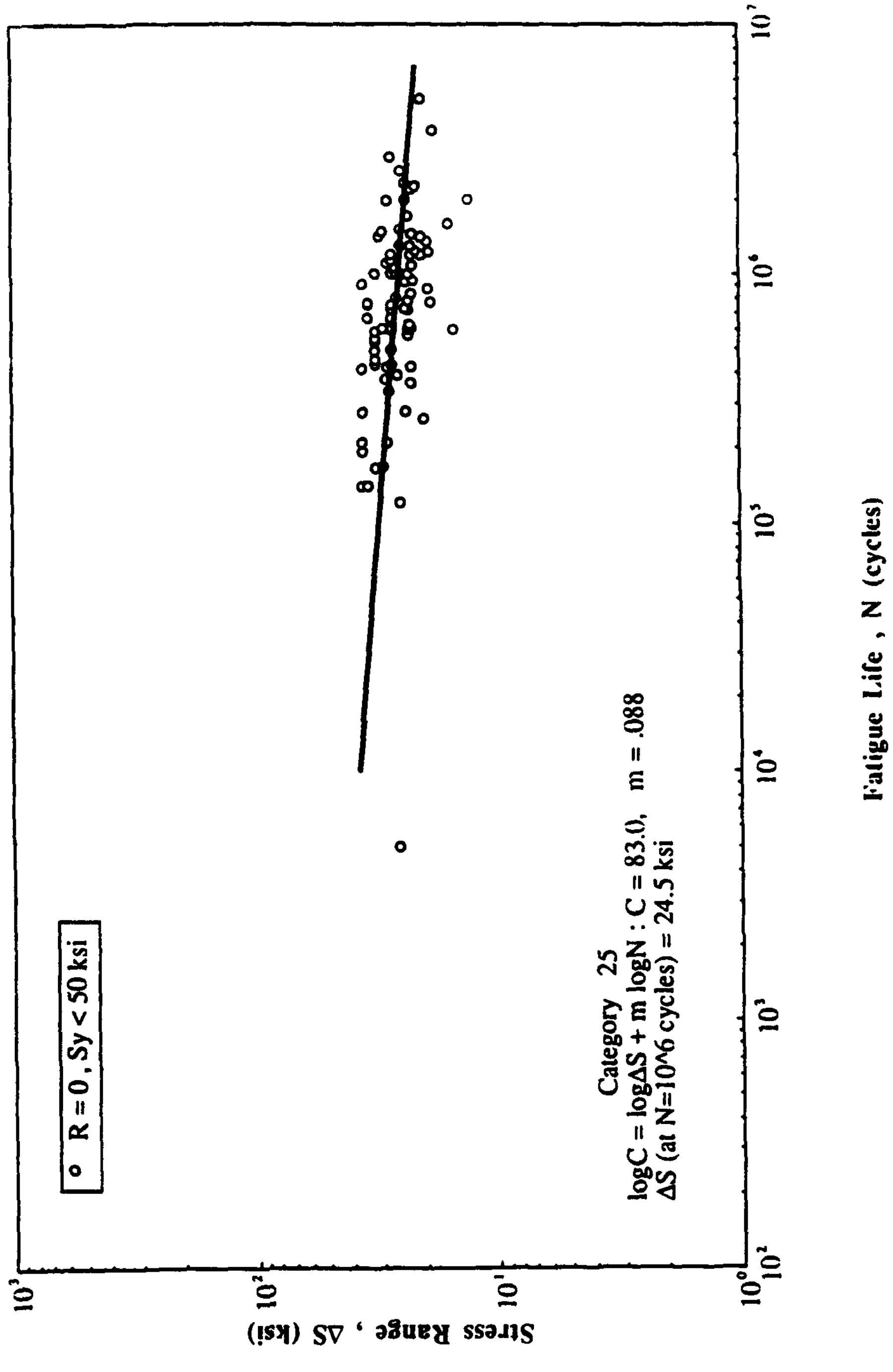

Fig. A-32 Detail Category 25

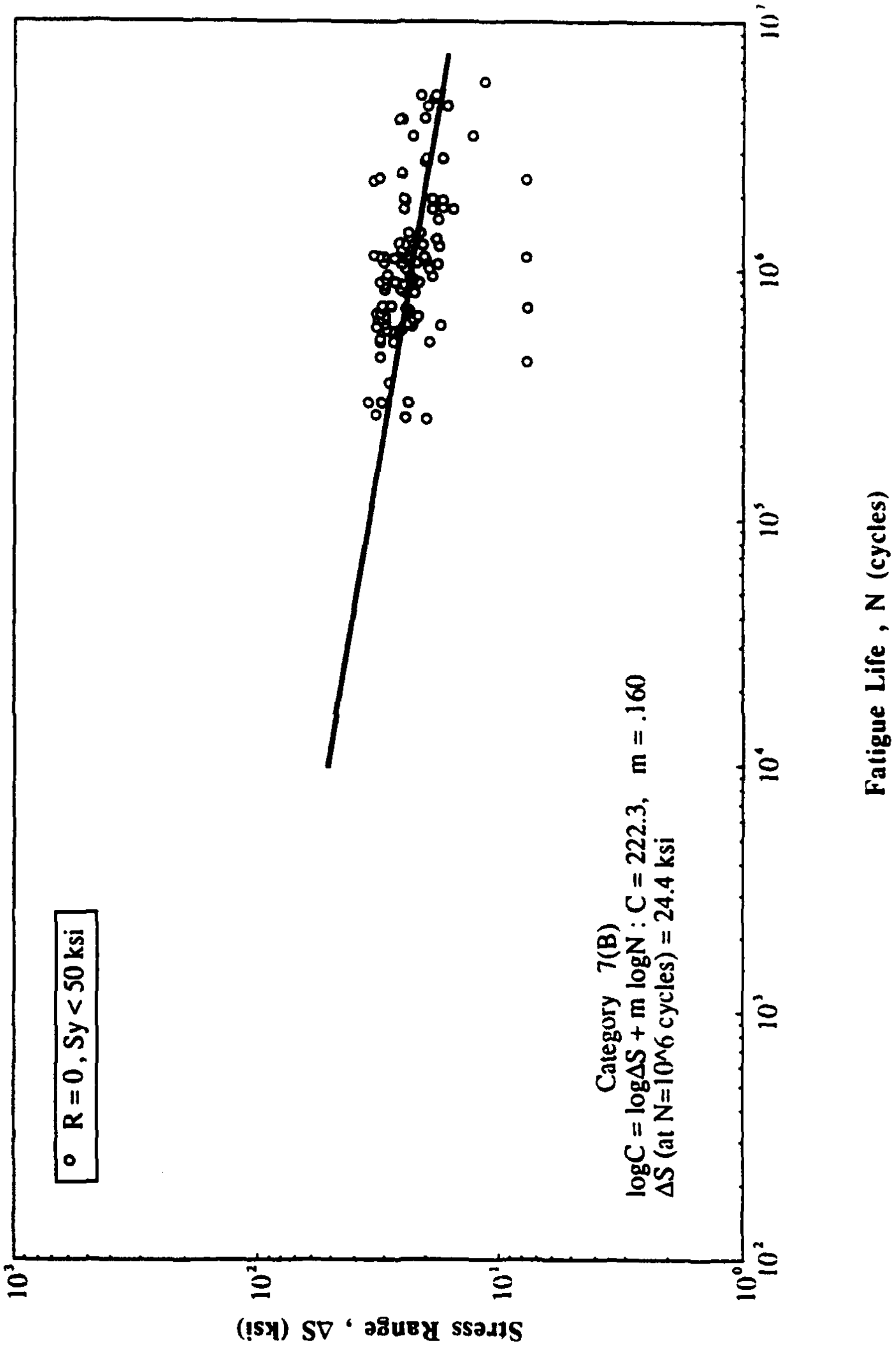

Fig. A-33 Detail Category 7(B)

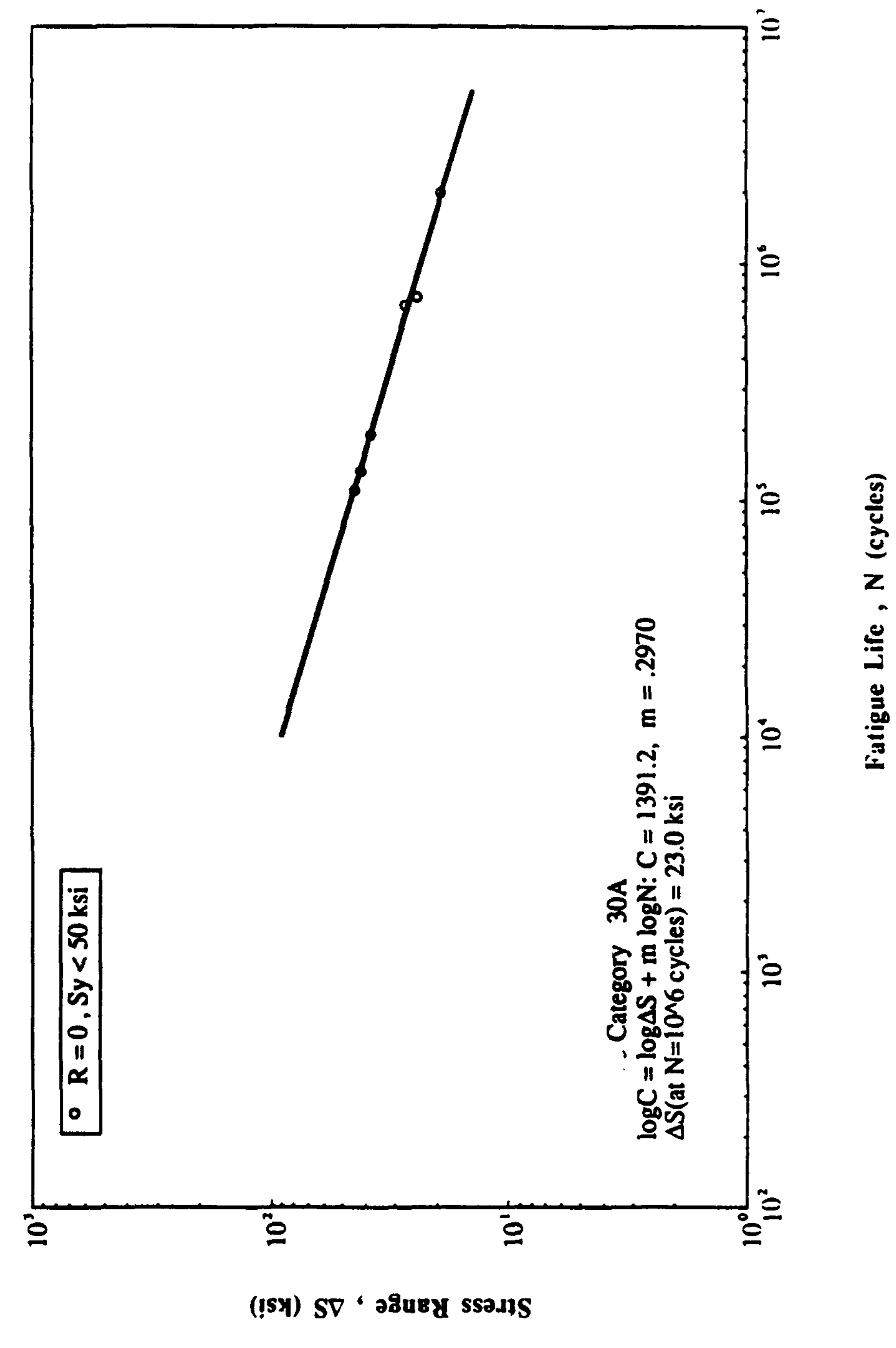

Fig. A-34 Detail Category 30A

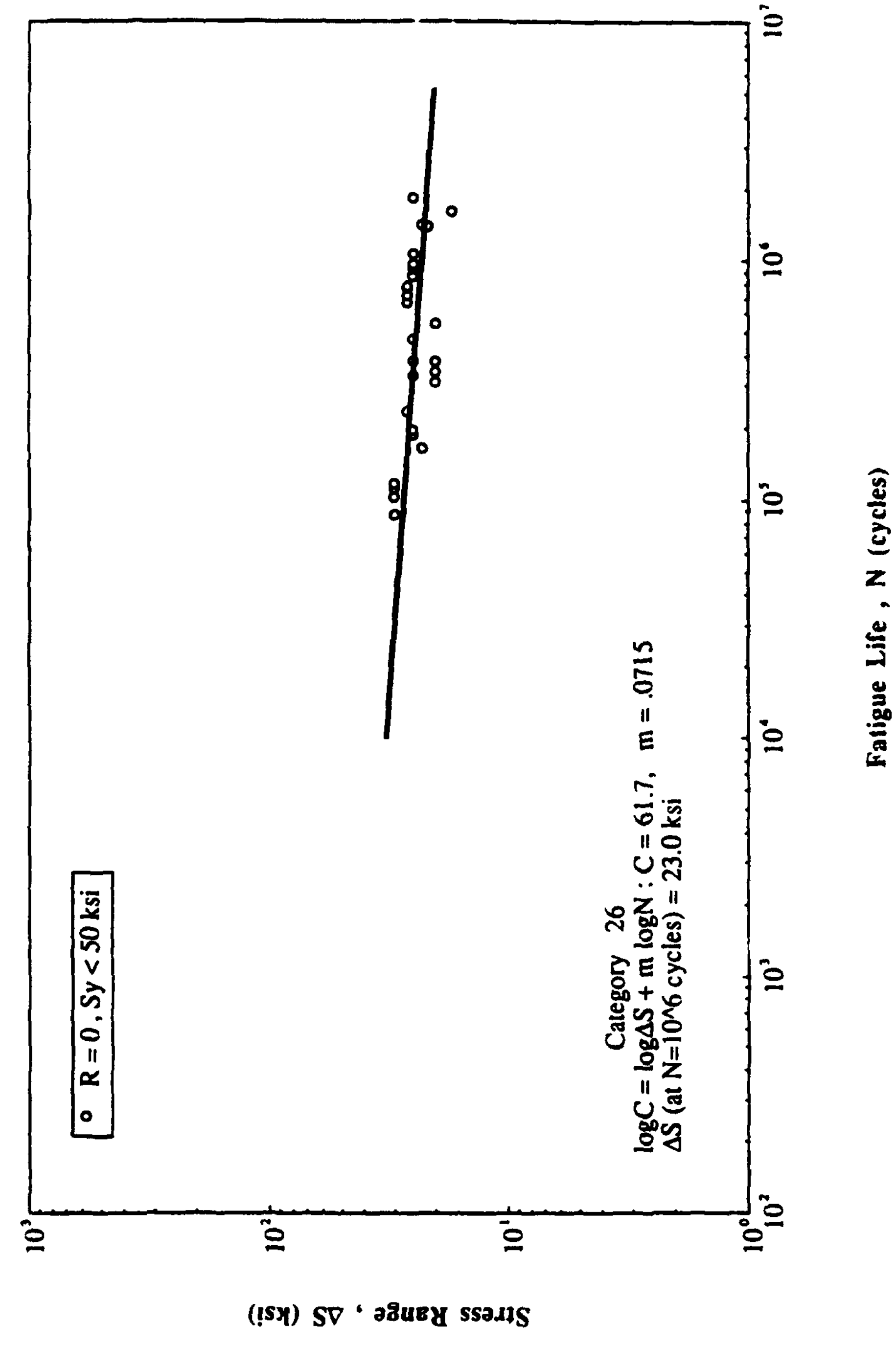

Fig. A-35 Detail Category 26

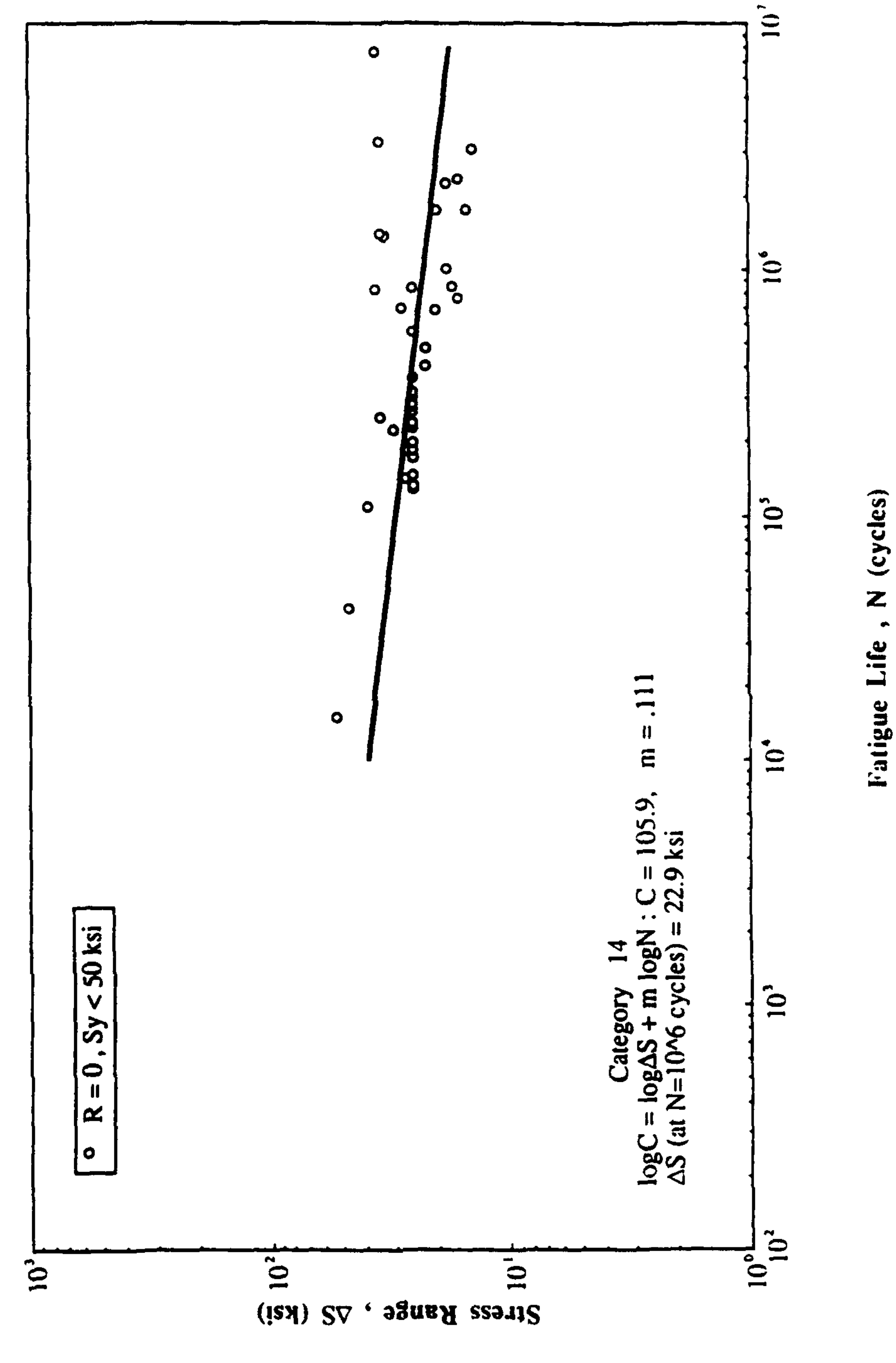

Fig. A-36 Detail Category 14

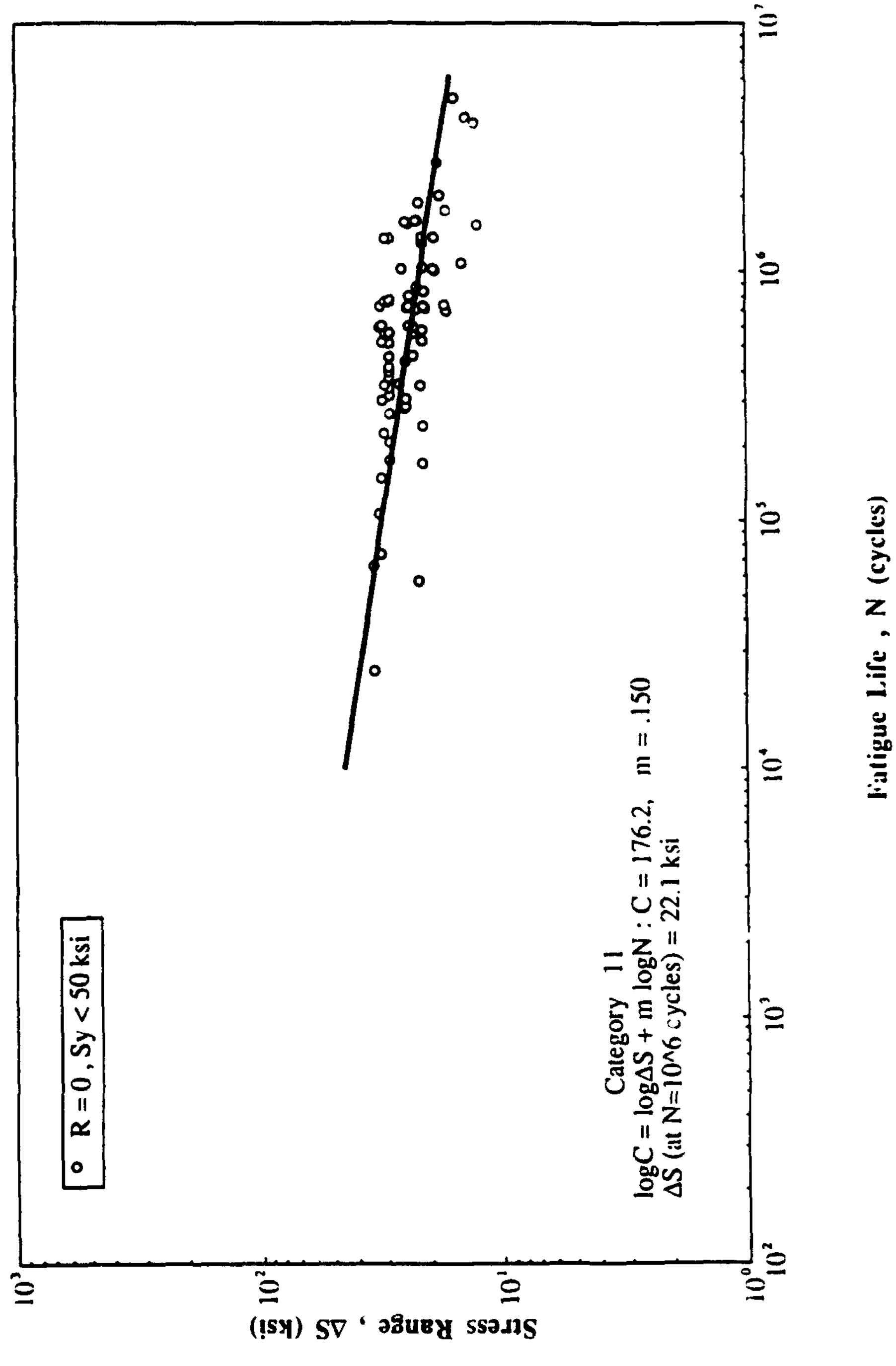

Fig. A-37 Detail Category 11

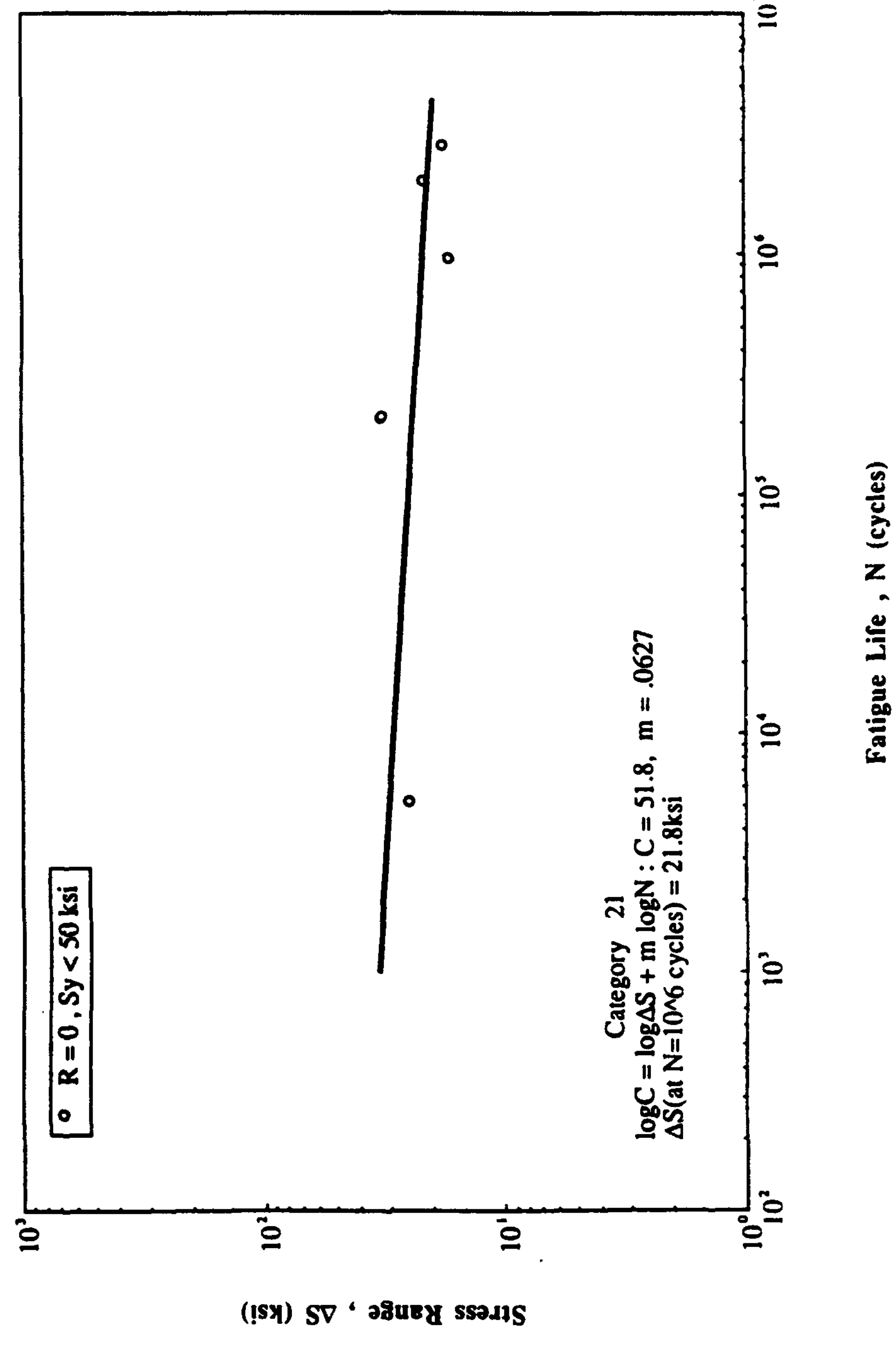

Fig. A-38 Detail Category 21

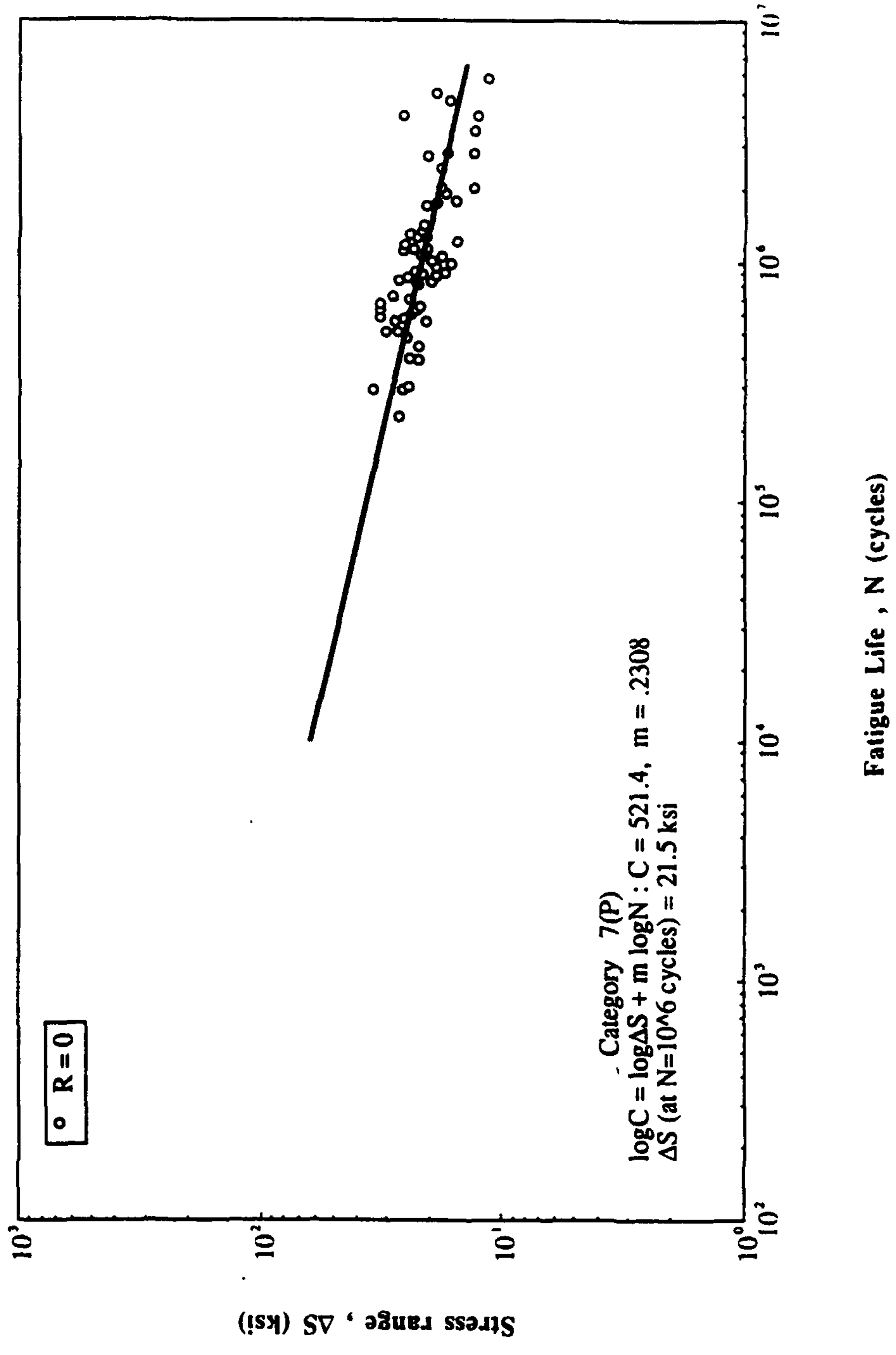

Fig. A-39 Detail Category 7(P)

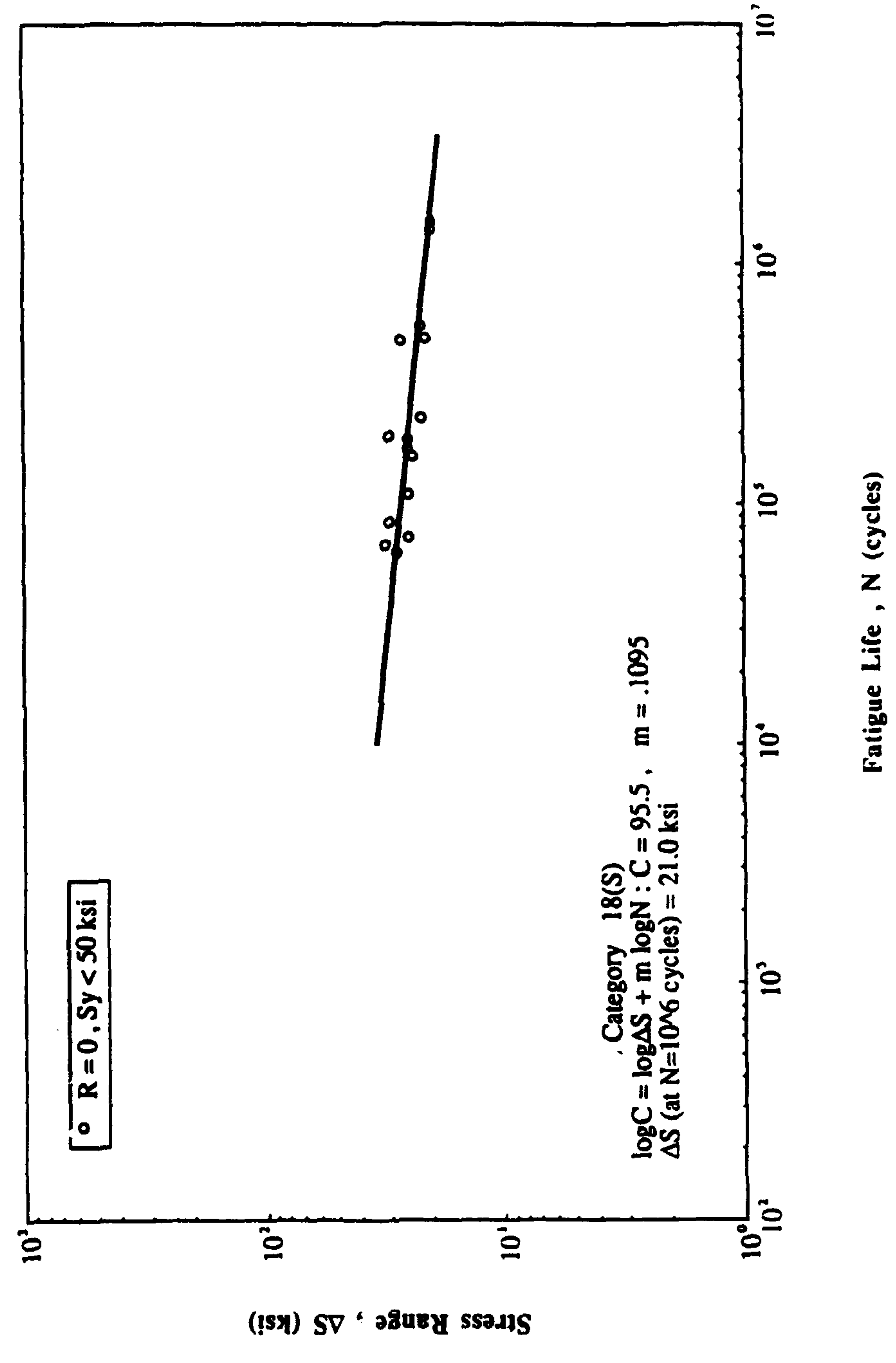

Fig. A-40 Detail Category 18(S)

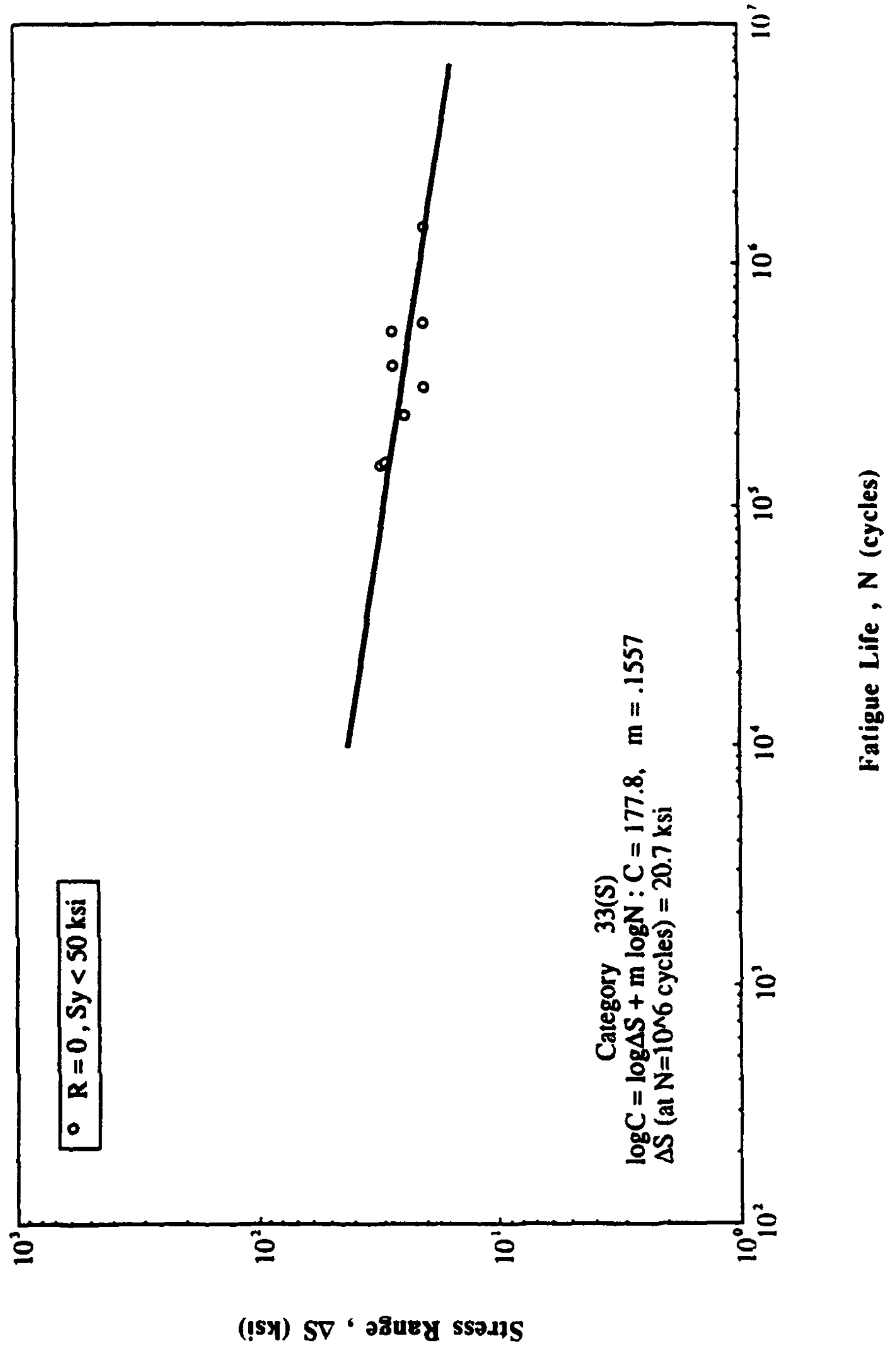

Fig. A-41 Detail Category 33(S)

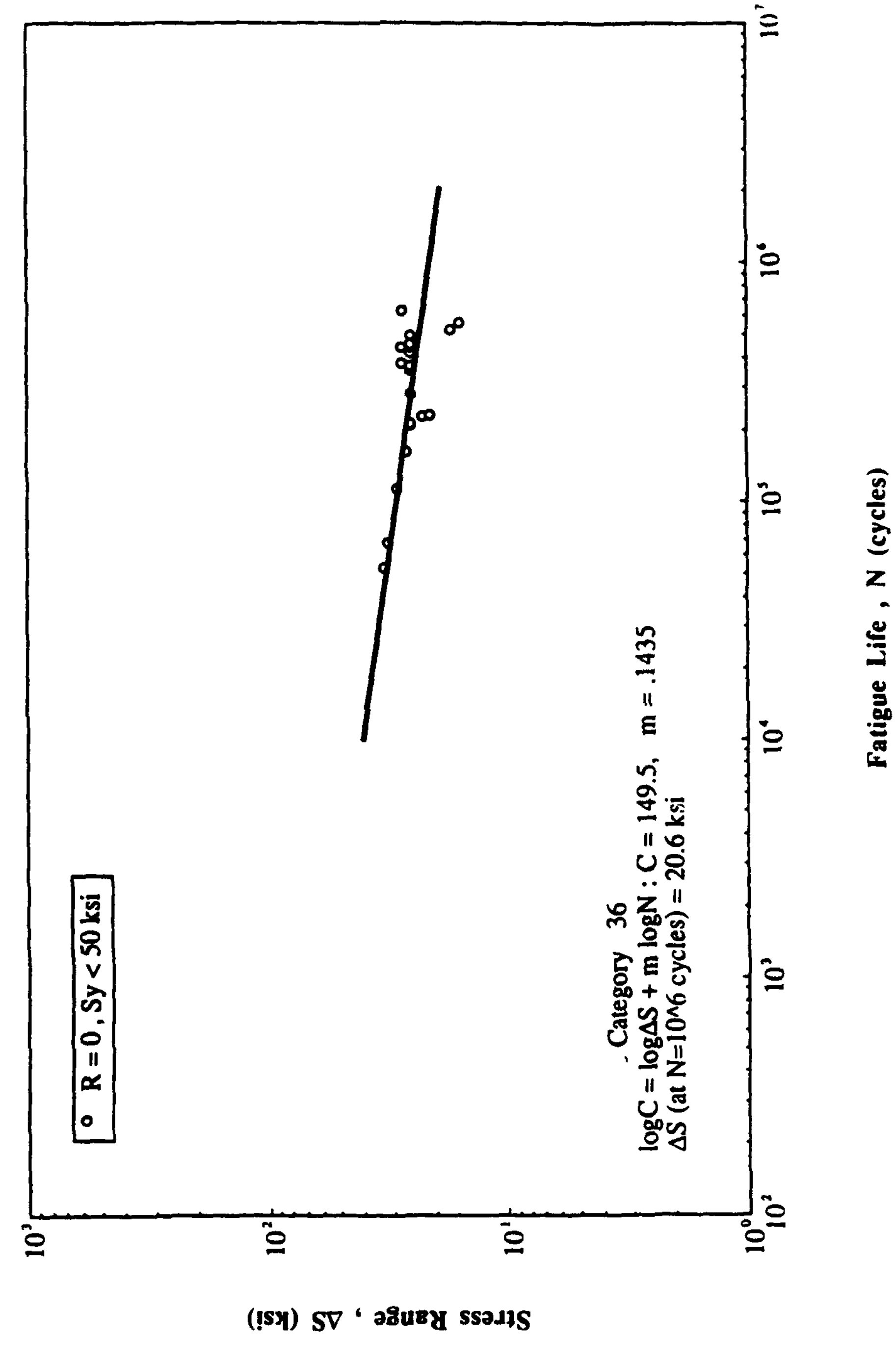

Fig. A-42 Detail Category 36

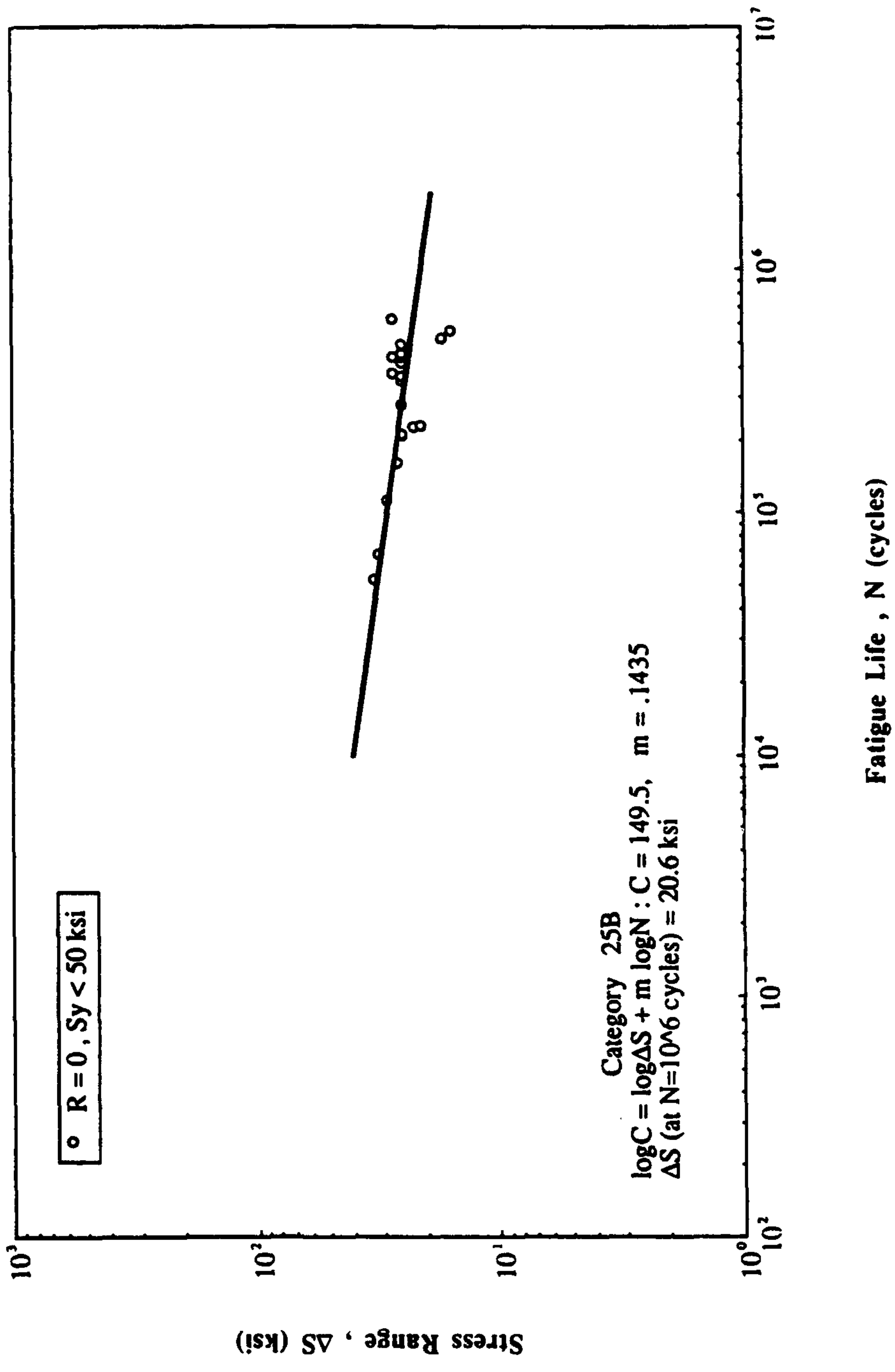

Fig. A-43 Detail Category 25B

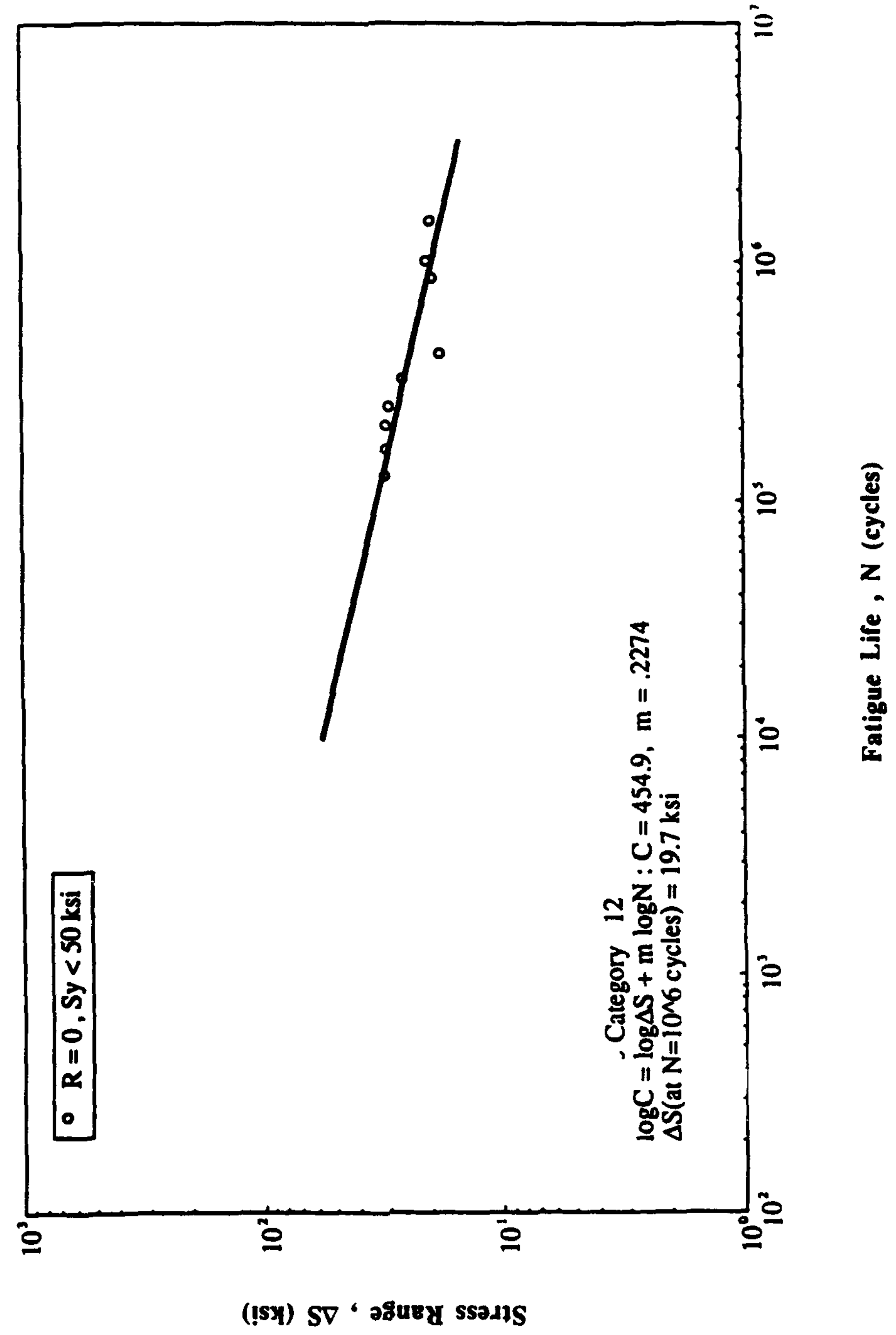

Fig. A-44 Detail Category 12

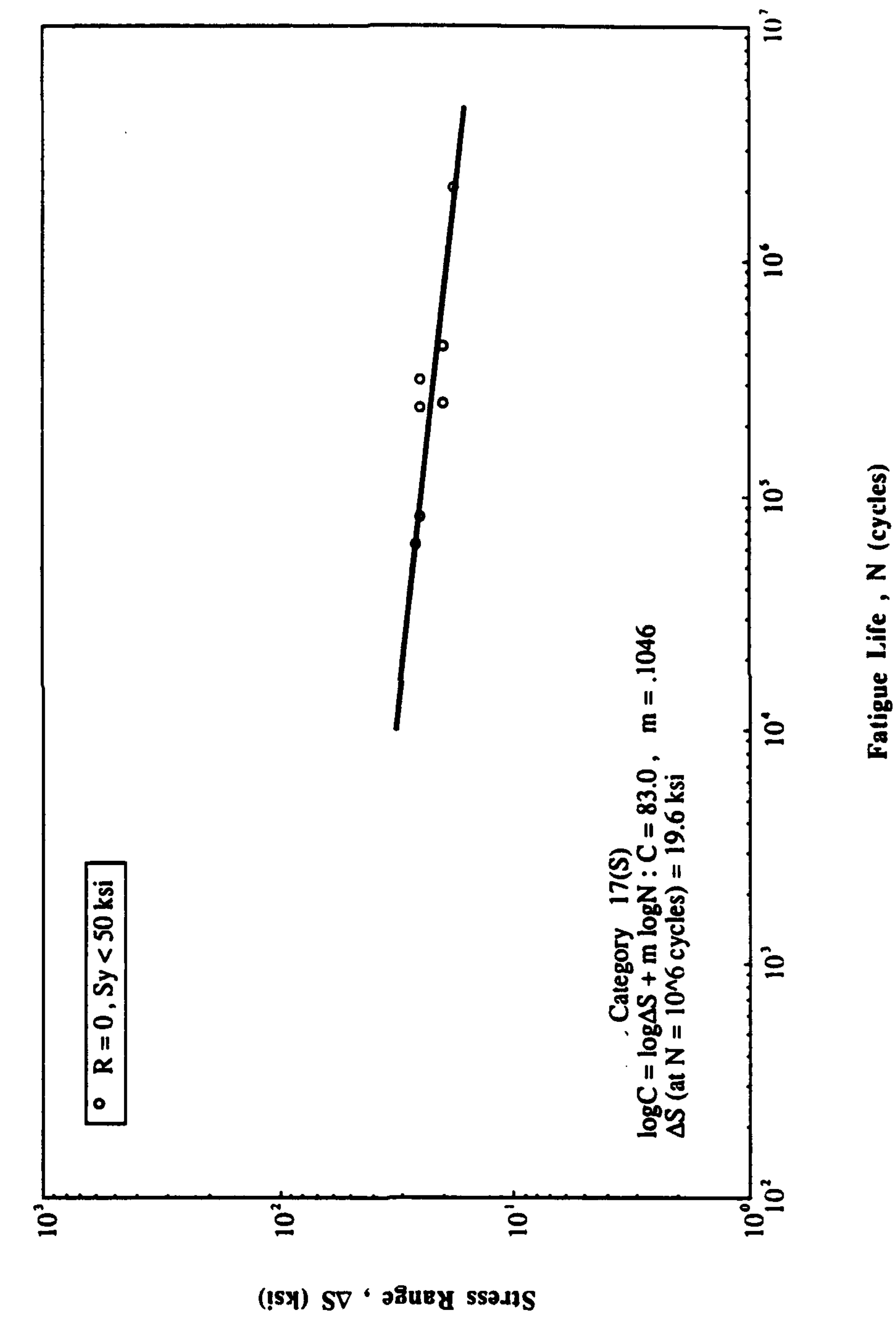

Fig. A-45 Detail Category 17(S)

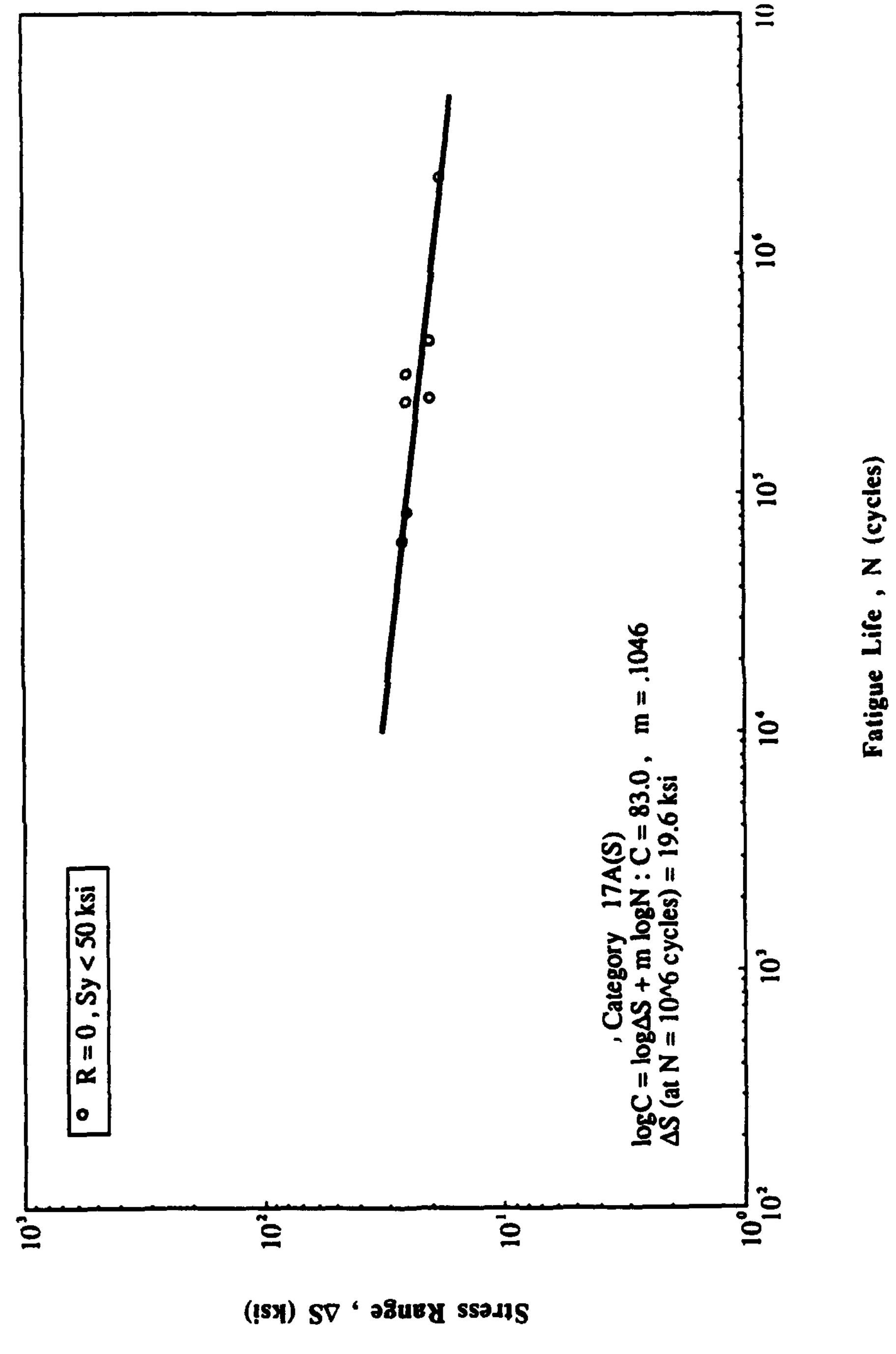

Fig. A-46 Detail Category 17A(S)

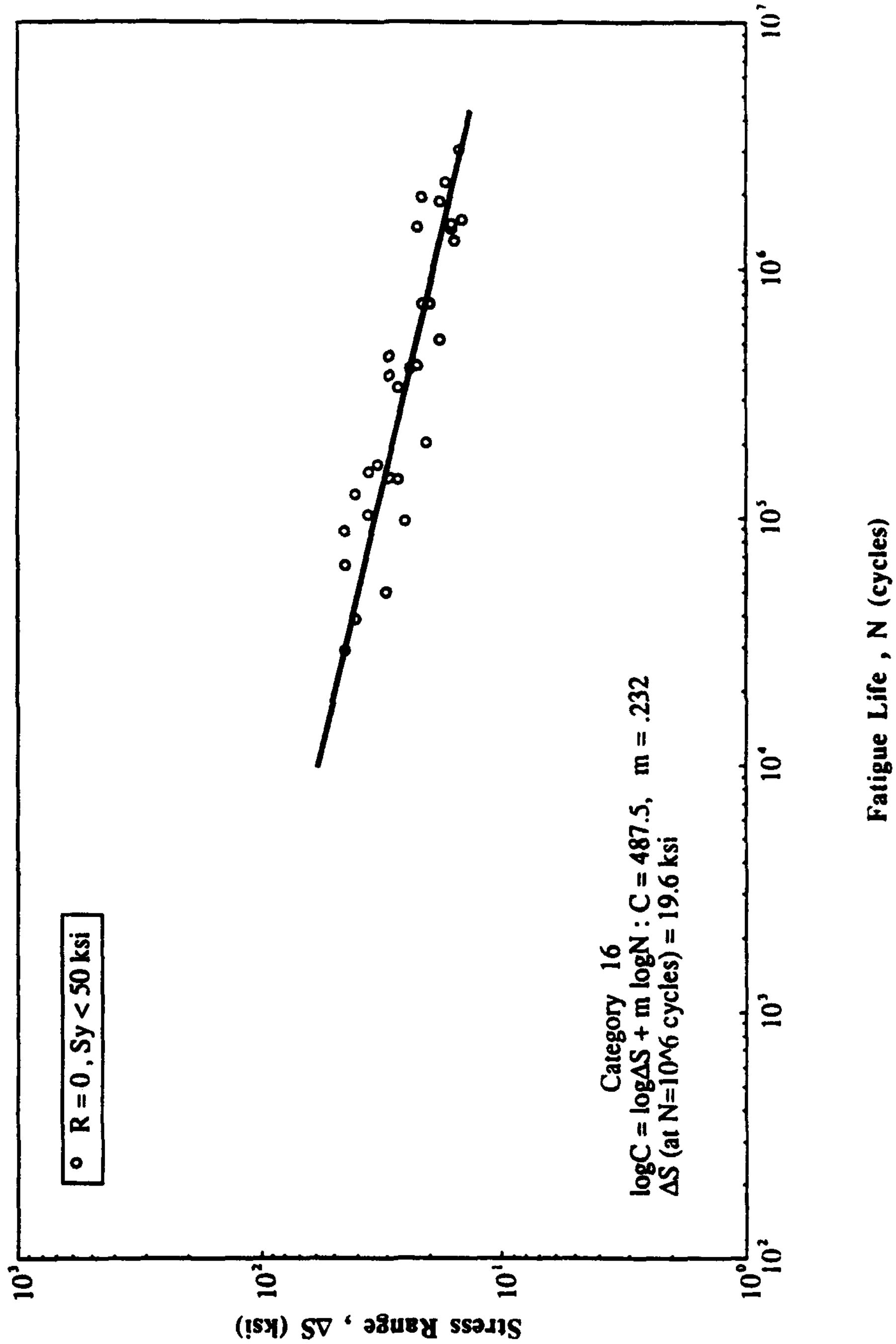

Fig. A-47 Detail Category 16

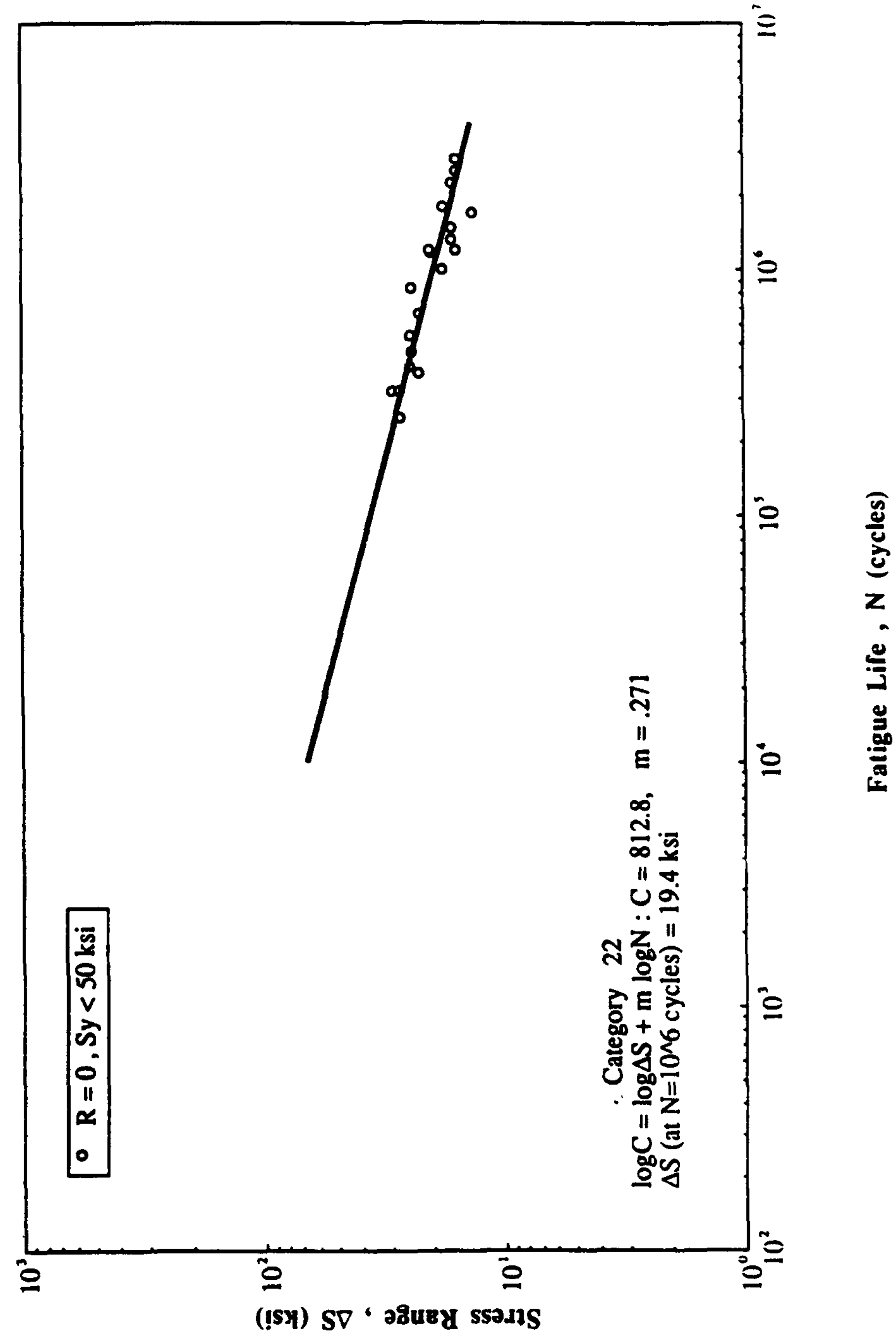

Fig. A-48 Detail Category 22

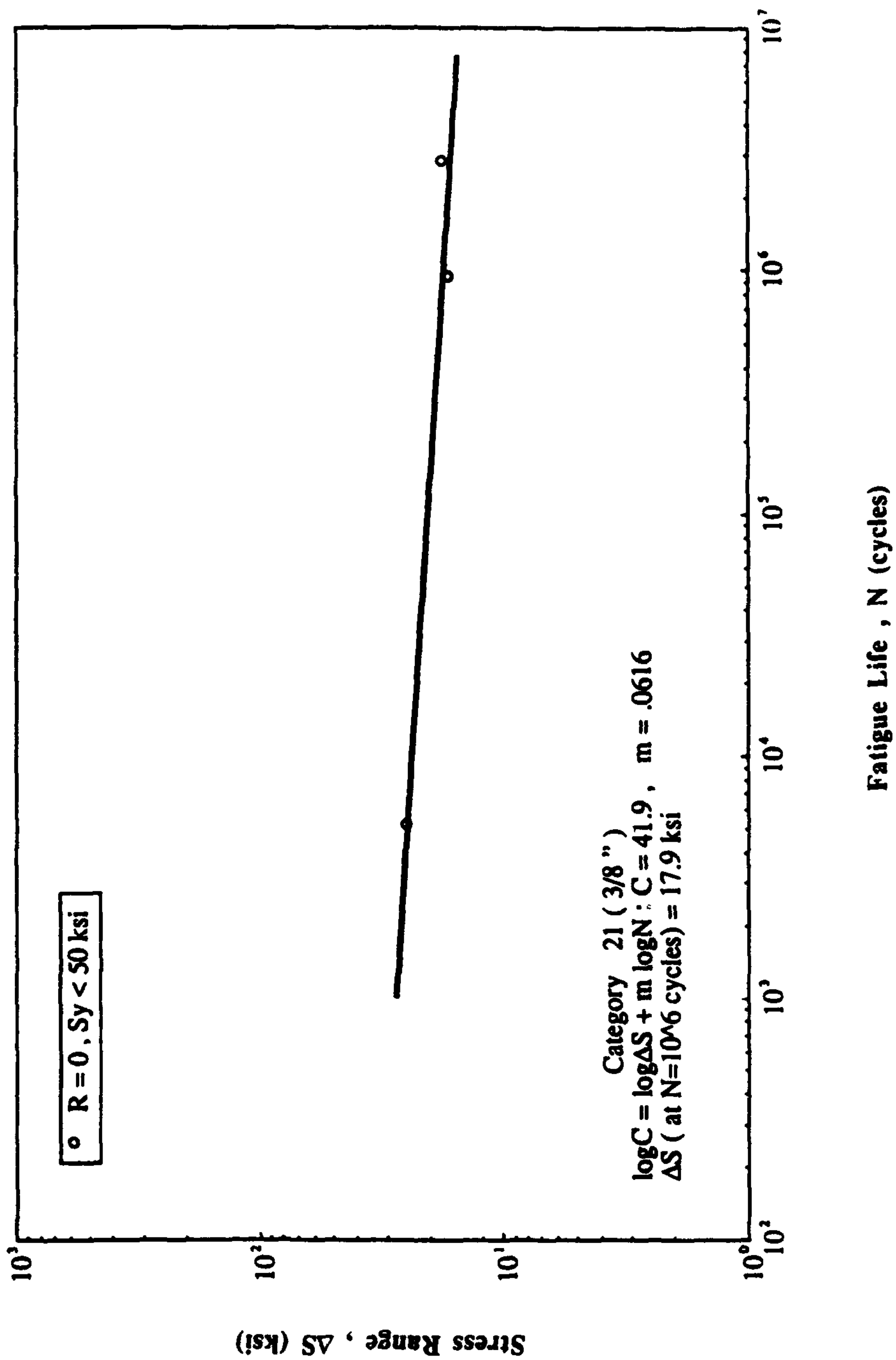

Fig. A-49 Detail Category 21(3/8")

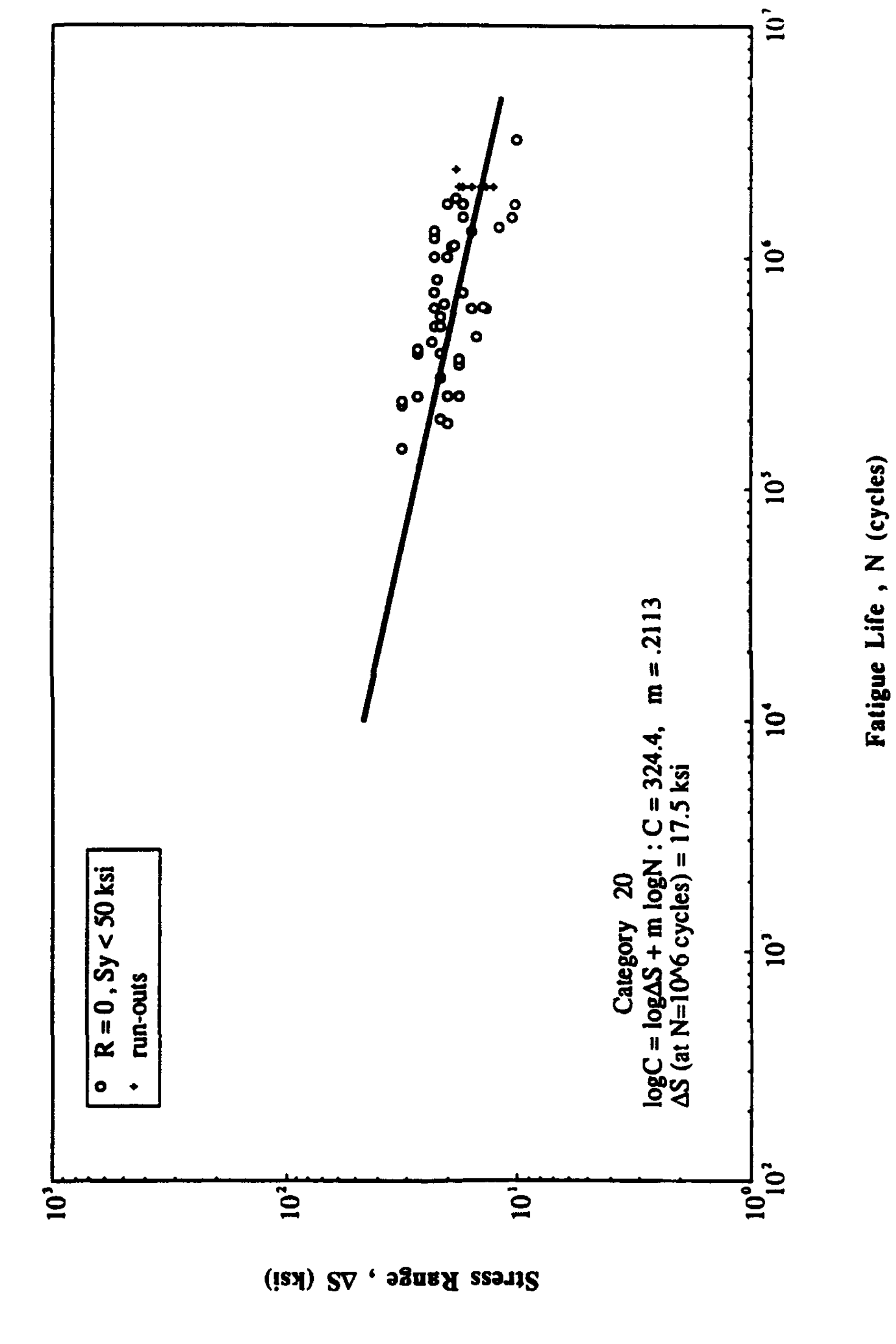

Fig. A-50 Detail Category 20

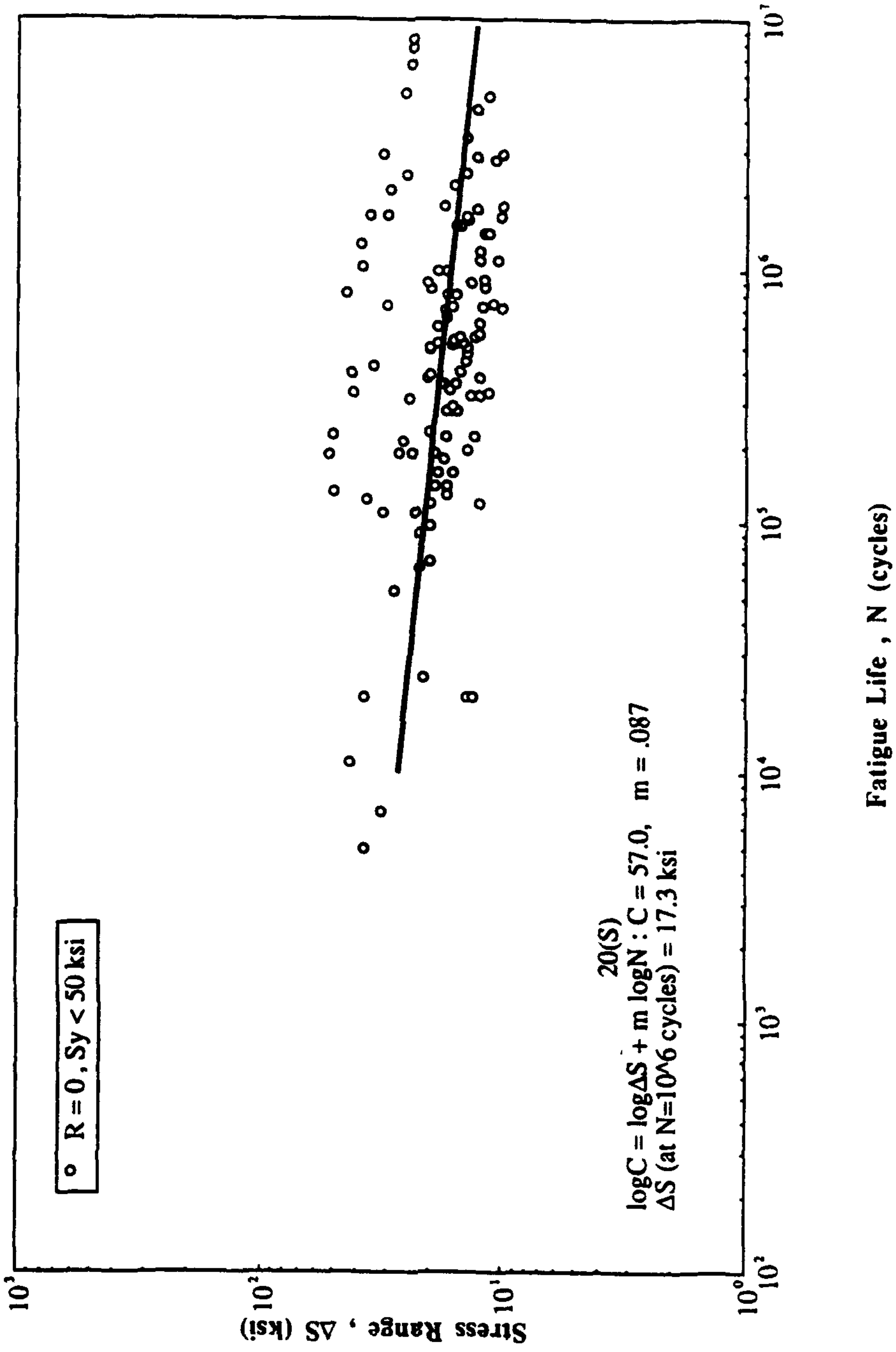

Fig. A-51 Detail Category 20(S)

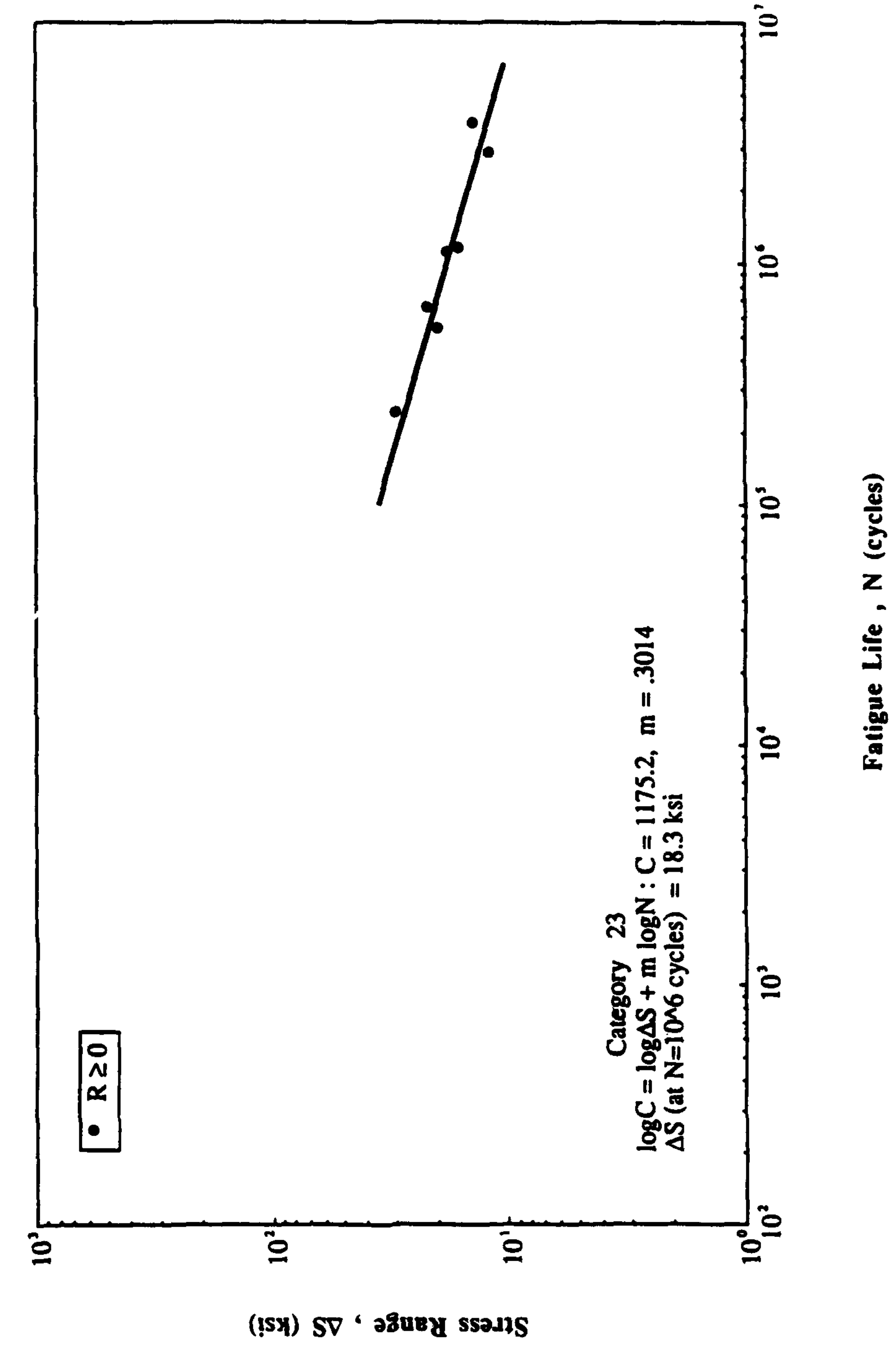

Fig. A-52 Detail Category 23

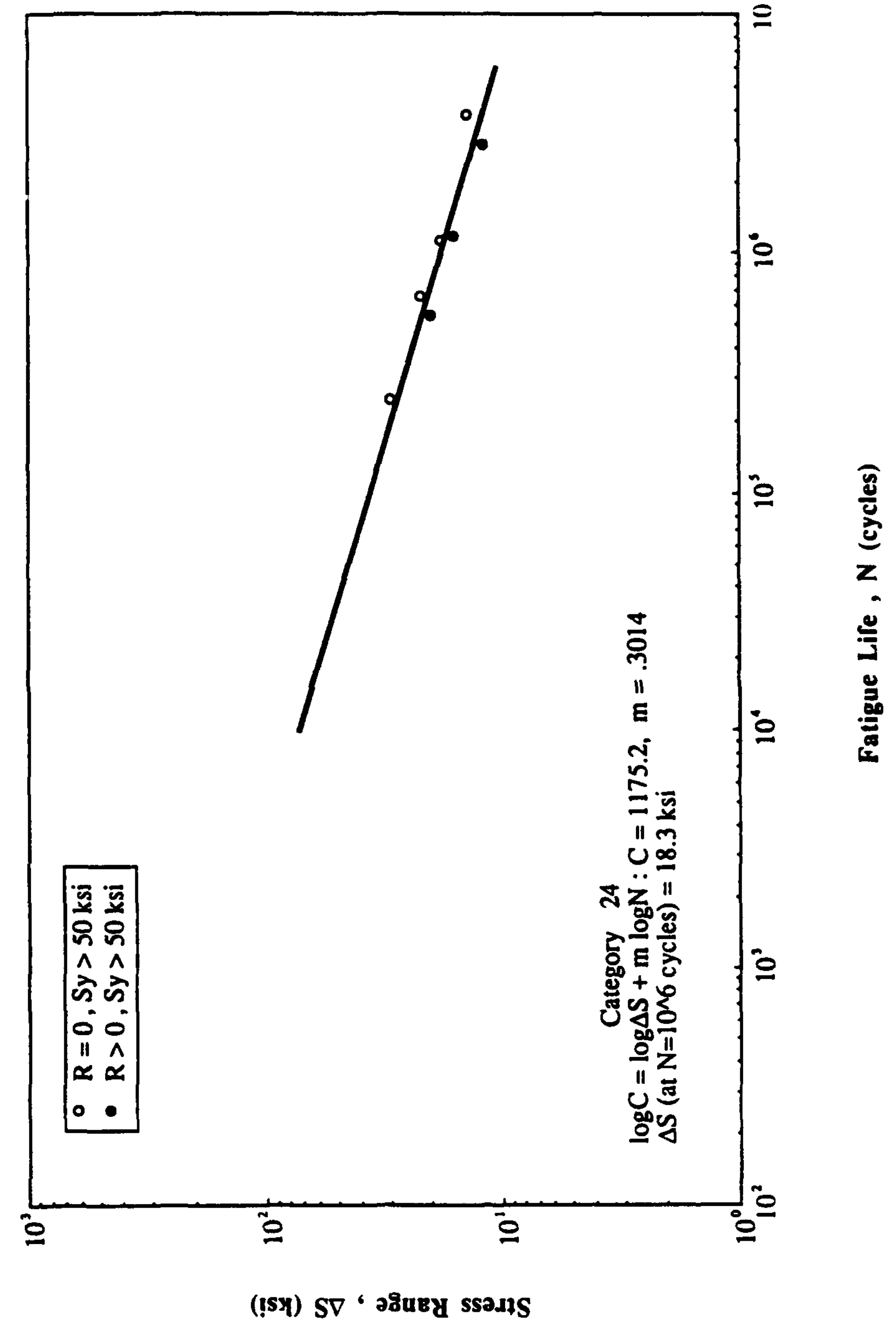

Fig. A-53 Detail Category 24

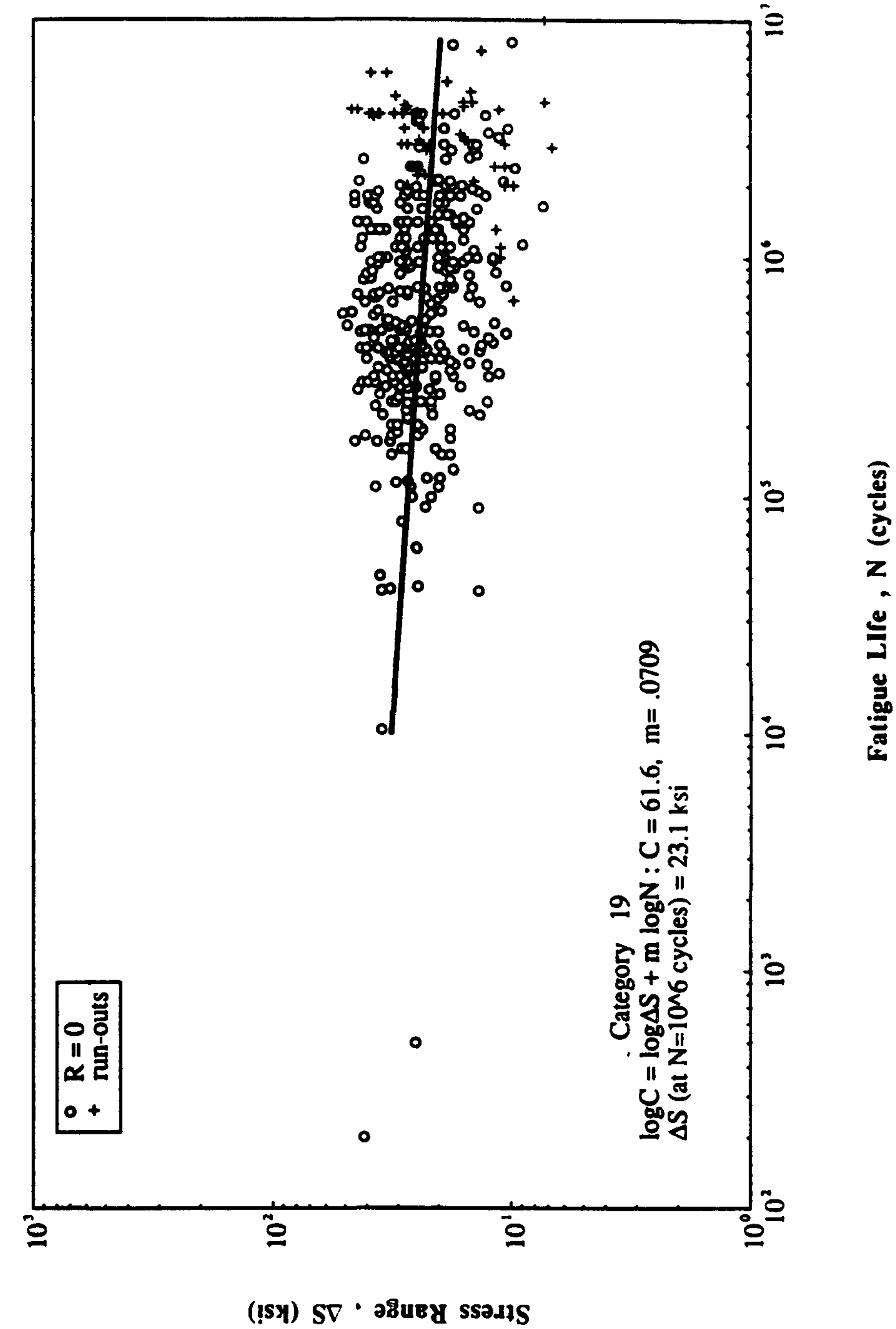

Fig. A-54 Detail Category 19

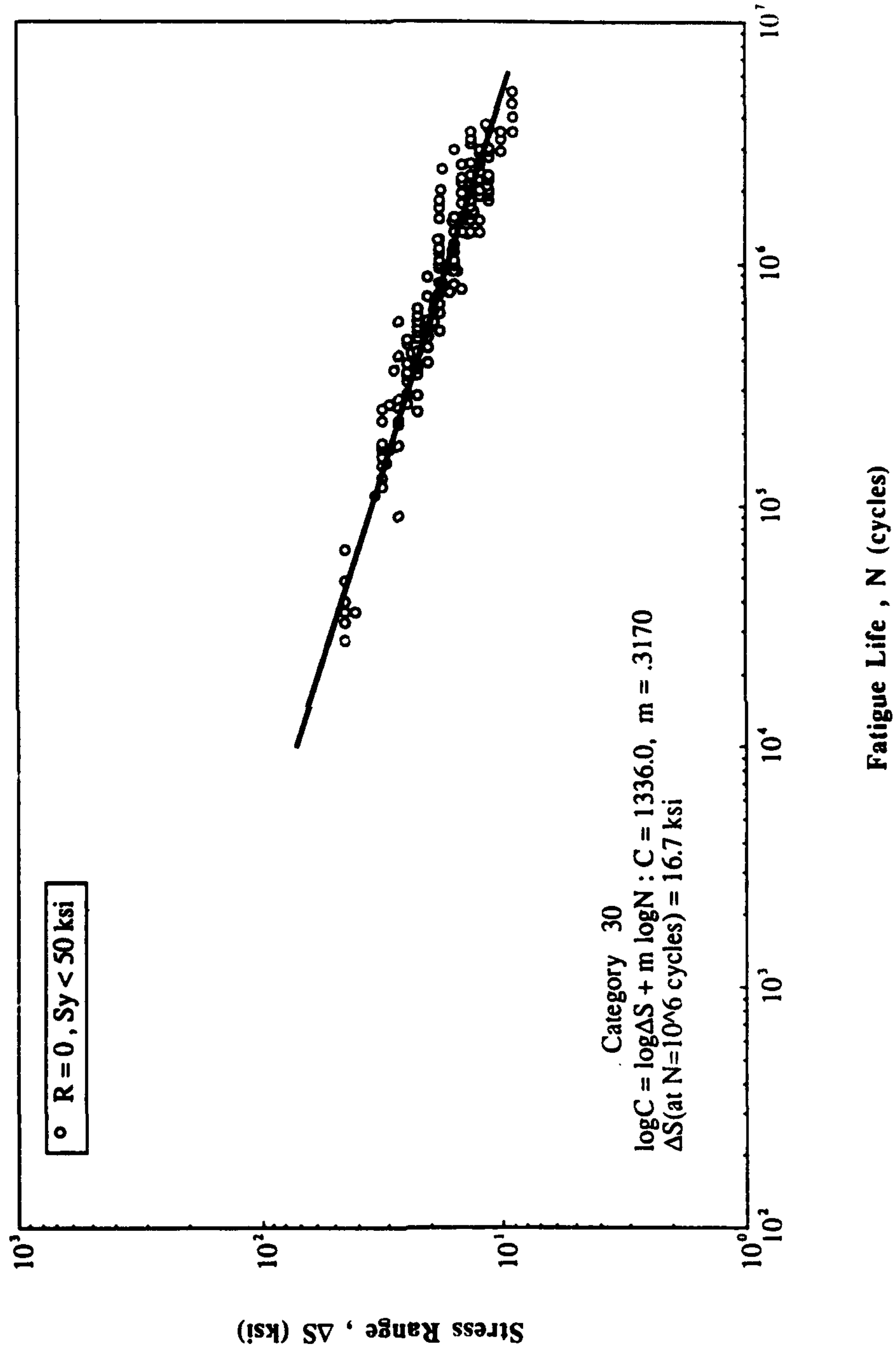

Fig. A-55 Detail Category 30

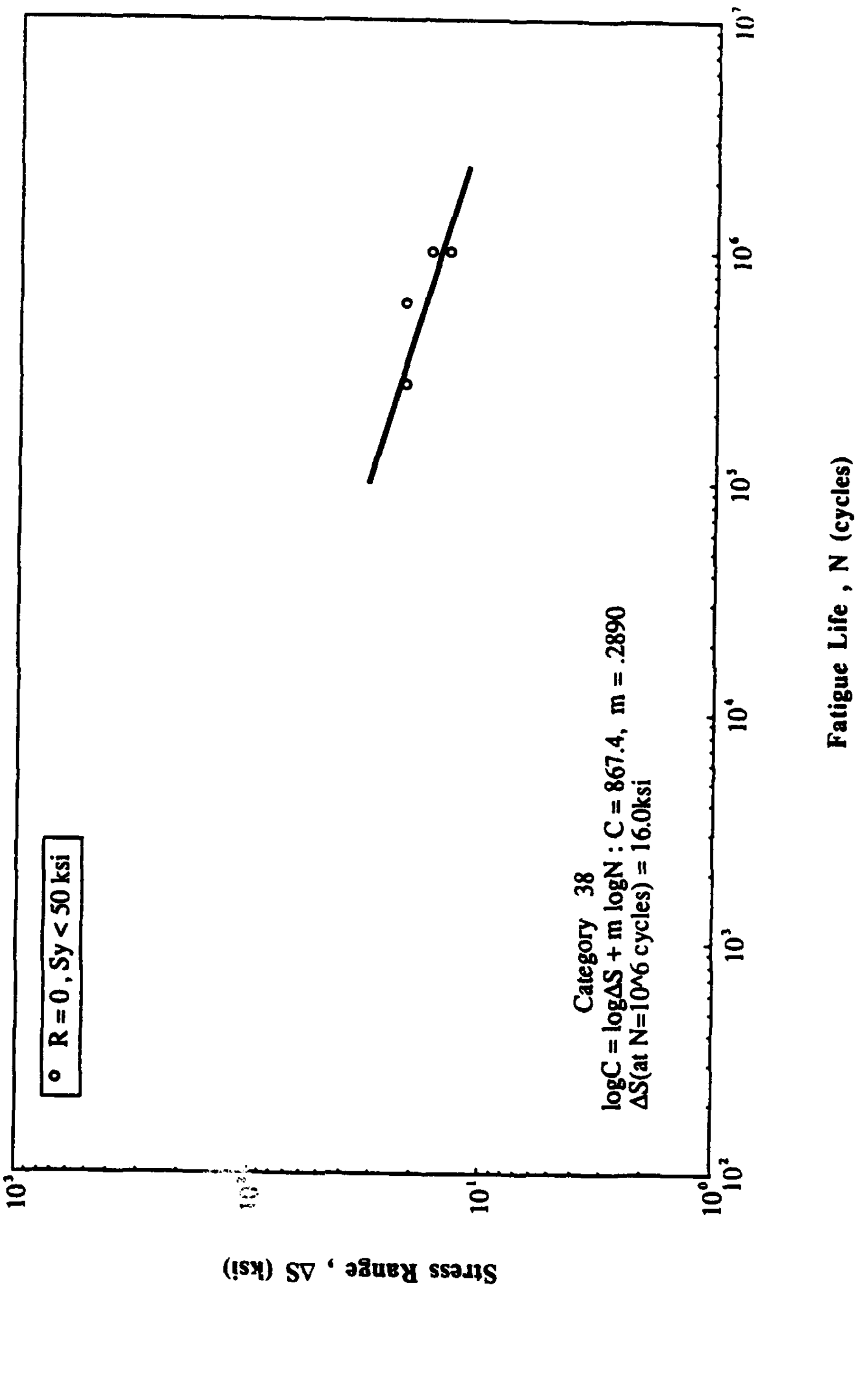

Fig. A-56 Detail Category 38

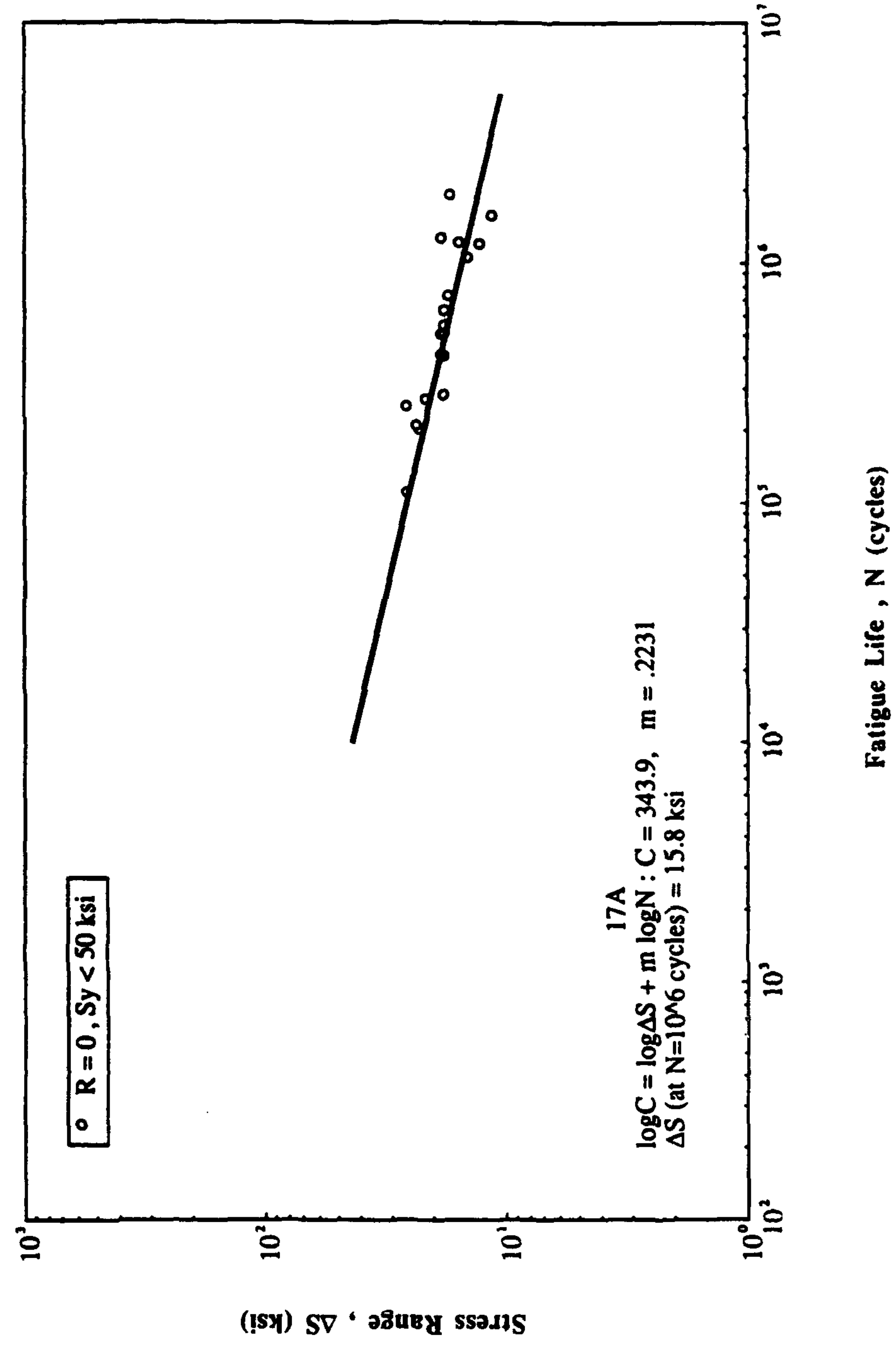

Fig. A-57 Detail Category 17A

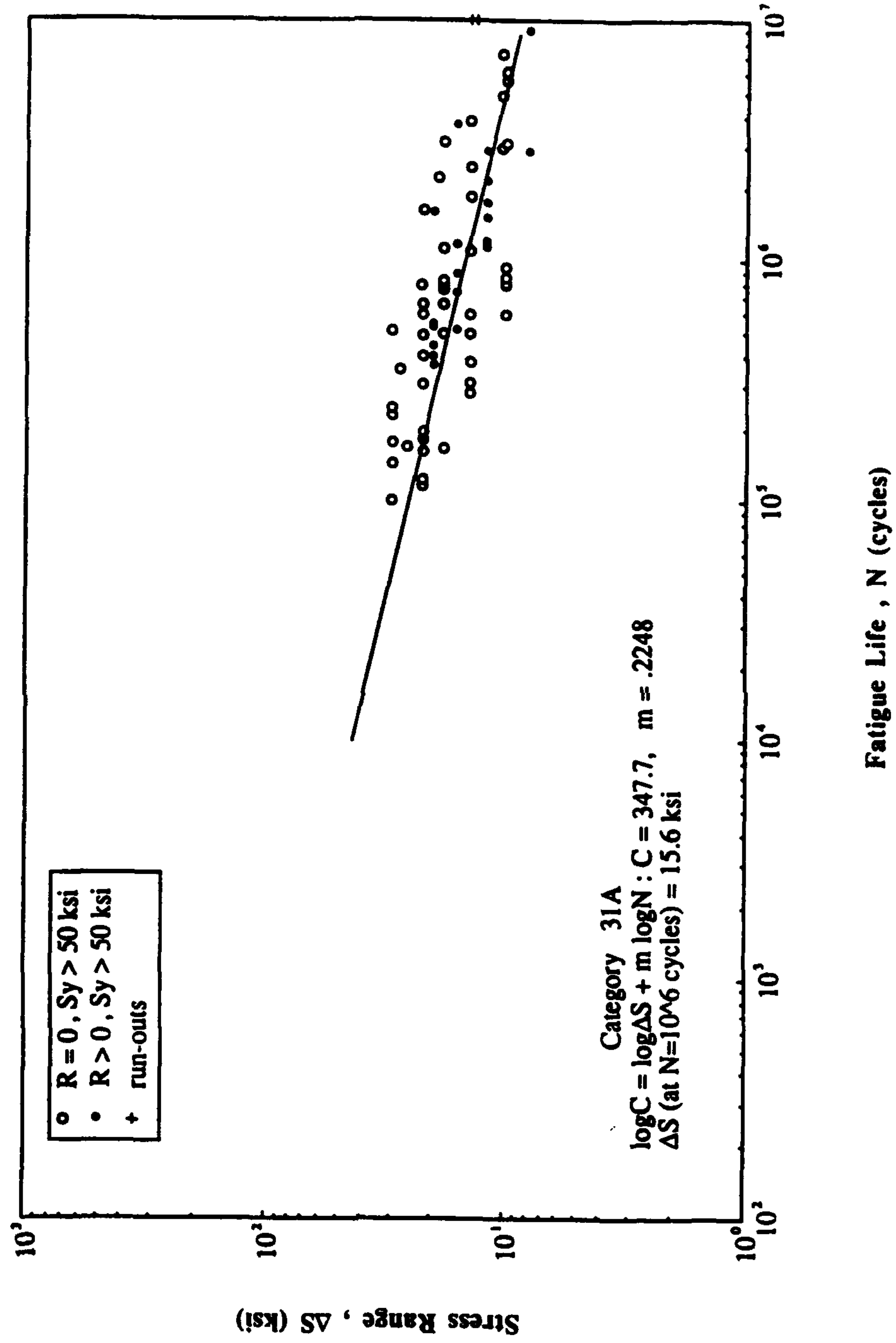

Fig. A-58 Detail Category 31A

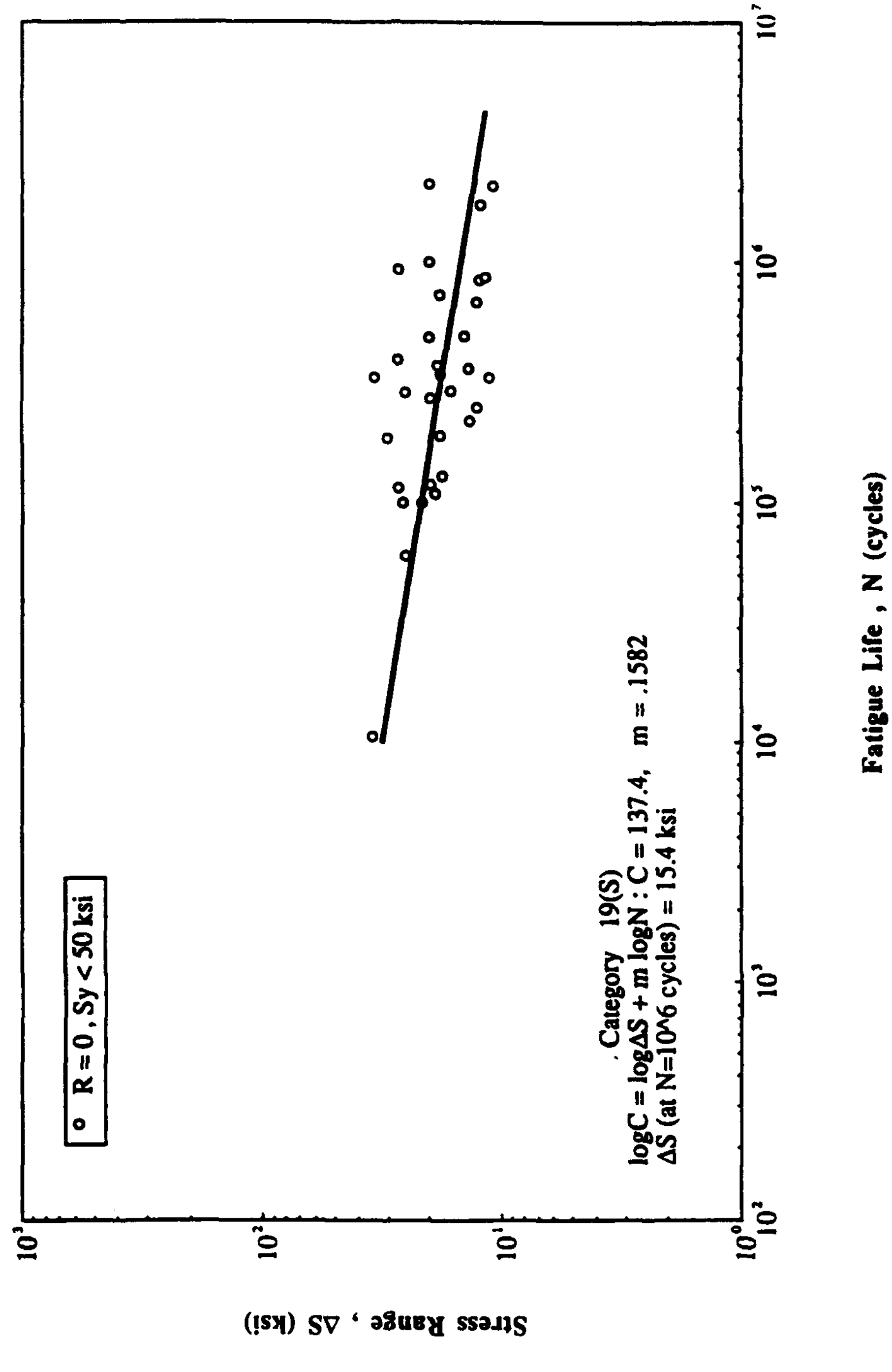

Fig. A-59 Detail Category 19(S)

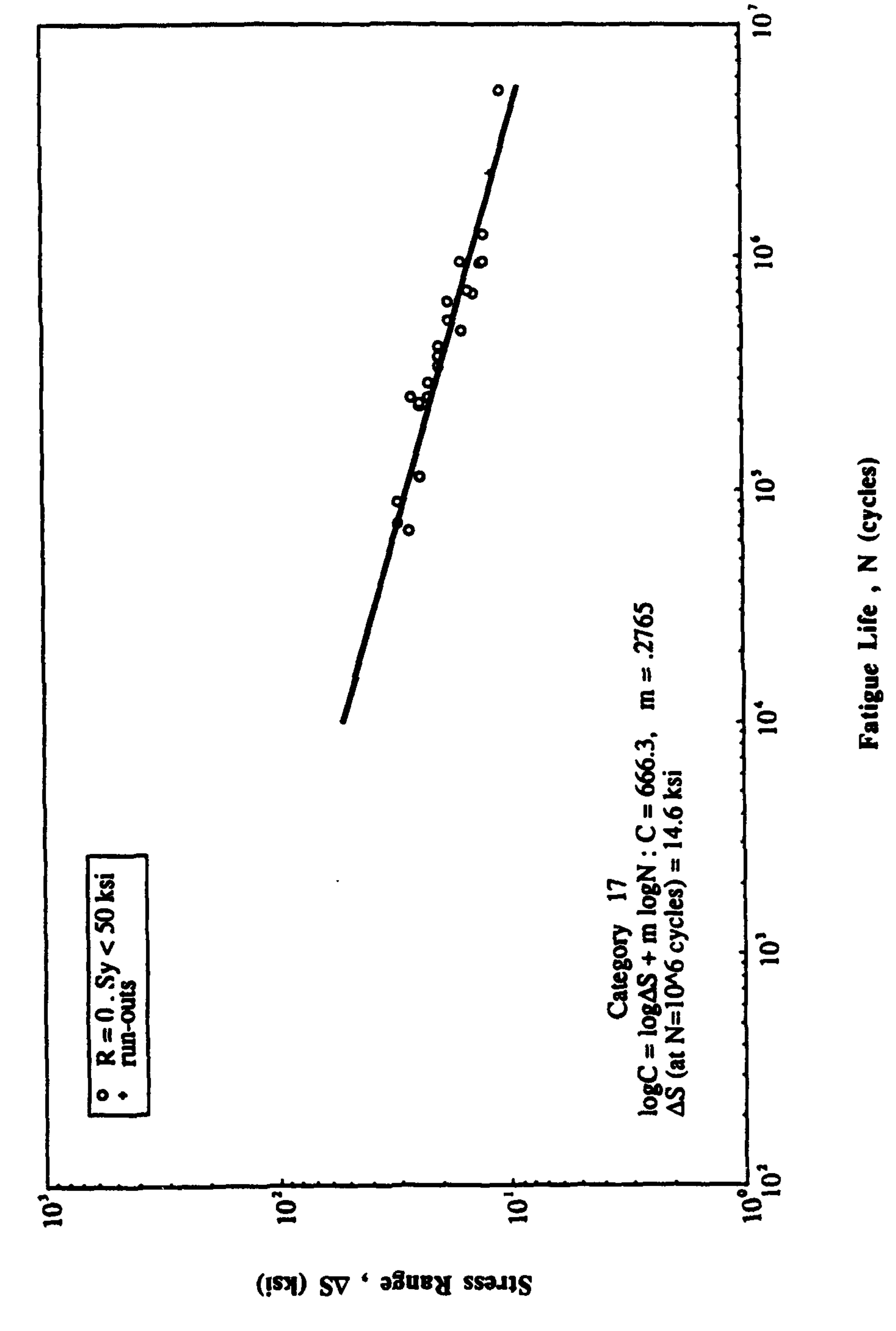

Fig. A-60 Detail Category 17

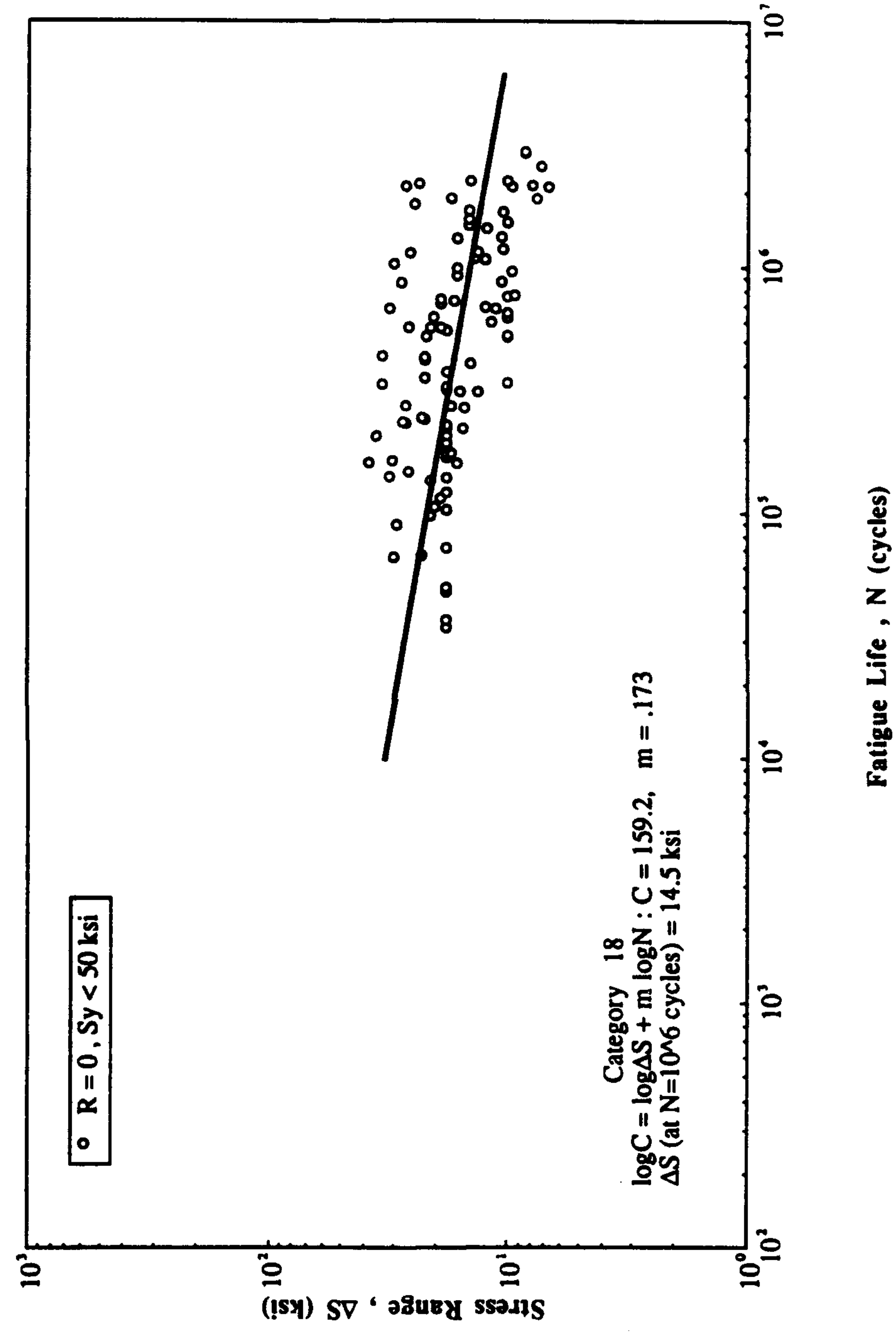

Fig. A-61 Detail Category 18

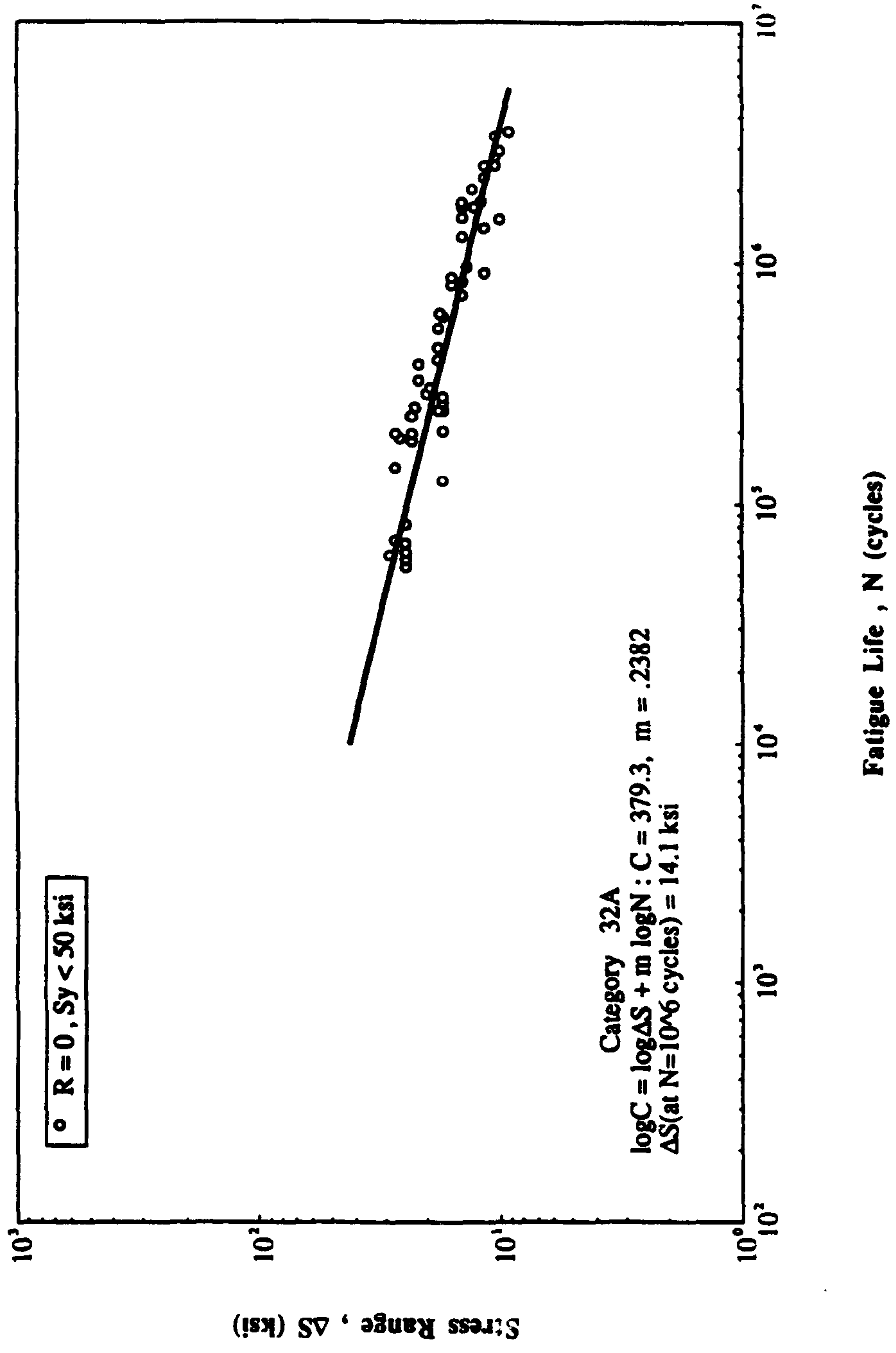

Fig. A-62 Detail Category 32A

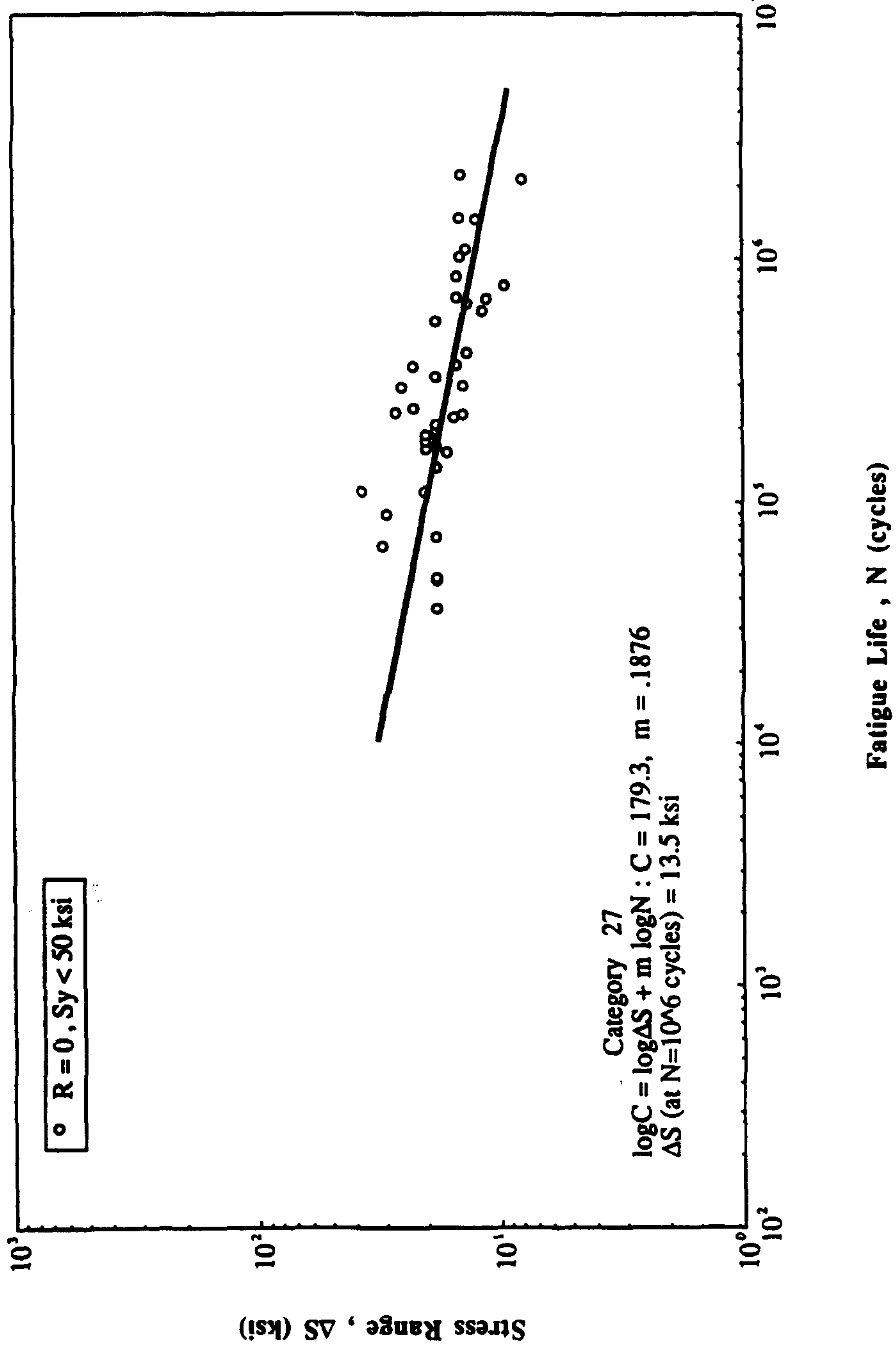

Fig. A-63 Detail Category 27

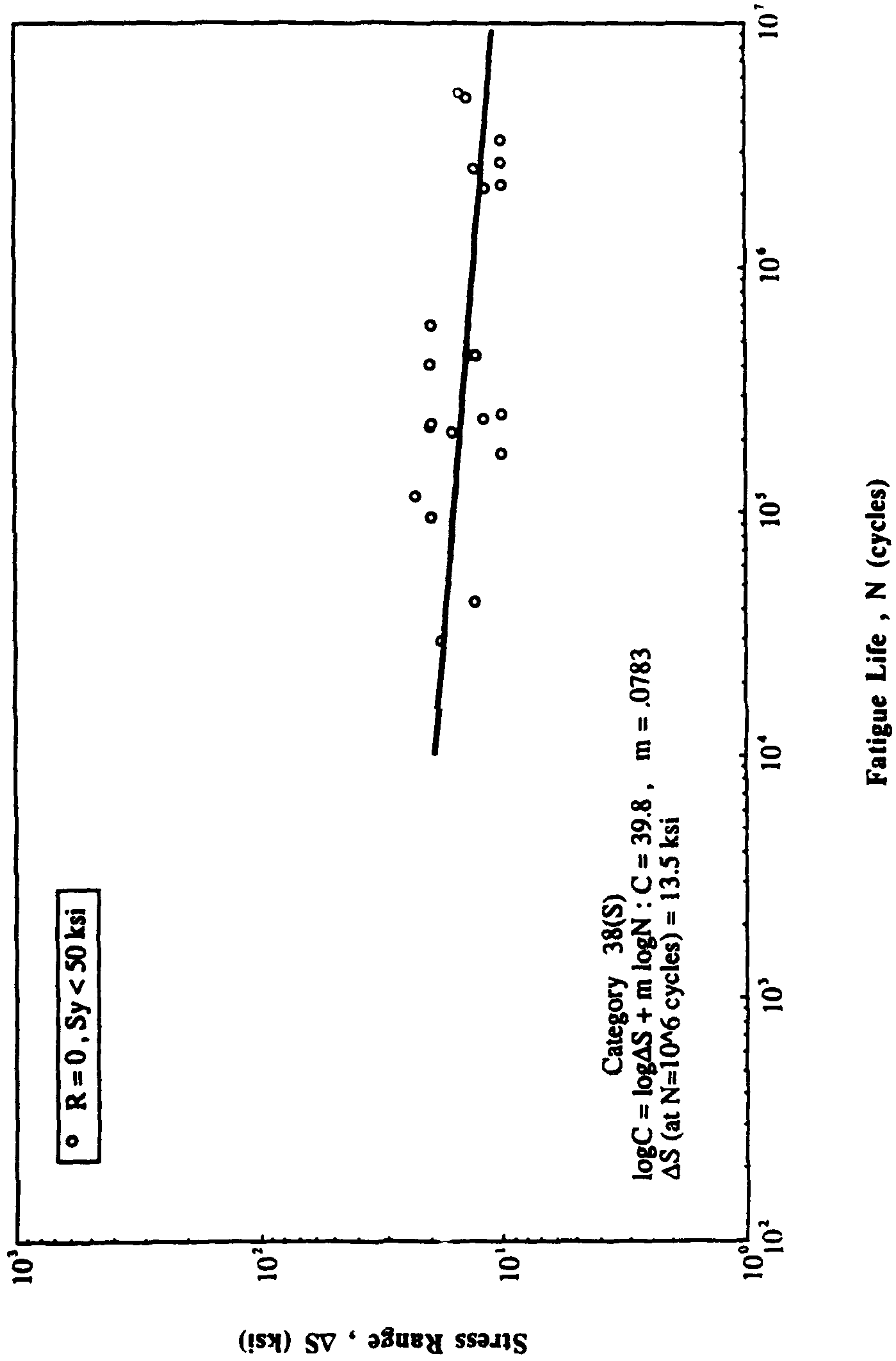

Fig. A-64 Detail Category 38(S)

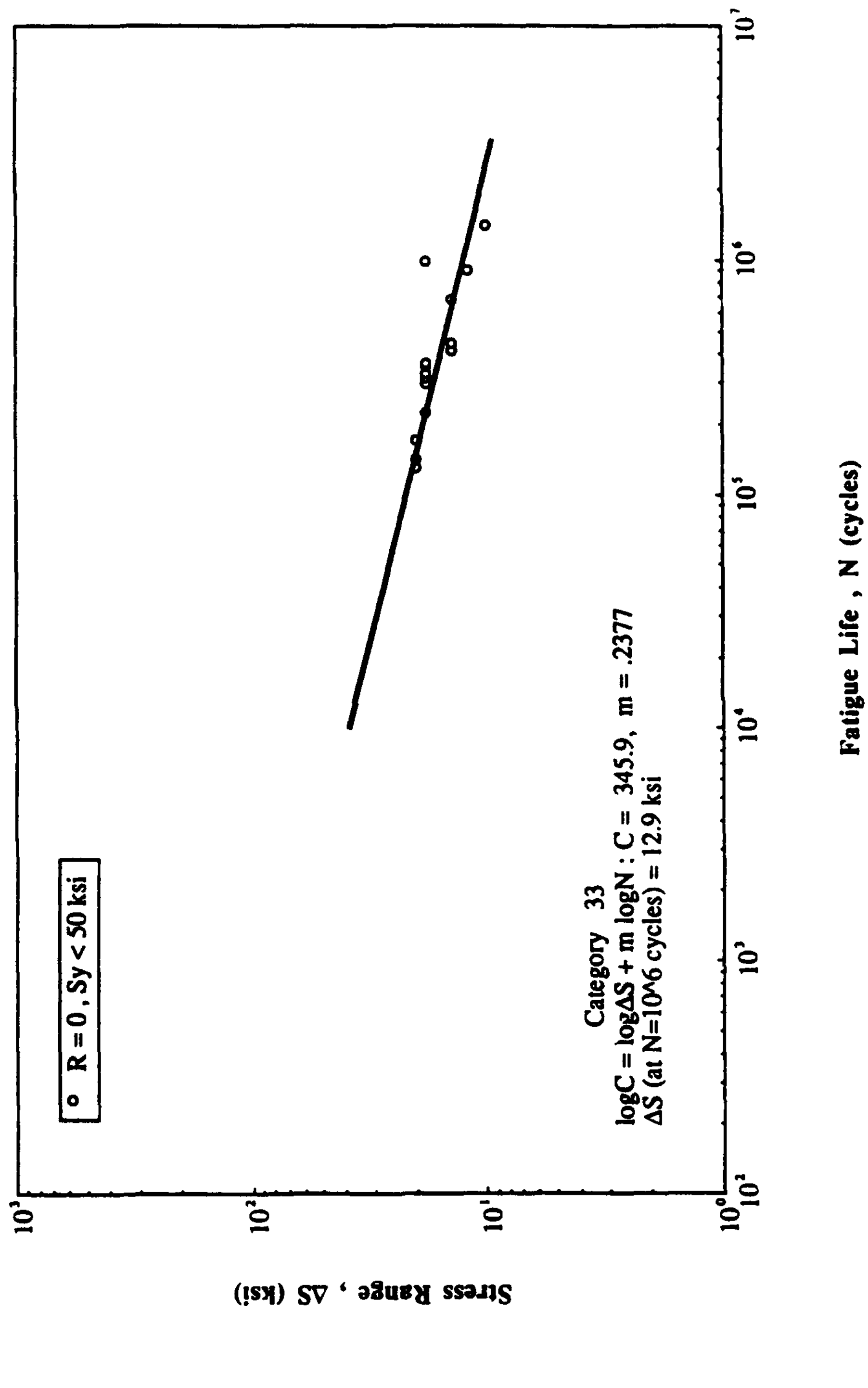

Fig. A-65 Detail Category 33

A-5 REFERENCES

A-1. Radziminiski, J. B., R., Srinivasan, D. Moore, C. Thrasher, and W. H. Munse (1973) "Fatigue Data Bank and Data Analysis Investigation," Structural Research Series No. 405, UILU-ENG-73-2025, University of Illinois at Urbana - Champaign.

A-2. Munse, W.H., T. W. Wilbur, M. L. Telalian, K. Nicol, K. Wilson (1983) "Fatigue Characterization of Fabricated Ship Details for Design," Ship Structure Committee Report SSC-318, Washington D.C.

A-3. Lawrence, F. V., Jr. and G. Banas (1990) "Fatigue Life Statistics for AISC Stress Categories (Task 1)," Report to Columbia Research Corporation, University of Illinois at Urbana - Champaign.

A-4. Stambaugh, K., private communication, February 1991.

A-5. Chang, S.-T. and F.V. Lawrence. "Improvement of Weld Fatigue Resistance," Fracture Control Program, Report No. 46, University of Illinois, January 1983.

A-6. Yung, J.-Y. and F.V. Lawrence, Jr., "Analytical And Graphical Aids for the Fatigue Design of Weldments," Fatigue Fract. Engng Mater. Struct., Vol. 8, NO. 3, pp 223-241, November 1985.

APPENDIX B

Thickness Effects in Welded Ship Details

B-1 <u>RECENT THINKING ON THE WELDMENT SIZE EFFECT</u>

B-1.1 EARLY CONCEPTS

There is currently much interest in the influence of weldment size on its fatigue strength at long lives. Most fatigue design curves were generated for welds fabricated from plates of 12.5 mm thickness. Unfortunately, the use of these design rules may overestimate the fatigue resistance of very large weldments. At present, for geometrically similar welds, larger weldments will sustain shorter fatigue lives; and in the U.K., the off-shore codes have recently been modified to reflect this effect of thickness (B-1).

The conclusion that thicker weldments should have shorter fatigue lives is suggested by analytical estimates of both the fatigue crack propagation lives and the fatigue crack initiation lives; however, the predicted influence of thickness is less for propagation than for initiation. Experimental evidence also confirms the existence of a size effect, but there is much scatter to this data (see Figure B-1). Thus, the magnitude of the thickness effect remains in question.

Gurney (B-2) suggests two empirical relationships based on experimental results:

$$\frac{S}{Sref} = \left(\frac{32}{t}\right)^{1/4} \quad \textit{for tubular joints} \tag{1}$$

$$\frac{S}{Sref} = \left(\frac{22}{t}\right)^{1/4} \quad \textit{for non-tubular joints} \tag{2}$$

where:

S	= Design stress at the thickness in question
S_{ref}	= Design stress for the reference thickness
t	= Thickness of weldment plates (mm)

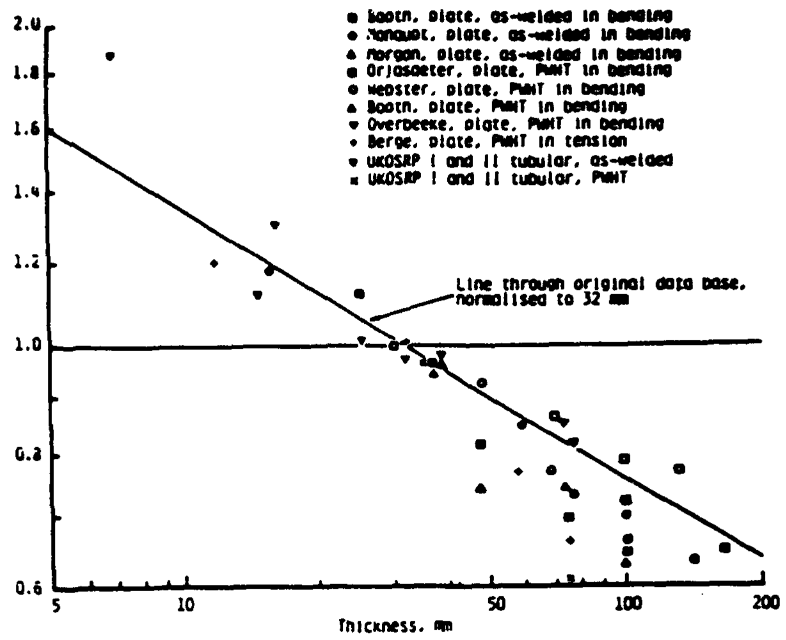

Fig. B-1 Relative fatigue strength at 10^6 cycles for various weld geometries and test conditions

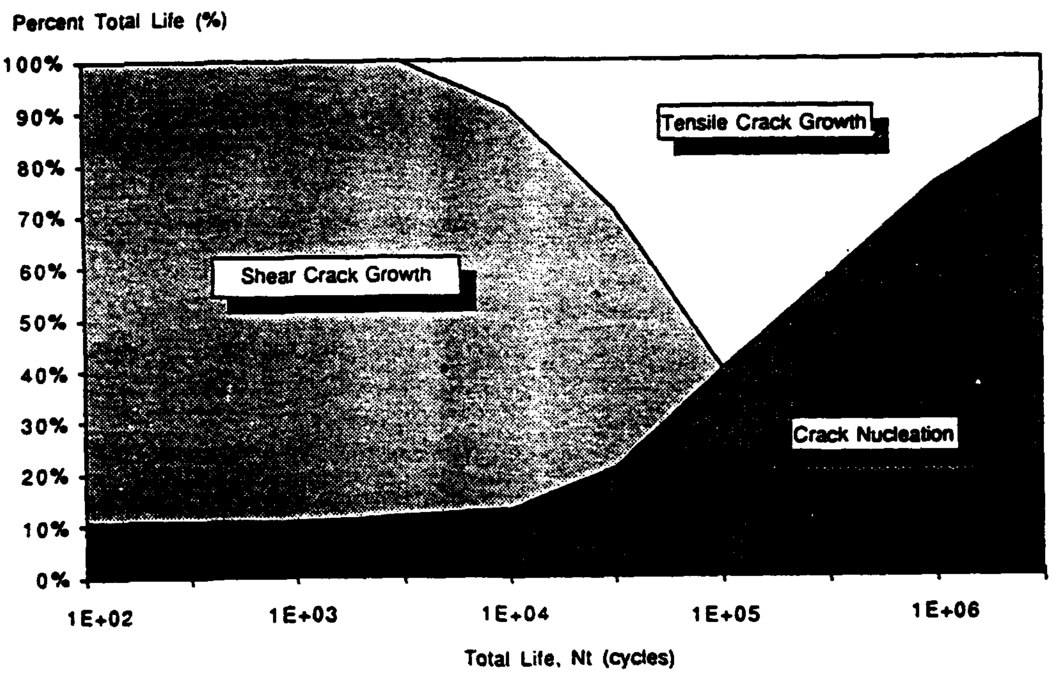

Fig. B-2 Relative importance of shear crack growth, tensile crack growth and crack nucleation as a function of total fatigue life for 1045 steel R=0

Smith (3) calculates the fatigue crack propagation lives of three weldments using fatigue crack propagation analyses, concluding that:

$$\frac{S_1}{S_2} = \left(\frac{t_1}{t_2}\right)^m \tag{3}$$

The value of the exponent m, which depends on geometry and loading condition, was found to be a function of thickness as well since the value of m for t < 22 mm appears to be less than that for t > 22 mm.

B-1.2 ANALYTICAL STUDIES BASED ON CRACK INITIATION

Yung and Lawrence (B-4) suggest that at long lives the fatigue life of weldments is principally governed by fatigue crack initiation; consequently, the thickness effect should be related to the fatigue notch factor for the weldment ($K_{f\,max}$), which in turn depends on the weld geometry, the nature of the applied loads, the strength of the material, and the weld thickness:

$$K_{f\ max}^{A} = 1 + 3.25e\text{-}3\alpha^{A} S_u^{0.9}\ t^{0.5} \tag{4}$$

$$K_{f\ max}^{B} = 1 + 3.25e\text{-}3\alpha^{B} S_u^{0.9}\ t^{0.5} \tag{5}$$

$$K_{f\ max}^{eff} = (1-x)K_{f\ max}^{A} + xK_{f\ max}^{B} \tag{6}$$

where:

$$x = S_\alpha^B / S_\alpha^T$$

$$S_\alpha^T = S_\alpha^A + S_\alpha^B$$

From Basquin's Law, Yung and Lawrence (B-4) derive an expression for the fatigue strength of weldments at long lives based on fatigue crack initiation:

$$S_\alpha^T = \frac{(\sigma'_f - \sigma_r)(2N_I)^b}{K_{f\,max}^{eff}\left(1 + \frac{1+R}{1-R}(2N_I)^b\right)} \tag{7}$$

Thus, the effect of thickness on the fatigue strength of weldments at long lives should be given by the expression:

$$\frac{S_1}{S_2} = \frac{K_{f\,max\,1}}{K_{f\,max\,2}} \tag{8}$$

For purely axial loading:

$$\frac{S_1}{S_2} = \frac{1 + 3.25e\text{-}3\alpha^A S_U^{0.9}\, t^{0.5}}{1 + 3.25e\text{-}3\alpha^B S_U^{0.9}\, t^{0.5}} \tag{9}$$

As shown in Figure B-2, fatigue crack initiation is expected to dominate in the long life region; consequently, Eq. 9 should describe the effect of thickness in this life period. According to Eq. 9, the influence of thickness on the long life fatigue strength of a weldment is modified by the ultimate strength of the notch root material and by the weldment geometry and loading condition (axial or bending). Consequently, the thickness effect should depend on the material (S_u), the life range (N_t), the weld geometry (α), the nature of the applied loads, as well as the absolute size of the weldment itself (t). Figure B-3 shows the predictions made using Eq. 9 compared with the work of Gurney (B-2) and Smith (B-3).

B-1.3 CURRENT SITUATION

Most recent thinking on the thickness effect was summarized at the 9th International Conference on Offshore Mechanics and Arctic Engineering in Houston, May 1990 (B-5 - B-11). An entire session was devoted to the topic; and the papers and subsequent panel discussion showed that controversy still surrounds this topic. Discussion of weld fatigue strength and the influence of size, complex in itself, is further complicated by several definitions of stress: nominal stress at the location of the notch, notch root stress (hot-spot stress), etc.

The controversy breaks into two positions. The European view (B-6) is that thickness can be entirely explained in terms of linear elastic fracture mechanics and is the result of a constant initial crack size (a_0) propagating through weldments of different thickness. This view does not admit any advantage to weld profiling or control of weld toe geometry or residual stress. The U.S. view (B-5) accepts the importance of the notch severity provided by the weld toe.

Most agree, however, that the original value of m (proposed by Gurney) of 1/4 is too low and that a value of 1/3 is more likely the proper value for weldments. The persistent problem is the lack of a comprehensive theory which can predict the fatigue life of a weldment, deal with the many variables which influence fatigue life, and predict the effect of thickness on a weldment's fatigue behavior.

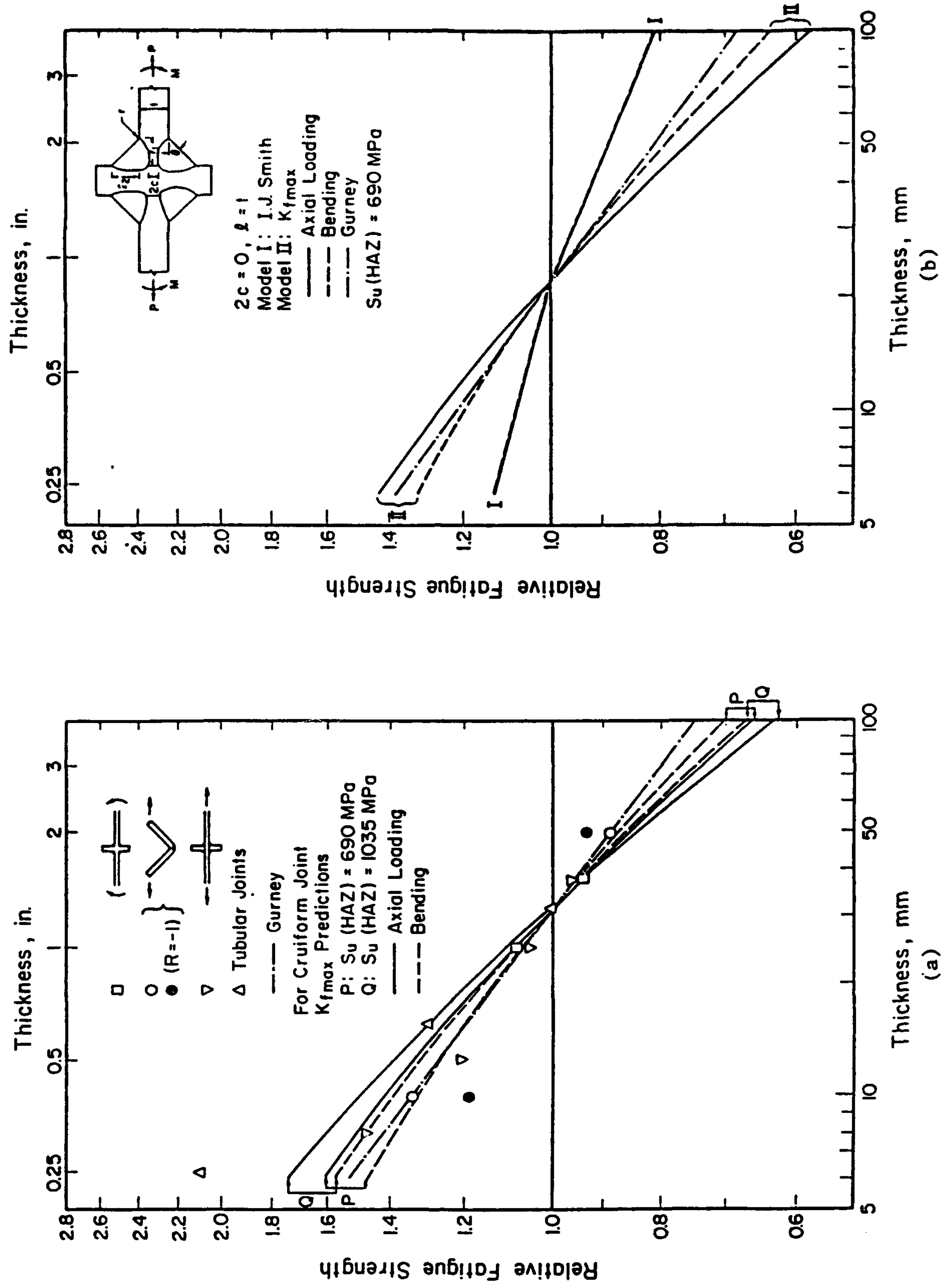

Fig. B-3 Predictions of the I-P Model compared with work of Gurney and Smith

B-2 EFFECT OF WELDMENT THICKNESS PREDICTED BY THE I-P MODEL

B-2.1 THE INITIATION-PROPAGATION MODEL FOR WELDMENT FATIGUE LIFE

The total fatigue life of a weldment (N_T) comprises a period devoted to fatigue crack initiation and early growth (N_I) and one devoted to the growth of a dominant crack (N_P):

$$N_T = N_I + N_P \tag{10}$$

Lawrence and his colleagues at the UIUC have during the last fifteen years developed an analytical model (called the I-P Model of Total Life Model) for estimating the fatigue life of weldments by summing independent estimates of N_I (using Eq. 7) and N_P using the Paris power law:

$$N_P = \frac{1}{C}\int_{\alpha_I}^{\alpha_f} \Delta K(\alpha)^{-n} d\alpha \tag{11}$$

To explore the influence of thickness on structural weldments, the N_T of steel weldments was estimated using Eqs. 7, 10 and 11. To operate the model, it is necessary to make the assumptions discussed below.

B-2.2 ASSUMPTIONS FOR ESTIMATES OF N_I

Similitude: It was assumed that all dimensions except the notch root radius remained in the same proportions as the plate thickness. The critical value of the notch root radius was kept constant at a value numerically equal to the material constant in Peterson's Equation (B-12).

Material: The material properties of ASTM A36 steel weldments were the only ones assumed by the study. Note from Eq. 9 that S_u is as influential a variable as α which describes the effect of the weld geometry and loading conditions. The properties of the HAZ were estimated from assumed nominal base material properties after McMahon (B-13) and from the work of Higashida (B-14).

Loading: Constant amplitude, pure axial loading was assumed. A load ratio of R=0 was assumed. This assumption diminishes the importance of N_I as predicted by Eq. 7. Under R=-1 conditions, N_I would be much larger.

Weld geometry: Three values of K_f at a thickness of 25 mm were assumed. These values correspond to the K_f values for weldments of Categories B, D, and F; that is, they had values of $K_{f\,max}$ equal to 2.0, 3.0, and 5.0 for weldments of 25 mm thickness. (Note that the K_f of a given geometrically similar weldment increases with thickness as described by Eq. 9.) The estimates of K_f for the weld categories were taken from the AISC Bridge Fatigue Guide (B-15) Table 1.3.13B and calculated as the ratio of the design stresses for AISC weld category A to the design stress of the category in question. The K_f for AISC category A (A36 plane plate) was taken to be 1.43 as suggested by Chang (B-16).

Residual stresses: It was assumed that the weldments were in the as-welded state; that is, the residual stresses were equal to the yield strength of the base metal.

B-2.3 ASSUMPTIONS FOR ESTIMATES OF N_P

Similitude: It was assumed that all dimensions except the initial value of fatigue crack length remained in the same proportions as the plate thickness. The initial value of the crack length was kept constant. It was also assumed that the weld toe had a constant radius equal to Peterson's material constant "a".

Geometry factor for N_p estimates: An expression for M_k given by Ho (B-17) for cruciform weldments under axial loads was used and rewritten in terms of K_f max since $2(K_{f\,max} - 1) = K_{t(a)} - 1$ for the worst case notch (B-12).

$$M_k = 1 + 2(K_{f\,max} - 1) \exp\left(-44.0(K_{f\,max} - 1)^{0.85\,a/t}\right) \tag{12}$$

Loading: Constant amplitude, pure axial loading was assumed. A load ratio of R=0 was assumed. $\Delta K = Y\Delta S\surd(\pi a_i)$. The effect of residual stresses was ignored.

Initial and final fatigue crack lengths: An initial crack length $a_0 = 0.1$ mm and a final crack length $a_f = 0.4t$ were assumed.

B-2.4 PREDICTED S-N DIAGRAMS

Figures B-4 through B-9 give the estimated S-N diagrams for AISC Categories B, D, and F weldments of 25 and 100 mm thickness under constant amplitude, R=0, axial loading. In each of these figures, the estimates of N_I, N_P and N_T are plotted. Because of interest in long-life behavior (lives of 10^6 and 10^7 cycles) most of the S-N curves have been developed principally for this life regime. As seen in Figures B-4, B-5, and B-6, N_I dominates the N_T of weldments in AISC Category B for both thicknesses and in AISC Category D for the 25 mm thickness. N_P dominates the N_T of Category F for both thicknesses and in Category D in the 100 mm thickness as seen in Figures B-7, B-8 and B-9. Figure B-10 compares the N_T estimates for the six case studies.

Except for AISC Category D, for which the UIUC Fatigue data base gives peculiar estimates, there is excellent agreement between the blind predictions given by the model and the UIUC fatigue data base, as is seen in the table below. The best fit lines to the UIUC data bank information reflect test data for all

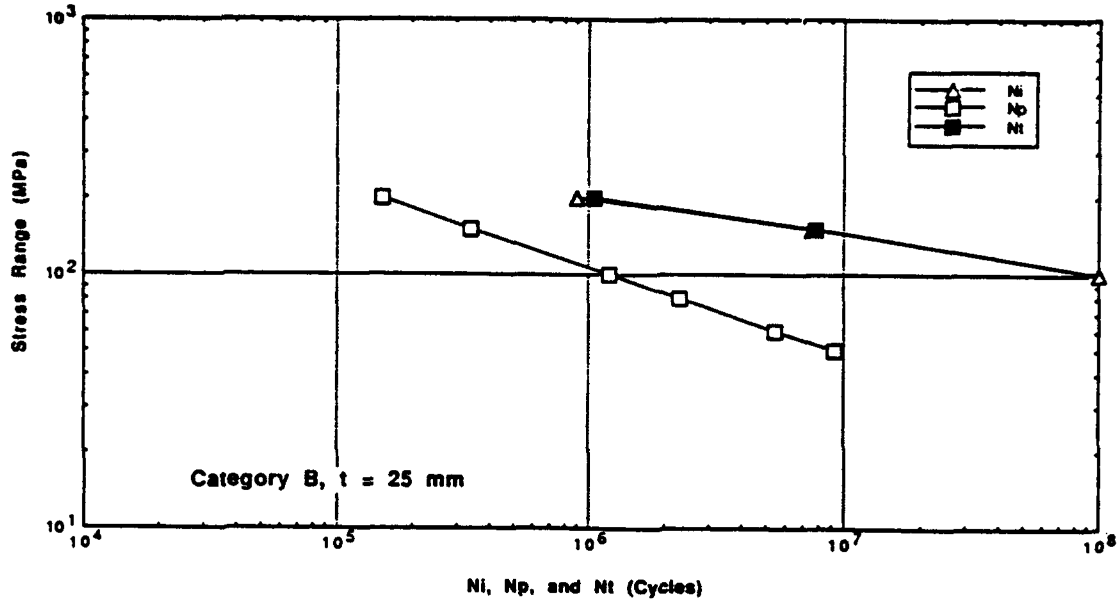

Fig. B-4 **Predicted N_I, N_p and N_T for Category B A36 steel weldments. Thickness = 25mm, K_{fmax} = 2.0.**

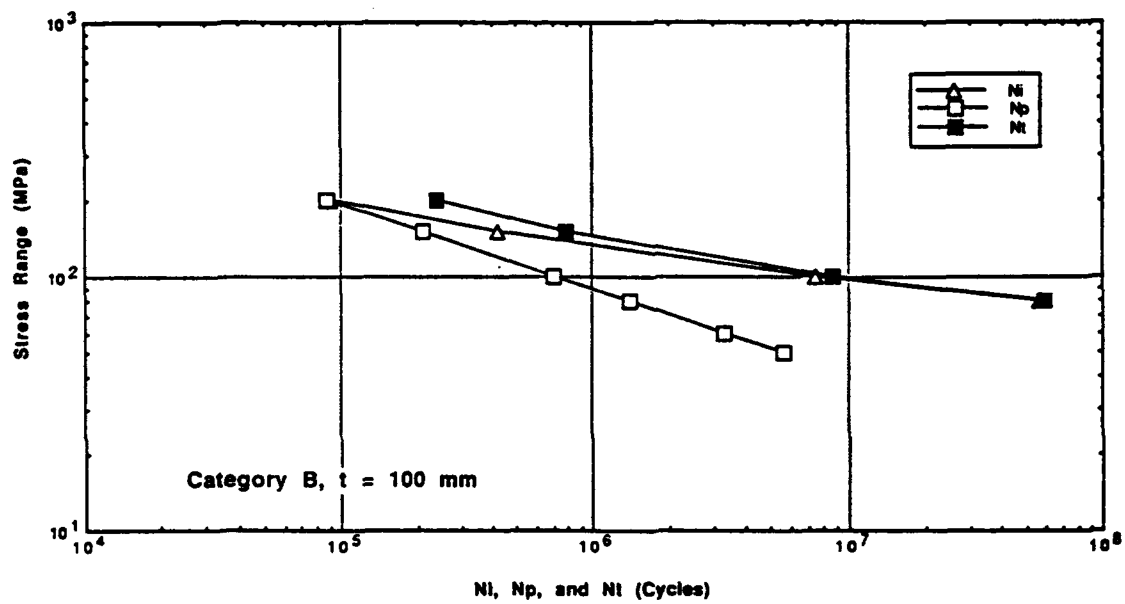

Fig. B-5 **Predicted N_I, N_p and N_T for Category B A36 steel weldments. Thickness = 100mm, K_{fmax} = 3.0.**

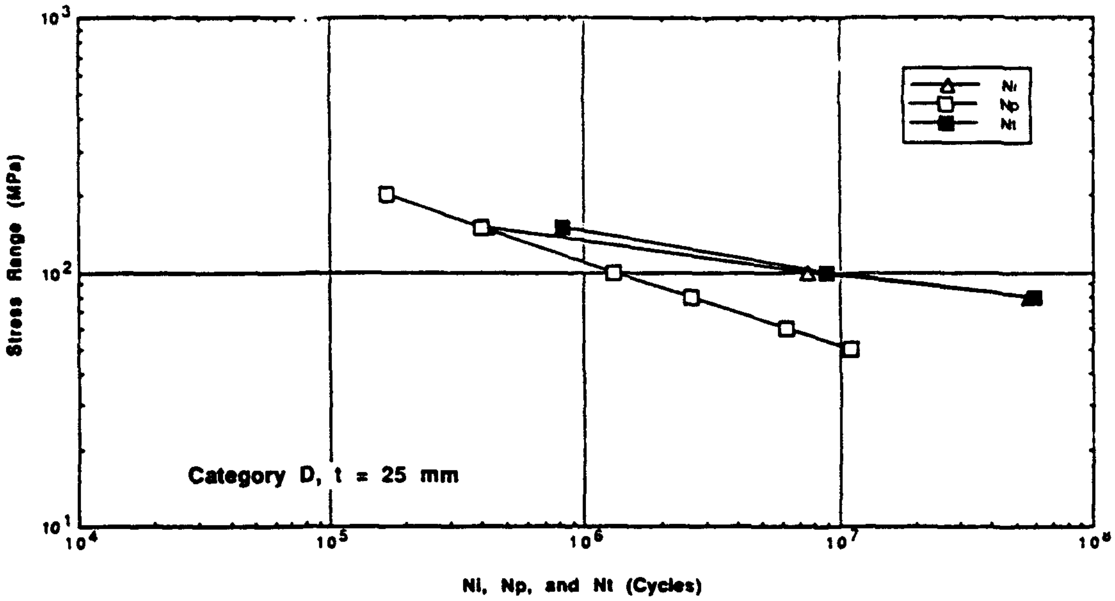

Fig. B-6 Predicted N_I, N_p and N_T for Category D A36 steel weldments. Thickness = 25mm, K_{fmax} = 3.0.

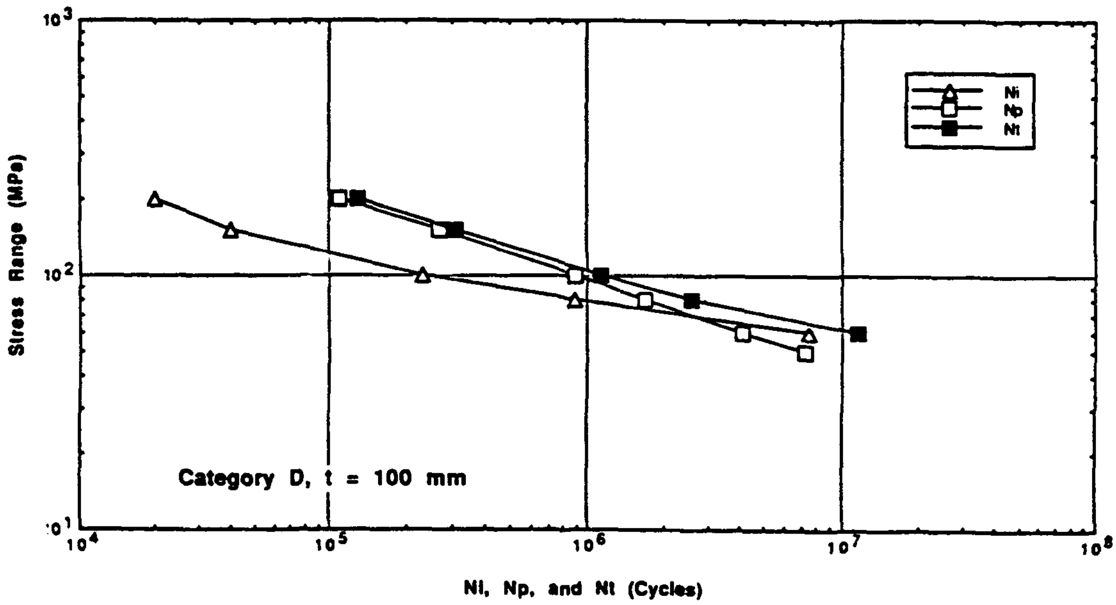

Fig. B-7 Predicted N_I, N_p and N_T for Category D A36 steel weldments. Thickness = 100mm, K_{fmax} = 5.0.

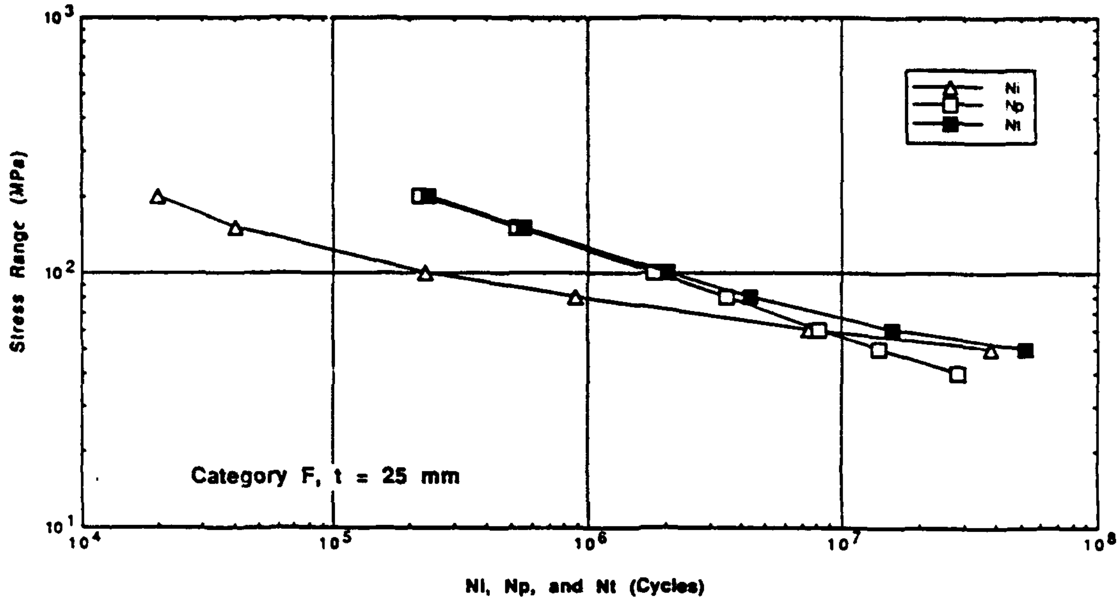

Fig. B-8 Predicted N_I, N_p and N_T for Category F A36 steel weldments. Thickness = 25mm, K_{fmax} = 5.0.

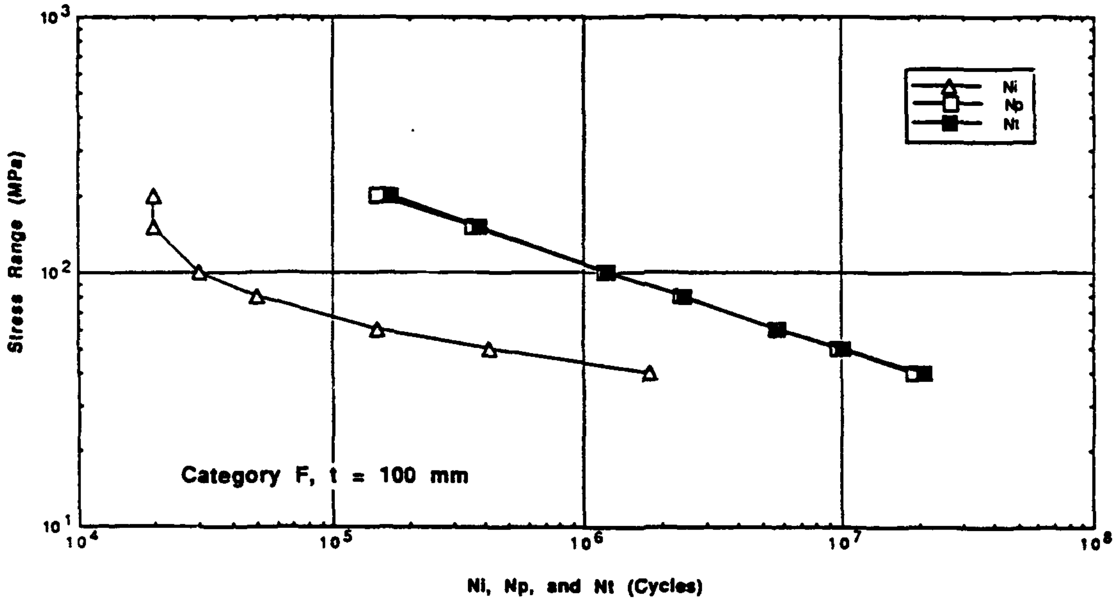

Fig. B-9 Predicted N_I, N_p and N_T for Category F A36 steel weldments. Thickness = 100mm, K_{fmax} = 9.0.

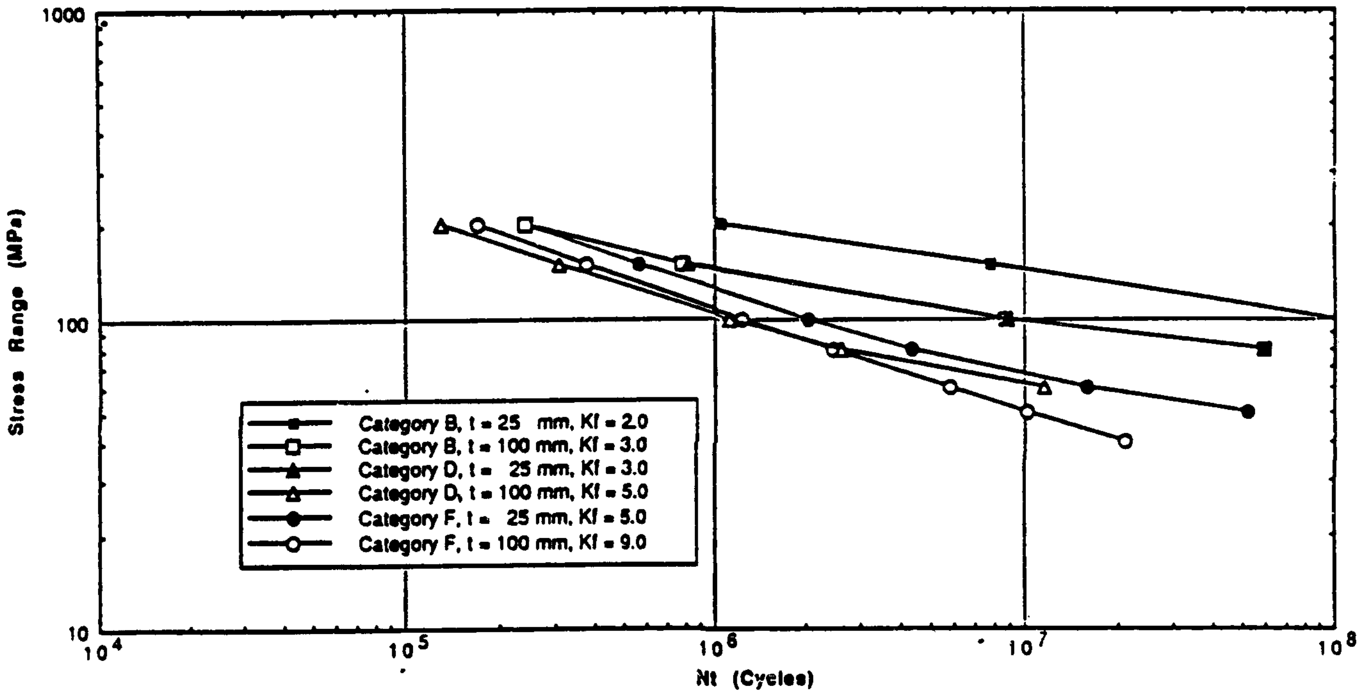

Fig. B-10 Predicted N_T for Category B, D and F A36 steel weldments. Thickness = 25 and 100mm.

materials and R ratios listed in the data base. Thus agreement between the UIUC data bank's mean S-N curves and the blind predictions for the general A36 steel weldment is quite good. The UIUC data bank regression analysis for AISC Category D was somewhat strange.

B-2.5 PREDICTED EFFECT OF PLATE THICKNESS

The calculated effect of plate thickness on the fatigue strength at 10^6 cycles for AISC categories B, D and F are given in Figure B-11. Also given in this figure are data of Booth (B-7) for AISC Category F detail tested in bending.

Detail	Calc. ΔS $N_T = 10^6$ cycles (MPa)	Exp. ΔS $N_T = 10^6$ cycles (MPa)	Calc. ΔS $N_T = 10^7$ cycles (MPa)	Exp. ΔS $N_T = 10^7$ cycles (MPa)
Category B	200	195	145	131
Category D	144	187	98	156
Category E	-	113	-	78
Category F	125	109	65	75

While the comparison is strained because the weldment was tested in four-point bending and because the estimates are for axial loading, the similarity between the trends for AISC Categories D and F and the experimental data reinforce confidence in the calculations made using the I-P model.

Figures B-12 and B-13 show the predicted effect of plate thickness on relative fatigue strength (S/S_{ref}). In this study, the reference thickness was taken as 25 mm. At 10^6 cycles, the fatigue strengths of the AISC Categories F and D weldments agree most closely with the m = -1/4 power dependence, particularly in the case of AISC Category D weldments of very large thickness (see Figure B-12). At 10^7 cycles, all weldments except those with the most severe geometries follow a m = -1/3 power

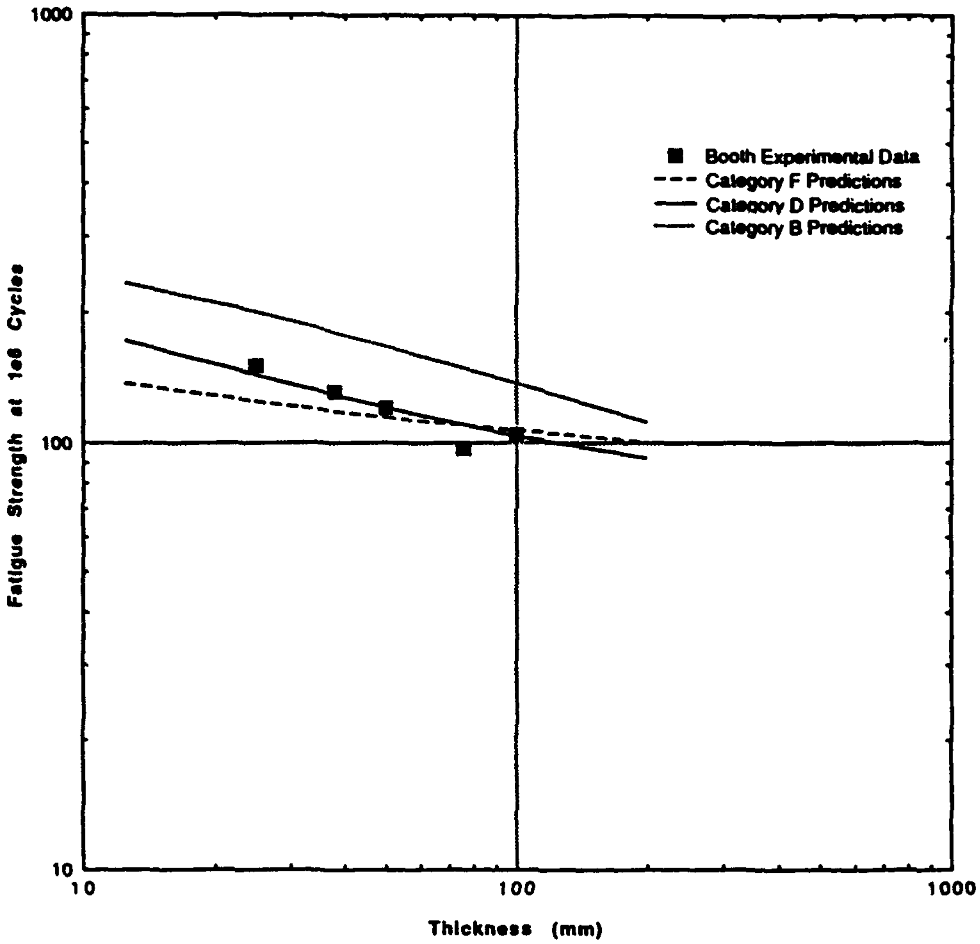

Fig. B-11 Predicted fatigue strength at 10^6 cycles for A36 steel weldments of Category B, D, and F (under axial loading).

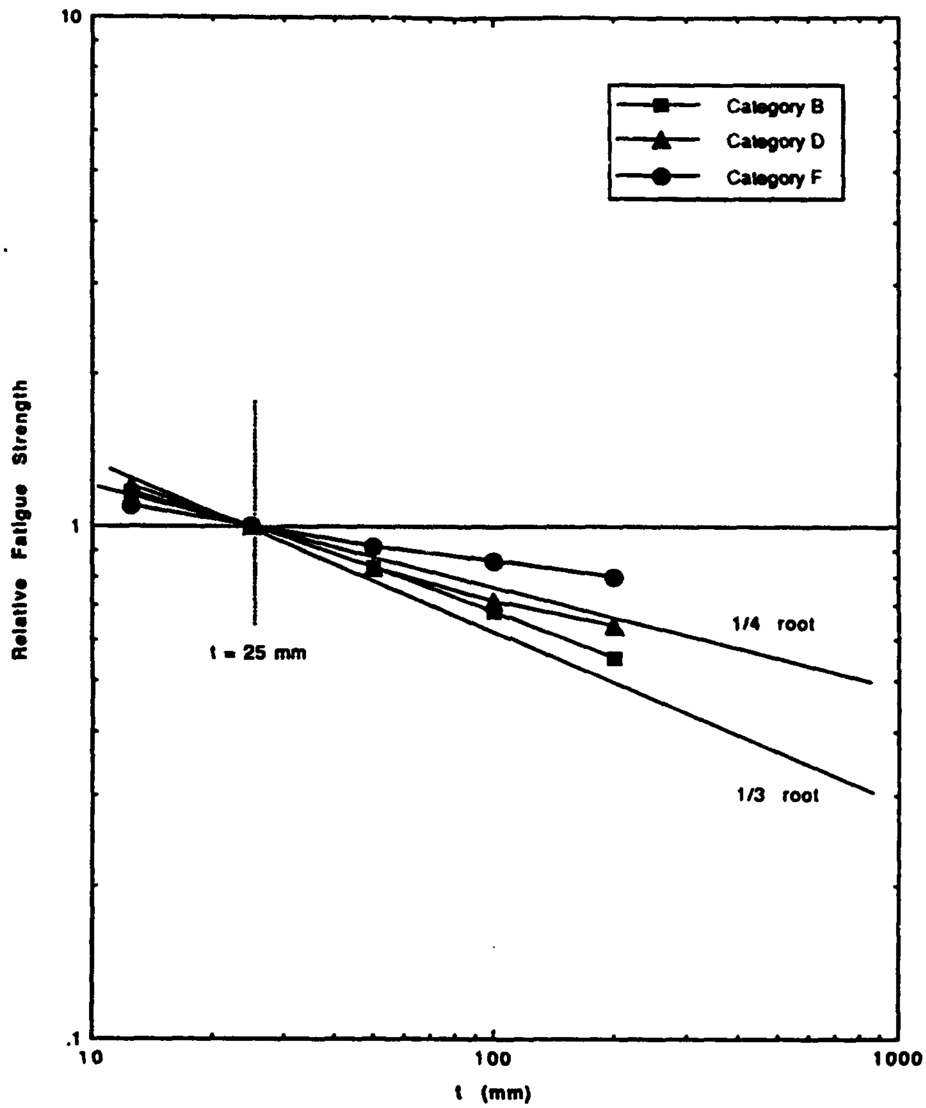

Fig. B-12 Predicted relative fatigue strength at 10^6 cycles versus plate thickness for Category B, D and F A36 steel weldments. Fatigue strengths were normalized to the values calculated for t=25mm.

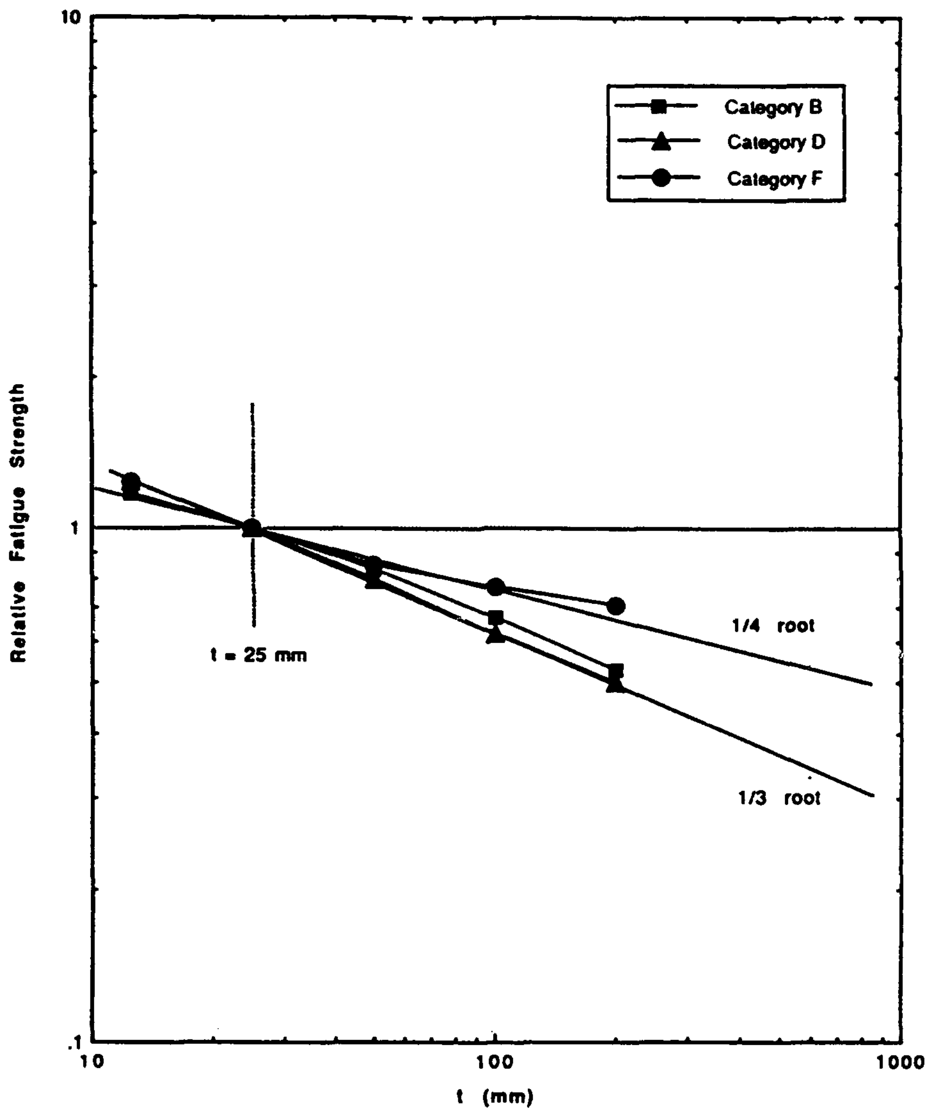

Fig. B-13 Predicted relative fatigue strength at 10^7 cycles versus plate thickness for Category B, D and F A36 steel weldments. Fatigue strengths were normalized to the values calculated for t=25mm.

dependence. Thus, both the experimental data of Figure B-1 and the predictions of the I-P model suggest that at sufficiently long lives and for thicknesses in the range 12.5 to 50 mm the dependency of relative fatigue strength on thickness is best described by m = 1/3.

Figures B-14 and B-15 plot relative fatigue strength versus $K_{f\,max}$. Figure B-14 shows the calculated values for 10^6 cycles; and it is apparent that basing the estimate of the thickness solely on N_I and Eq. 8 or 9 is valid only for weldments having notch severity, ultimate tensile strengths, and thicknesses which give $K_{f\,max}$ values of 3.0 or less, e.g., AISC Categories A through D in thickness up to 50 mm for mild steel weldments. Figure B-15 shows the calculated values for 10^7 cycles. It is apparent that Eq. 8 or 9 may be used to estimate the thickness effect for AISC Categories B, D, and F. This is applicable to severely notched weldments (like those of AISC Category F) where crack initiation dominates (see Figure B-8).

B-3 SUMMARY OF FINDINGS

Experimental data, recent thinking, and analytical studies using the I-P Model favor a dependency of the relative fatigue strength on the -1/3 power of thickness.

Analytical studies of the thickness effect using the I-P Model suggest that the thickness effect depends on the relative importance of fatigue crack initiation and propagation and hence upon the notch severity of the weldment, the ultimate tensile strength of the notch root materials, the nature of the applied loads, the life regime, and the thickness of the weldment.

For long lives (10^7 cycles), analytical studies using the I-P Model suggest that $K_{f\,max}$ provides a rational basis for estimating the thickness effect.

The I-P Model appears to predict correctly the weldment size effect at both long and short lives.

B-4 REFERENCES

B-1. Hicks, J.G. (1984) "Modified Design Rules for Fatigue Performance of Offshore Structures." Welding in Energy Relate Projects, pp 467-475. Welding Institute of Canada.

B-2. Gurney, T.R. (1983) Revised Fatigue Design Rules. Metal Construction 15, pp 37-44.

B-3. Smith, I.J. (1984) "The effect of Geometry Change upon the predicted Fatigue Strength of Welded Joints," Proc. 3rd Int. Conf. on Numerical Methods in Fract. Mech., pp 561-574.

B-4. Yung, J.-Y. and F.V. Lawrence, Jr. (1985) "Analytical and Graphical Aids for the Fatigue Design of Weldments," Fatigue Fract. Engng Mater. Struct., Vol. 8, No. 3, pp 223-241, November 1985.

B-5. Marshall, P.W. (1990) "Fatigue Design Rules in the U.S.A-.," Proceedings of the 9th International Conference on Offshore Mechanics and Arctic Engineering Houston, May 1990, edited by M/M. Salama, H.C. Rhee, J.G. Williams and S. Liu, Volume III, Part A pp 175-184.

B-6. Berge, S. (1990) "The Plate Thickness Effect - Again," Proceedings of the 9th International Conference on Offshore Mechanics and Arctic Engineering Houston, May 1990, edited by M/M. Salama, H.C. Rhee, J.G. Williams and S. Liu, Volume III, Part A pp 185-190

B-7. Booth, G.S. (1990) "The Fatigue Properties of Plate Welded Joints of Various Thicknesses," Proceedings of the 9th International Conference on Offshore Mechanics and Arctic Engineering Houston, May 1990, edited by M/M. Salama, H.C. Rhee, J.G. Williams and S. Liu, Volume III, Part A pp 191-198.

B-8. Sablok, A.K. and W.H. Hart (1990) "An Experimental Investigation of Plate Thickness and Weld Profile Effects Pertaining to Fatigue Design of Offshore Structures," Proceedings of the 9th International Conference on Offshore Mechanics and Arctic Engineering Houston, May 1990, edited by M/M. Salama, H.C. Rhee, J.G. Williams and S. Liu, Volume III, Part A pp 185-190.

B-9. Eide, O.I. and S. Berge (1990) "Fatigue Capacity of Stiffened Tubular Joints," Proceedings of the 9th International Conference on Offshore Mechanics and Arctic Engineering Houston, May 1990, edited by M/M. Salama, H.C. Rhee, J.G. Williams and S. Liu, Volume III, Part A pp 209-216.

B-10. Haagensen, P.J., T. Sind, and O. Oerjaeter (1990) "Scale Effects in Fatigue Design Data for Welded and Unwelded Components," Proceedings of the 9th International Conference on Offshore Mechanics and Arctic Engineering in Houston, May 1990, edited by M/M. Salama, H.C. Rhee, J.G. Williams and S. Liu, Volume III, Part A pp 217-227.

B-11. Haagensen, P.J. (1990) "Size Effects of Non-Welded Components," Proceedings of the 9th International Conference on Offshore Mechanics and Arctic Engineering in Houston, May 1990, edited by M/M. Salama, H.C. Rhee, J.G. Williams and S. Liu, Volume III, Part A pp 689-699.

B-12. Lawrence, F.V., Jr.; R.S. Mattos; Y. Higashida; and J.D. Burk. (1978) "Estimating the Fatigue Crack Initiation Lives in Welds." Fatigue Testing of Weldments, ASTM STP 648, Hoeppner, Ed., American Society for Testing and Materials, STP 648 (July 1978): 134-158.

B-13. McMahon, J.C. and F.V. Lawrence (1948) "Predicting Fatigue Properties Through Hardness Measurements." Fracture Control Program Report No. 105, University of Illinois.

B-14. Higashida, Y.; J.D. Burk; and F.V. Lawrence, Jr. (1987) "Strain-Controlled Fatigue Behavior of ASTM A36 and A514 Grade F Steels and 5083-0 Aluminum Weld Materials." Welding Journal, pp 334s-344s.

B-15 Fisher, J.W. (1977) Bridge Fatigue Guide, American Institute of Steel Construction, New York.

B-16 Chang, S-T. and F.V. Lawrence (1983) "Improvement of Weld Fatigue Resistance," Fracture Control Program, Report No. 46, University of Illinois.

B-17. Ho, N.J. and F.V. Lawrence, Jr. (1984) "Constant Amplitude and Variable Load History Fatigue Test Results and Predictions for Cruciform and Lap Welds." Theoretical and Applied Fracture Mechanics, Vol. 1, No. 1, pp 3-21.

B-18 Socie, D.F. (1987) "Fatigue Damage Maps," Third Int. Conf. of Fatigue and Fatigue Thresholds, Charlottesville, V. II, pp 599-616.

APPENDIX C

Glossary

Cathodic protection	A means of reducing corrosive attack on a metal by making it the cathode of an electrolytic cell. This can be done by applying an external direct current from a power source (impressed) or by coupling it with a more electro-positive metal (sacrificial).
Constant amplitude fatigue limit	The fatigue strength at $5 \cdot 10^6$ cycles. When all nominal stress ranges are less than the constant amplitude fatigue limit for the particular detail, no fatigue assessment is required.
Continuous termination	Termination from continuous weld
Cruciform or transverse load-carrying joint	Specimen made from two lengths of plate welded, via fillet or full penetration welds, to either side of a perpendicular cross piece of the same section thickness.
Cut-off limit	The fatigue strength at 10^8 cycles. This limit is calculated by assuming a slope corresponding to $m = 5$ below the constant amplitude fatigue limit. All stress cycles in the design spectrum below the cut-off limit may be ignored unless the detail is exposed to a corrosive environment.
Design life	The period during which the structure is required to perform without repair.
Detail category	The designation given to a particular structural detail to indicate which of the fatigue strength curves should be used in the fatigue assessment. The category takes into consideration the local stress concentration at the detail, the stress direction, and residual stresses.
Discontinuity	An absence of material causing a stress concentration. Typical discontinuities are cracks, scratches, corrosion pits, lack of penetration, slag inclusions, cold laps, porosity, and undercut.
Discontinuous termination	Termination from intermittent weld.
Fatigue	The damage of a structural part by gradual crack propagation caused by repeated stresses.
Fatigue Limit	See "cut-off" limit.

Fatigue loading	Fatigue loading describes the relevant variable loads acting on a structure throughout the design life. The fatigue loading in ships is composed of different load cases.
Fatigue notch factor	Ratio of stress of a notched detail to stress for a plan detail at a constant fatigue life.
Fatigue strength	The stress range corresponding to a number of cycles at which failure occurs.
Geometric stress	The stress at any point around the detail intersection necessary to maintain the compatibility of displacements. This stress excludes local stress and depends on the nominal stress and overall geometry of the intersecting members.
Hot spot stress	The stress which controls fatigue endurance in tubular nodal joints. It can be defined experimentally or in design by the product of the nominal stress and the design hot spot stress concentration factor. This form is used primarily for offshore structural details.
Load case	A part of the fatigue loading defined by its relative frequency of occurrence as well as its magnitude and geometrical arrangement.
Load stress	The stress due to the discontinuity at the weld and which is superimposed on the geometric stress.
Nominal stress	The detail stress remote from the intersection. This includes geometric stress at the weld toe in the absence of weld.
Nominal stress range	The algebraic difference between two extremes (reversals) of nominal stress. Usually, this difference is identified by stress cycle counting. Stress extremes may be determined by standard elastic analysis and applying forces and moments to the cross-sectional areas. Exceptions to this definition are details near cut-outs, man-holes, or other stress concentrations not shown in Table 3-1.
Ripple	Uneven weld surface.
Weld profiling	Process of mechanically altering weld surface geometry.

Weld toe — The intersection of the weld profile and parent plate.

Project Technical Committee Members

The following persons were members of the committee that represented the Ship Structure Committee to the Contractor as agency resident subject matter experts. As such they performed technical review of the initial proposals to select the contractor, advised the contractor in cognizant matters pertaining to the contract of which the agencies were aware, and performed technical review of the work in progress and edited the final report.

Mr. Chao Lin	Maritime Administration
Mr. Gary North	Maritime Administration
Mr. Gary Larimer	U.S. Coast Guard
Mr. James White	U.S. Coast Guard
Mr. Ash Chatterjee	U.S. Coast Guard
Dr. Y.N. Chen	American Bureau of Shipping
Mr. Dave Kihl	Carderock Division, Naval Surface Warefare Center
Mr. Jerry Snyder	Naval Sea Systems Command
Prof. William Munse	University of Illinois
Dr. Pedro Albrecht	University of Maryland
Mr. William Siekierka	Naval Sea Systems Command, Contracting Officer's Techical Representative
Mr. Alex Stavovy Dr. Robert Sielski	National Academy of Science, Marine Board Liaison
CDR Mike Parmelee CDR Steve Sharpe	U.S. Coast Guard, Executive Director Ship Structure Committee

*U.S. G.P.O.:1994-301-717:80489

COMMITTEE ON MARINE STRUCTURES

Commission on Engineering and Technical Systems

National Academy of Sciences – National Research Council

The COMMITTEE ON MARINE STRUCTURES has technical cognizance over the interagency Ship Structure Committee's research program.

LOADS WORK GROUP

MATERIALS WORK GROUP

SHIP STRUCTURE COMMITTEE PUBLICATIONS

SSC-354	Structural Redundancy for Discrete and Continuous Systems by P. K. Das and J. F. Garside 1990
SSC-355	Relation of Inspection Findings to Fatigue Reliability by M. Shinozuka 1989
SSC-356	Fatigue Performance Under Multiaxial Load by Karl A. Stambaugh, Paul R. Van Mater, Jr., and William H. Munse 1990
SSC-357	Carbon Equivalence and Weldability of Microalloyed Steels by C. D. Lundin, T. P. S. Gill, C. Y. P. Qiao, Y. Wang, and K. K. Kang 1990
SSC-358	Structural Behavior After Fatigue by Brian N. Leis 1987
SSC-359	Hydrodynamic Hull Damping (Phase I) by V. Ankudinov 1987
SSC-360	Use of Fiber Reinforced Plastic in Marine Structures by Eric Greene 1990
SSC-361	Hull Strapping of Ships by Nedret S. Basar and Roderick B. Hulla 1990
SSC-362	Shipboard Wave Height Sensor by R. Atwater 1990
SSC-363	Uncertainties in Stress Analysis on Marine Structures by E. Nikolaidis and P. Kaplan 1991
SSC-364	Inelastic Deformation of Plate Panels by Eric Jennings, Kim Grubbs, Charles Zanis, and Louis Raymond 1991
SSC-365	Marine Structural Integrity Programs (MSIP) by Robert G. Bea 1992
SSC-366	Threshold Corrosion Fatigue of Welded Shipbuilding Steels by G. H. Reynolds and J. A. Todd 1992
SSC-367	Fatigue Technology Assessment and Strategies for Fatigue Avoidance in Marine Structures by C. C. Capanoglu 1993
SSC-368	Probability Based Ship Design Procedures: A Demonstration by A. Mansour, M. Lin, L. Hovem, A. Thayamballi 1993
SSC-369	Reduction of S-N Curves for Ship Structural Details by K. Stambaugh, D. Lesson, F. Lawrence, C-Y. Hou, and G. Banas 1993
SSC-370	Underwater Repair Procedures for Ship Hulls (Fatigue and Ductility of Underwater Wet Welds) by K. Grubbs and C. Zanis
SSC-371	Establishment of a Uniform Format for Data Reporting of Structural Material Properties for Reliability Analysis by N. Pussegoda, L. Malik, and A. Dinovitzer
None	Ship Structure Committee Publications - A Special Bibliography